Università degli Studi della Tuscia di Viterbo

Dipartimento di Scienze Ecologiche e Biologiche

Corso di Dottorato di Ricerca in

Ecologia e Gestione Sostenibile delle Risorse Ambientali - XXXVI ciclo

Landscape and climatic drivers of diversity patterns in a topographically heterogeneous hotspot of biodiversity

Settore scientifico-disciplinare

BIO/07 - ECOLOGIA

Tesi di dottorato di:
Dott. Daniele Delle Monache
Firma

Coordinatore del corso
Prof. Claudio Carere
Firma

Tutore
Prof. Daniele Canestrelli
Firma

Co-tutore
Prof. Luigi Maiorano
Firma

A.A. 2023/24

Index

Thesis structure

This thesis aimed to identify the environmental drivers that shape the distribution of biological diversity in highly heterogeneous hotspots of biodiversity. I devoted the introduction (Chapter 1) to illustrating the landscape and climatic features that render mountain regions capable of hosting outstanding biodiversity levels. Prominent among these is certainly topographic heterogeneity. In the introduction, I also framed the general aims of the research and described the study area.

Topographic heterogeneity can pose significant challenges when deriving high-resolution climate surfaces relevant to ecologists. In Chapter 2, I thus compared state-of-the-art interpolation and downscaling techniques to assess which are suitable for local climate forecasting when topography gets overly complex. This activity led to submitting a research paper to the *Ecological Informatics* peer-reviewed journal, which has been accepted pending minor revision.

Chapter 3 investigated the landscape and climatic factors giving rise to a genetic diversity mountain hotspot using the fire salamander (*Salamandra salamandra gigliolii* Eiselt & Lanza, 1956) as a candidate species. I will soon submit this research study to the *Landscape Ecology* peer-reviewed journal.

In Chapter 4, I explored the role of land use/cover, microclimatic stability, and forest structure in promoting the diversification of biological communities in a mountain hotspot of biodiversity. Here, I draw my attention to pollinating insects. This Chapter constitutes a preliminary study, which will be improved with further analyses.

The thesis ends with Chapter 5, where I conclude from the results of the previous Chapters and outline their relevance from a conservation perspective.

Abstract

Mountain regions feature some of the richest biodiversity hotspots on Earth. Among the many factors that make mountains unique, topography stands out for its prominence. It drives fine-scale variations in climate and influences soil moisture and nutrient availability; these physiographic effects have become known for decades. Likewise, how mountain biodiversity responds is increasingly studied. However, disentangling how climates and landscapes shape diversity patterns at all hierarchical levels becomes challenging when topographic heterogeneity gets overly complex.

In this thesis, I leveraged an exceptionally heterogeneous mountain region in Southern Italy, the Aspromonte, to investigate how landscapes and climates in topographically challenging contexts drive diversity patterns at remarkably small spatial scales. I started by finding the best technique to account for the region's climatic variability completely. Once the best technique was selected, I examined the population genetic structure of the fire salamander (*Salamandra salamandra gigliolii*), elucidating its relationships with the region's topographic, climatic, and habitat components. The species here is distributed continuously and is tightly bonded to habitat quality, which renders it an optimal candidate. Then, I rose to the community level and investigated whether microclimatic stability, forest characteristics, and land use/cover explain the region's outstanding pollinator diversity.

Results showed that interpolating weather station data got an edge over downscaling macroclimate grids as it provided more detailed high-resolution monthly climate surfaces. Environmental heterogeneity influenced biodiversity distribution at both intraspecific and community levels. On the one hand, I found *S. Salamandra* populations highly genetically structured, with fine-scale habitat configuration and climatic variation primarily driving population differentiation. Old-growth forests, prominent habitats for the Aspromonte region, also seemed to promote differentiation in the species. In addition, *S. salamandra* was predicted to move upslope in response to near-future climate warming. On the other hand, pollinator diversity depended on land use/cover, with the most heterogeneous semi-natural habitats being the most diverse. Moreover, old-growth forests were prominent for pollinating insects, too, increasing pollinator diversity in their proximity.

In conclusion, this thesis proposed an integrated framework to simultaneously identify the environmental drivers of biodiversity distribution at all hierarchical levels. When applying it to the Aspromonte, I found that climatic and habitat heterogeneity influence its biodiversity patterns at intraspecific and community levels and even at the smallest spatial scales. I also compiled evidence confirming the relevance of old-growth forests to biodiversity conservation.

1. Introduction

As human activities exert unprecedented pressure on worldwide ecosystems, biodiversity hotspots increasingly emerge as priority targets for nature conservation. These regions concentrate more than 50% of endemic plant species and 42% of endemic terrestrial vertebrate species in 2.4% of the Earth's land surface (CEPF, 2014). Biodiversity hotspots are also home to a disproportionate share of Earth's people (Cincotta et al., 2000), and human communities rely heavily on the ecosystem services they provide. Conserving biodiversity hotspots is, hence, as much an ecological problem as an economic and social one (Zachos & Habel, 2011). The threats facing hotspots closely mirror, albeit typically more severe than, those confronting global biodiversity. Habitat destruction drives extinctions in many hotspots (Brooks et al., 2002). Climate change threatens a significant fraction of species by altering global climates and fueling further habitat loss (Thomas et al., 2004; Turner et al., 2010). Many natural populations in hotspots were impacted by the introduction of non-native species (Groves & di Castri, 1991; Steadman, 1995), while others were severely exploited for trade or meat (van Dijk et al., 2000; Bakarr et al., 2001). Diseases and infections can also affect biodiversity hotspots, like chytridiomycosis, which threatens hotspots that harbor 59% of all amphibians as endemics (Stuart et al., 2004; Wake & Vredenburg, 2008). In other words, as biological richness, anthropogenic pressures, and socioeconomic risks converge in hotspots, biodiversity conservation here is critically important.

Some biodiversity hotspots are remarkably richer than others. In their seminal study, Myers et al. (2000) identified five main hotspots that comprise astounding proportions of endemics – as much as 45% of all the hotspots' endemic plants and vertebrate species. Among the many habitat types they include, these hotspots feature some of the most prominent mountain regions worldwide (CEPF, 2014; Camacho-Sanchez et al., 2018; Noroozi et al., 2018). Similarly, and at broader scales, mountain regions are home to more than 87% of global amphibian, bird, and mammal biodiversity while covering less than 25% of the Earth's land surface, excluding Antarctica (Kapos et al., 2000; Rahbek et al., 2019). Mountains are rich in endemic species (Steinbauer et al., 2016); this is strikingly the case for Alpine floras (Körner, 2003; Ozenda & Borel, 2003; Pauli et al., 2003; Aeschimann et al., 2004) and vascular plant diversity in general (Barthlott et al., 1996; Mutke & Barthlott, 2005), but it remains valid for many other organisms as well (Smythies, 1964; Rodgers & Homewood, 1982; Leo, 1995; Martino et al., 2022). Significant hotspots of plant species diversity encompass tropical and subtropical mountains like the tropical eastern and subtropical Andes, northern Borneo, and the Atlantic forests of Brazil (Mutke & Barthlott, 2005; Barthlott et al., 2007). Further biodiversity hotspots occur in the Mediterranean mountains, the Caucasus, and the Alps (Spehn et al., 2010); plant

diversity in the Mediterranean basin, for instance, concentrates in 10 hotspots, most of which include mountainous areas (Médail & Quézel, 1997). Southeast Asia also features relevant mountain hotspots, housing approximately half of Earth's mountain forests (Hansen et al., 2013; Körner et al., 2017). The usual belief is that the highest biodiversity on Earth occurs in Equatorial rainforest ecosystems (Molles & Tibbets, 2002); however, the observation that mountain biotas are often more diverse than tropical ones challenges this belief so much that it has been granted the name of the "Humboldt's enigma" (Rahbek et al., 2019).

So, what makes mountain regions so unique? Arguably, the most impactful prerogative of mountains on biological diversity is topographic conformation; it indeed underlies many, if not all, eco-evolutionary processes occurring here. For instance, mountain uplifting influences drainage patterns and river flows in young mountain ranges, often leading to evolutionary radiations (Hoorn et al., 1995). Likewise, mountain uplifting creates novel climatic conditions that drive the adaptation of plants and their associated biota (Antonelli et al., 2018). To appreciate the depth of this topic, see the thorough review from Favre et al. (2015). Heterogeneous topographies also compress contrasting climatic zones over short distances, rivaling those found along much broader elevational or latitudinal gradients (Scherrer & Körner, 2010). At local scales, many species with slightly different climatic niches can thus coexist, allowing biological diversity to cumulate (Körner, 2004; Hoorn et al., 2018). Within these mosaics of contrasting microclimates, favorable microhabitats also abruptly alternate with unfavorable ones, causing populations to split and diverge despite physical proximity (Särkinen et al., 2012; Stein et al., 2014).

Likewise, with their differing slopes and aspects, mountain ranges are home to unique short- and long-term climatic oscillations. Day-to-day weather variations in high-altitude landscapes can be extreme (Barry & Blanken, 2016) and, when interacting with seasonality, create small patches of peculiar climate types that further fuel specialization (Janzen et al., 1967; Ohlemüller et al., 2008; Chan et al., 2016). In longer-term oscillations, such as under Quaternary climatic shifts, mountains acted as refugia, repeatedly allowing species to track their climatic niche by upward and downward shifts (Carnaval et al., 2009; Stewart et al., 2010). When climates oscillate, mountains also undergo fewer species extinctions due to their contrasting microclimates facilitating climatic niche tracking through short-term migrations (Sandel et al., 2011; Scherrer & Körner, 2011). Concurrently, species incur cyclical range expansions and contractions that cause habitat connectivity to "flicker" (see Flantua et al., 2019), leading to species-pump effects that drive diversification in naturally fragmented landscapes (Nevado et al., 2018; Vasconcelos et al., 2020). These effects cumulate and produce tangible outcomes on the biological diversity of entire regions. Back to the Mediterranean basin

example, out of the 52 refugia identified by Médail & Diadema (2009), 33 refugia fall within mountain ranges, and 26 refugia occur within the 10 plant diversity hotspots (Médail & Quézel, 1997).

Paradoxically, ecologists knew that exposure, slope inclination, and steep altitudinal clines create unique local climatic (i.e., topoclimatic) and microclimatic conditions for over a century; suffice to mention that the first edition of Geiger's classical text, *The Climate Near the Ground*, dates to 1927. They had, however, to wait the last few years to make groundbreaking progress in modeling the mountains' climatic components at appropriate resolutions. They can now finally benefit from advances in remote sensing and other technologies (Zellweger et al., 2019; Lembrechts & Lenoir, 2020) and the widespread awareness that mountains are cornerstones for species conservation under contemporary anthropogenic change (Luoto & Heikkinen, 2008; Pastore et al., 2022). Given the complexity of the topic, I dedicated Chapter 2 to illustrating the challenges of modeling high-resolution local climates in topographically heterogeneous mountain regions. I did so by comparing the performance of two of the most widely used statistical techniques for the task – statistical interpolation and downscaling – when predicting the local climates of the Aspromonte, an outstandingly complex mountain region in Southern Italy.

The Aspromonte is an epitome of the diversity and heterogeneity typical of mountain regions. Still, several distinctive features make it shine as a critical priority for biodiversity conservation at national and continental levels. The Aspromonte region is located at the southern end of the Italian peninsula and hosts a mountain massif reaching almost 2000 meters asl (Fig. 1a). Its topographical conformation and its being surrounded by the Mediterranean Sea set the stage for intricate topoclimatic and microclimatic mosaics. The region also harbors peculiar natural habitats that, in some cases, are still devoid of human impacts; prominent examples are old-growth forests, which are its flagship forest environments (Piovesan et al., 2020). The Aspromonte region has recently been the scene of intense research (see Zampiglia et al., 2019, and literature therein) that revealed fascinating complexity. The region was identified as a glacial/interglacial refuge for temperate species to endure climate shifts and sea level variations during the Pleistocene glacial cycles (Todisco et al., 2010; Iannella et al., 2018). Consequently, a non-negligible – and probably vastly underestimated – proportion of its biodiversity is endemic or sub-endemic. In addition, many species' expanding evolutionary lineages from the Sicilian and more northern areas often intermix within the Aspromonte, making the region a vital genetic melting pot. When these combine with Aspromonte's endemic lineages, biological diversity in the region is boosted even further (Chiocchio et al., 2019).

The Aspromonte region, in fact, belong to the Mediterranean Basin biodiversity hotspot sensu Myers et al. (2020). The region also falls among the Mediterranean refugia of plants identified by Médail & Diadema (2009), within which it constitutes a critical hotspot for all biodiversity levels, from community assemblages to interspecific and intraspecific genetic diversity (Martino et al., 2022). The latter can reach regional to global relevance, as in the case of *Talpa romana*, whose genetic diversity here is among the highest in mammals worldwide (Canestrelli et al., 2010). Intraspecific genetic diversity plays a primary role in conservation as it establishes the evolutionary potential of populations to cope and adapt to anthropogenic change (Benito Garzón et al., 2011). This is a particularly pressing matter in Aspromonte, given that the region houses the only resilient populations left for many species, like the Apennine yellow-bellied toad (Zampiglia et al., 2019). Accordingly, I devoted Chapter 3 to investigating the genetic population structure of the fire salamander (*Salamandra salamandra gigliolii* Eiselt & Lanza, 1956) and its connections with the climatic and landscape features of the Aspromonte region. The species here is continuously distributed (Lanza, 2007) and is generally sensitive to habitat degradation and fragmentation because of its philopatry and dispersal limitations (Schulte et al., 2007). In this respect, I also took the opportunity to examine whether old-growth forests could help vulnerable species face contemporary anthropogenic change, which could be relevant to the preservation of forested habitats and the organisms inhabiting them.

The Aspromonte region also features extraordinarily diverse biological communities. Pollinator communities are particularly relevant for their precious ecosystem roles (Klein et al., 2007; Gallai et al., 2009). Pollinating insects currently suffer from widespread declines, projected to have far-reaching consequences for the stability of natural and agricultural systems (Potts et al., 2010). Therefore, understanding how reduced pollinator diversity affects pollination function is imperative (Kremen & Ostfeld, 2005). Pollinator diversity in the Aspromonte has been recently investigated, both taxonomically and genetically. These studies elevated the region to an absolute hotspot of diversity at national to continental scales, with rich and well-differentiated pollinator populations that could prove irreplaceable for the long-term conservation of these taxa. Building on samples collected in 2020 and microclimates recorded by several data loggers, I thus had the chance to combine Aspromonte's outstanding pollinator diversity with its unique landscape heterogeneity. In Chapter 4, I examined which microclimatic, forest, and landscape features could help explain pollinators' diversification in highly heterogeneous mountain hotspots.

Within the Aspromonte region lies the Aspromonte National Park. Since 1989, it has protected and safeguarded the territories of the Aspromonte section of the former Calabria National Park, which existed until 2002; it has also been part of UNESCO's Global Geoparks Network since 2021. Along

with the Park are 57 Natura 2000 areas, including 55 Special Areas of Conservation (SACs) and two Special Protection Areas (SPAs). In recent years, research highlighted the need to reassess the Park's conservation management strategies, including the criteria for defining its zonation. The Aspromonte National Park is currently divided into six functional zones (Fig. 1b). From a conservation perspective, the most relevant ones are the A and B zones. Zone A is an integral reserve area found among those of the highest naturalistic value. Therefore, its conservation purpose excludes, as a rule, the carrying out of anthropic activities, except in the case of recovering and upgrading existing artifacts or the preservation of cultural heritage. On the other hand, B zones are general reserve areas targeted at renaturalisation; they still comprehend areas of high naturalistic and landscape value but with greater anthropization than A zones. Tourism and productive activities are allowed in Zone B as long as they do not increase the territory's vulnerability. Then come the C and D zones, which are progressively more affected by anthropization. The list ends with special zones Cs and Ds, functional zones with different classifications since they require substantial redevelopment, adaptation, completion, and enhancement to ensure their better insertion in the natural environment. Having broadened the perspective to the entire Aspromonte region as a prominent exponent of mountain hotspots, I conclude the thesis by framing its results within the framework of the Aspromonte National Park and its functional zonation.

This thesis, therefore, aims to develop an integrated framework to disentangle the influences of fine-scale environmental complexity on multiple hierarchical levels of biodiversity. To this end, we calibrated our framework to Aspromonte's topographical and climatic heterogeneity. Then, we applied it to study the environmental determinants of intraspecific diversity in fire salamander populations and community diversity in pollinating insects.

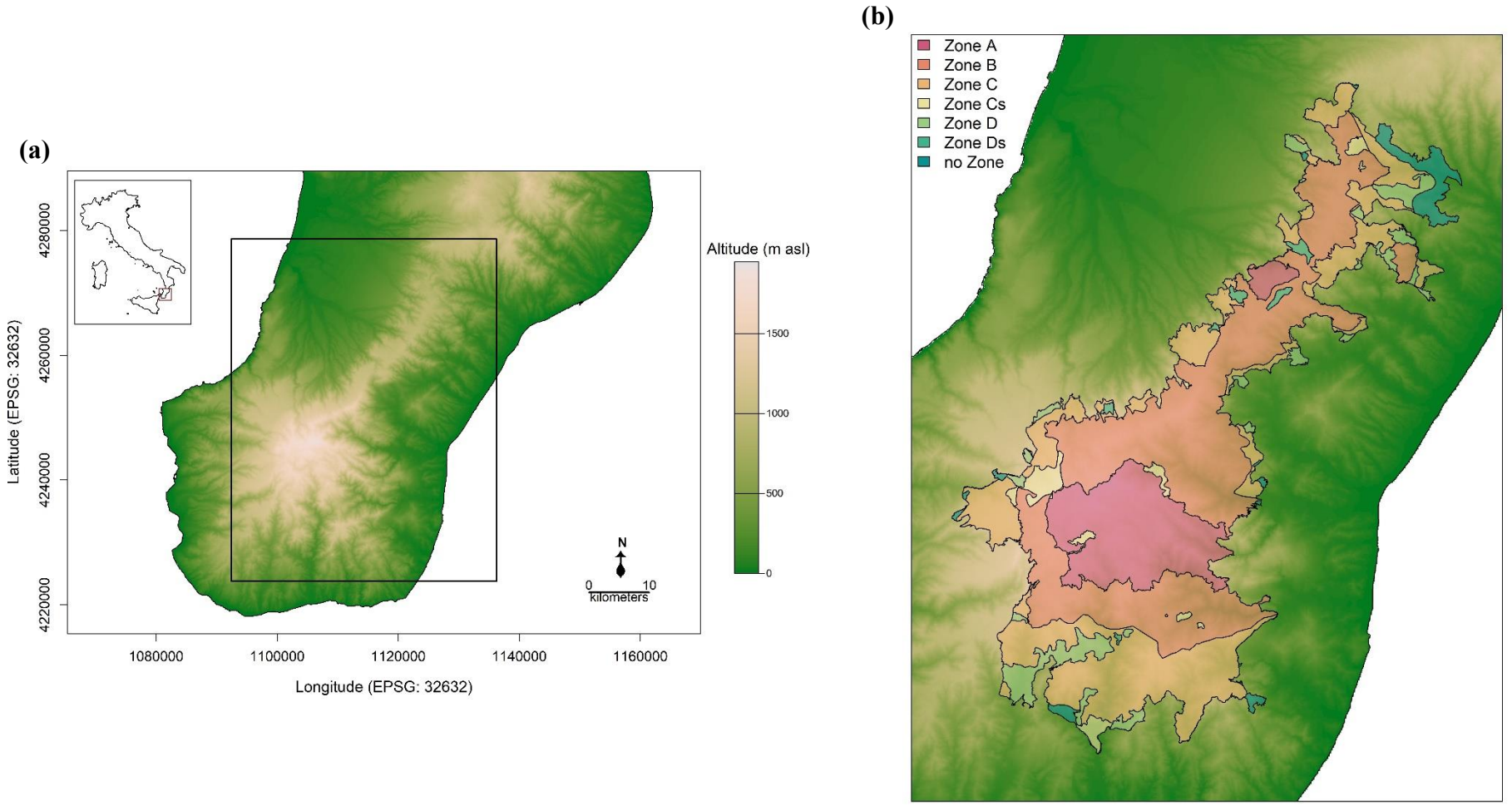

Figure 1. **(a)** Geographic position and topographic conformation of the Aspromonte region. The box indicates the extent of subplot **(b)**. The inset shows the borders of the Italian peninsula, while the red box represents those of the study area. **(b)** The Aspromonte National Park and its current zonation.

2. Mapping local climates in highly heterogeneous mountain regions: interpolation of meteorological station data vs. downscaling of macroclimate grids

Authors: Daniele Delle Monache[a], Giuseppe Martino[a], Andrea Chiocchio[a], Antonino Siclari[b,c], Roberta Bisconti[a], Luigi Maiorano[d] & Daniele Canestrelli[a]

[a] Department of Ecological and Biological Sciences, Tuscia University, Viterbo, Italy
[b] Aspromonte National Park, Santo Stefano in Aspromonte, Italy
[c] Città Metropolitana di Reggio Calabria, Piazza Italia, 89100, Reggio Calabria, Italy
[d] Department of Biology and Biotechnologies «Charles Darwin», Sapienza University, Rome, Italy

Abstract

Topography modulates air and soil temperature and gives rise to local climates that may strongly deviate from regional macroclimates. These local climatic conditions determine the distribution of many organisms but are hardly accounted for by coarse-grained macroclimate grids. Downscaling macroclimate grids or interpolating high-resolution climate surfaces from weather station data has thus become a staple in ecological research. Against this background, topographically complex territories pose a challenge, as downscaling and interpolation techniques are susceptible to high topographic heterogeneity. Simultaneously, these regions will act as refugia and preserve biodiversity amidst the challenges of climate change. This contrast renders choosing the technique to derive local climatic conditions under high topographic complexity critically relevant.

In this study, we compared how interpolation and downscaling techniques predict the local climates of topographically heterogeneous territories. We interpolated monthly average temperatures from weather stations in a Southern Italy mountain region and downscaled WorldClim and CHELSA macroclimatic grids from their native 30 arcsecs to 10 m resolution. We carried out the interpolation and downscaling procedures by employing four commonly used statistical algorithms and by including physiographic descriptors (altitude, northness, eastness, distance to the coast, and monthly average of daily clear-sky insolation time) known to determine local climatic conditions. We compared the techniques' predictive performance via leave-one-out cross-validation. We extended the comparison over the study area to identify where the techniques most strongly diverged and evaluated how interpolation and downscaling techniques fare against environmental extrapolation.

Although the interpolations scored the best values across all error metrics, interpolating weather station data and downscaling WorldClim yielded essentially equivalent predictions of local climates in the cross-validations. Differences between the two techniques emerged during the spatial comparison, where downscaling WorldClim produced biased and less detailed monthly climate surfaces. On the contrary, weather station interpolation was affected by environmental extrapolation in the study area's most internal and topographically heterogeneous landscapes. Downscaling CHELSA severely over-smoothed local climatic conditions during both cross-validations and spatial comparisons, possibly due to lacking climate variability in the native product itself.

We demonstrated that technique and data source choice affect the prediction of local climates in topographically heterogeneous territories. Despite its limitations, we argue that interpolating weather station data better accounted for local-scale topographic effects. These effects form an integral part of the microrefugia that will shelter mountain communities from warming climates. We thus recommend carefully considering the techniques chosen to unravel the intricate climatic mosaics of topographically heterogeneous territories.

Keywords

high-resolution local climates, topographic heterogeneity, interpolation, downscaling, climate products

Introduction

Amidst the socio-economic consequences of globalization, climate change is arguably the most impactful on the world's ecosystems (Rosenzweig et al., 2008). Climate change prompts many terrestrial organisms to redistribute upslope and poleward to follow their climatic niche (Parmesan, 2006; Chen et al., 2011). It also forces many organisms to modify their physiology and seasonal activity to remain synchronous with environmental conditions favorable for growth and reproduction (Parmesan & Yohe, 2003; Canestrelli et al., 2017). Although climate change is occurring globally, it impacts some ecosystems more than others; in this respect, mountain ecosystems seem to be among the most vulnerable ones. The rate of warming increases with elevation, meaning that high-elevation environments are exposed to faster thermal changes than low-elevation ones (Pepin et al., 2015; McCullough et al., 2016). Such thermal changes strongly affect mountain biological communities. For instance, in a recent and extensive review concerning the European Alps (Vitasse et al., 2021), several taxa were shown to have shifted spring phenology and distribution range over recent decades. In addition, most of them struggled to keep track of the broad-scale isotherm shifts induced by climate warming.

At the same time, mountain species may experience lower extinction rates under warming climates than lowland species (Scherrer & Körner, 2011). The reason is the outstanding variety of temperature contrasts that mountain ranges house over short linear distances. These contrasts are comparable to those found along much broader elevational or latitudinal gradients (Scherrer & Körner, 2010). They facilitate vulnerable taxa coping with climate changes, allowing them to track the isotherm shifts easily by short-range migration (Sandel et al., 2011). Mountain ranges offered refuge to cold-adapted species during interglacials (Stewart et al., 2010; Camacho-Sanchez et al., 2018). Under warming climates, we should thus deem the preservation of mountain ranges of paramount importance. In particular, we should focus on preserving those small-scale climate niches expected to shelter biodiversity more effectively from climate change (Luoto & Heikkinen, 2008; Lenoir et al., 2013).

These areas of unusual microclimates relative to their surroundings are known as microrefugia or cryptic refugia (Rull, 2009; Ashcroft, 2010). Microrefugia are now finally recognized as game-changers for biodiversity conservation under climate change, and emerging technologies are increasingly facilitating their identification. Early microrefugia identification was qualitative, with microrefugia being equated with elements of the territory like boulder fields (Shoo et al., 2010) and old, climatically buffered, infertile landscapes (OCBILs sensu Hopper, 2009). Also, microrefugia were equated with areas that house stable climatic conditions becoming increasingly rare (Dobrowski,

2011) or that harbor climate-relict populations (Hampe & Jump, 2011). Instead, only one decade after these first attempts, microrefugia are identified by quantitatively modeling their climatic components. We can locate them in many ways, for example, via spatial interpolation of field measurements (Frey et al., 2016; Milling et al., 2018) or mechanistic models of fine-scale microclimates (Kearney & Porter, 2017; Maclean et al., 2019).

The growing availability of macroclimate grids is also coming in handy. These products provide information about free-air macroclimates concerning large shares of the Earth's surface and are commonly used to model species distributions over large spatial extents (Elith & Leathwick, 2009). Unfortunately, macroclimate grids are usually too coarse to capture the range of microclimates available at smaller scales (Potter et al., 2013). Thus, macroclimate grids might need to be downscaled to the appropriate spatial scales before they can be effectively used (Lenoir et al., 2017). High-resolution free-air temperature products are routinely obtained by linking macroclimates to the physiographic descriptors that drive local climatic conditions (McCullough et al., 2016). Then, after modeling the offset between local climates and microclimates (Lenoir et al., 2017; Maclean et al., 2019) or relying on available maps of temperature offsets (Haesen et al., 2021), these free-air climatic conditions can help characterizing the in-situ microclimates that organisms experience. However, downscaling free- air temperatures propagate the underlying uncertainty of the macroclimate grids; these products are built upon the interpolation of weather station data. In this respect, using weather station data to produce high- resolution climate surfaces directly might prevent the uncertainty from affecting the estimation of local climates.

Weather station data have been successfully employed in many studies so far. For example, Aalto et al. (2017) integrated weather station data with topographic information. They witnessed substantial improvements in estimating local climates compared to a more conventional approach involving only geographical location, elevation, and water cover. Meineri and Hylander (2017) similarly linked weather station data with topography via three different linear mixed models to obtain fine-grain climatic grids. They then supplemented these grids with coarser climate data to produce more refined species distribution models (SDMs) for 78 vascular alpine plants over Sweden. Lastly, Stark and Fridley (2022) compared SDMs generated using interpolated meteorological station data at two spatial scales, with one based on a previously validated microclimate model (Fridley, 2009). Their results reaffirm the importance of explicitly considering microclimates when projecting organismal response to climate change.

Ultimately, interpolating weather station data and downscaling macroclimate grids are valuable allies for mapping local climatic conditions. However, both techniques are likely to be

challenged by high topographic complexity. On the one hand, weather stations tend to be located in low-elevation and relatively flat terrains, which puts predicting local climates in otherwise impervious mountain ranges under threat of environmental extrapolation (Phillips et al., 1992; Daly et al., 1994; Bolstad et al., 1998). Weather stations must also be densely distributed across the territory to be successfully interpolated (Guisan & Zimmermann, 2000; Lookingbill & Urban, 2003). On the other hand, downscaling techniques are likewise susceptible to extrapolation since they are calibrated on coarse-resolution products that lack the topographic information of the territory. These techniques might thus fail to encompass the fine-scale relationships between local climates and their physiographic drivers when the latter interact in extremely complex ways, as in highly heterogeneous mountain ranges (Barry & Blanken, 2016).

That is where we come to a paradox; interpolation and downscaling techniques could fail precisely where their contribution would be most decisive. Assessing how interpolating weather station data and downscaling macroclimate grids compare in highly heterogeneous mountain ranges is therefore urgently needed. Here, we leverage a highly climatically complex and topographically heterogeneous mountain range in Southern Italy to perform this comparison by interpolating monthly climate data from 33 weather stations and by downscaling two of the most widely used macroclimate grids, namely WorldClim (version 2.1; Fick & Hijmans, 2017) and CHELSA (version 1.1; Karger et al., 2017). We started by following a pointwise leave-one-out cross-validation approach to compare the techniques' predictive performance at the weather stations' locations. We then extended the comparison over the entire study area by constructing monthly climate surfaces for each technique, which we confronted to highlight the regions where the techniques most strongly diverged. Finally, we compared the robustness of interpolation and downscaling techniques to environmental extrapolation by investigating how similar their local climate estimates were and whether they remained coherent as the extrapolation increased.

Materials & Methods

Study area

Our study area encompasses the Aspromonte region, located at the southern tip of the Apennines in Calabria, south Italy (Fig. 1). This region is home to the homonymous Aspromonte mountain range, which, by its conformation and topography, features a solid inner-outer macroclimatic gradient. Its rainfall distribution is typically Mediterranean, with abundant precipitation during autumn, winter, and spring that becomes scarce in summer; annual average rainfall over the region amounts to about 1000 mm, 83% of which is recorded from October to April (Colacino et al., 1997). Due to moderate-

altitude reliefs reaching 1957 m asl, interior areas are colder and wetter than the peripheral; they indeed belong to a temperate oceanic bioclimate, while those along the coast to a Mediterranean rain-seasonal oceanic bioclimate (Brullo et al., 2001). Annual average temperatures reach about 18 °C along the coast and 13 °C inland; annual average rainfall above 800 m usually reaches 1100 mm while drops to 900 mm in valleys and coastal areas. On top of this macroclimatic gradient, the prevalently north-south disposition of the Aspromonte adds another east-west gradient in local climatic conditions. Westerlies cause humid air masses to be intercepted by the western side of the Aspromonte, which leaves a rain shadow on its eastern side. Consequently, local climates on the west are markedly wetter and cooler (annual average rainfall: 900 mm), and those on the east are warmer and drier (annual average rainfall: 700 mm). These inner-outer and east-west gradients give rise to a remarkable range of climate niches over short horizontal distances. In this light, it is no surprise that the Aspromonte mountain range represents a biodiversity hotspot for plant and animal communities at all levels of biological organization (Spampinato et al., 2008; Zampiglia et al., 2019). The region is also identified as a glacial refuge and constitutes a hotspot of genetic diversity for many temperate species (Martino et al., 2022; Chiocchio et al., 2024).

Weather station data

From the regional environmental agency for Calabria (http://www.arpacal.it/), we retrieved daily average temperatures for 33 weather stations from 1923 to 2020. As these climate time series suffered from severe data deficiencies (Table A.1 in Appendices), we imputed the missing temperatures using the bootstrap algorithm implemented in the AMELIA II R package (Honaker et al., 2011). The algorithm leverages the correlation among incomplete time series, which is expected in weather station data, to produce multiple completed time series via multiple imputation. We ran the algorithm to impute 500 complete replicas of each weather station's time series. Then, for each weather station, we filled in the missing temperatures by taking the average of these replicas. We assessed the quality of the imputation procedures by checking the overimputation diagnostic plots and calculating the R^2 and root-mean-square errors (RMSE) of the overimputations (Figure A.1, Fig. A.2, and Fig. A.3 in Appendices). After the imputation procedures, we converted the daily average temperatures for the 33 weather stations into monthly average temperatures. Then, we averaged a subset of the monthly average temperatures (1970-2000) to obtain 12 datasets valid for 1970-2000, one for each month.

Weather station interpolation

We interpolated weather station data through four statistical algorithms: a generalized additive model (GAM), an artificial single-hidden-layer neural network (ANN), a random forest (RF), and a generalized boosting regression model (GBM). We employed physiographic descriptors known to

drive local climatic conditions as predictors in the algorithms; these descriptors were altitude, northness, eastness, distance to the coast, and monthly average of daily clear-sky insolation time. We derived most of these descriptors (altitude, northness, eastness, distance to the coast) from a digital terrain model at 10 m resolution in R, version 4.1.3 (R Core Team, 2022). Monthly averages of daily clear-sky insolation times were calculated by averaging the daily daylight lengths provided by the R.SUN routine available in GRASS GIS, version 7.8.5. We fitted GAMs by defining a cubic regression spline for each descriptor and using the MGCV R package (Wood, 2011). We fitted ANNs via the NNET R package (Venables & Ripley, 2002) after performing cross-validation over five decays (0, 0.2, 0.4, 0.6, 0.8, 1) and sizes (1, 2, 3, 4, 5). We fitted RFs using the RANDOMFOREST R package (Liaw & Wiener, 2002) with 500 trees, five as the minimum size of terminal nodes, and by sampling all descriptors for splitting at each node; these RFs were thus equivalent to bagged decision trees. Finally, we fitted GBMs via the GBM R package (Greenwell et al., 2020) by ensembling a maximum of 10,000 trees, with shrinkage and interaction parameters equal to 0.01 and 1, respectively; each tree was thus equivalent to a decision stump. After model calibration, we identified the most relevant physiographic descriptors for each algorithm and each month. For GAMs, we evaluated the predictors' relative importance by considering their F statistics. We assessed variable importance in ANNs by employing the Olden method (Olden et al., 2004) implemented in the NEURALNETTOOLS R package (Beck, 2018). GBMs' variable importance was quantified by retrieving the computed relative influences, normalized to sum to 100. We finally assessed RFs' variable importance by computing the increase in node purity associated with each predictor.

To ensure that the weather stations sampled sufficient portions of landscape complexity, we first synthesized all five physiographic descriptors via principal component analysis (PCA) and quantified the contribution of each principal component (PC) to the explained variance. Then, we extracted its first two PCs and inspected the spatial sparsity of the weather stations' locations in the resulting monthly bivariate plots. For each month, we also evaluated the proportion of overlap between the study area's distribution of PCA scores along all five PCs and the sampling distribution created by the weather stations. These overlapping proportions were calculated using the OVERLAPPING R package (Pastore et al., 2022). Finally, we inspected where the interpolations extrapolated by deriving each month's surface of the Shape extrapolation metric. The Shape method measures the degree of extrapolation in environmental space by calculating the distance between training and projection data; higher Shape values thus indicate higher extrapolation degrees (Velazco et al., 2023). We calculated Shape values by considering the Mahalanobis distance and using the FLEXSDM R package (Velazco et al., 2022).

WorldClim and CHELSA data

We downloaded version 2.1 of WorldClim's historical monthly climate rasters ("tavg 30s") from the WorldClim website (https://www.worldclim.org/). These 12 rasters cover 1970-2000 and come at 30 arcsec resolution (~ 1 km2). For CHELSA, we downloaded the CHELSA-EUR11 (https://chelsa-climate.org/high-resolution-climate-data-for-europe/) high-resolution (30 arcsecs; ~ 1 km2) monthly average temperature rasters for each year from 1981 to 2005 ("CHELSA_EUR11_tas_mon_1981-2005_V1.1"). We then averaged these monthly average temperatures, similar to what we did for the weather station data, to produce 12 rasters of monthly climate covering 1981-2005.

WorldClim and CHELSA downscaling

Before downscaling WorldClim and CHELSA, we cropped the monthly climate rasters to the extent of the study area (Fig. 1). We resampled the altitude, distance to the coast, and monthly average of daily clear-sky insolation time rasters we employed in the interpolation to match the extent and resolution (30 arcsecs) of the WorldClim and CHELSA monthly climate data. Northness and eastness rasters at 30 arcsec resolution were derived from the resampled altitude raster. Then, we fitted the same four statistical algorithms (GAM, ANN, RF, GBM) we employed when interpolating weather station data to the set of centroids of each monthly climate raster, constituting our calibration points. We calibrated each algorithm by replicating the same modeling procedures we followed during the interpolations and using the resampled altitude, northness, eastness, distance to the coast, and monthly average of daily clear-sky insolation time as physiographic descriptors. As with the interpolations, we finally inspected where WorldClim and CHELSA downscalings extrapolated by comparing the training data at the calibration points with the projection data over the study area. By doing so, we obtained 12 surfaces of the Shape extrapolation metric for both WorldClim and CHELSA, one for each month.

Methodological comparison

For each monthly climate dataset, we assessed the quality of the interpolations via leave-one-out cross-validation. Therefore, each weather station was excluded once from the dataset and used as a validation point. The quality of the downscalings was evaluated by calibrating the algorithms on the set of centroids of each monthly climate raster and then cross-validating them on the weather stations' locations. The predictive performance of the techniques was compared by using four validation metrics, namely the Kling-Gupta efficiency (KGE) scores, percent biases (*pbias*), mean absolute errors (MAE), and root-mean-square errors (RMSE). KGE is a composite measure that

simultaneously accounts for correlation, variability errors, and bias errors among observed and predicted data (Gupta et al., 2009) and was calculated as follows:

$$\mathrm{KGE} = 1 - \sqrt{(\rho - 1)^2 + \left(\frac{\sigma_{pred}}{\sigma_{obs}} - 1\right)^2 + \left(\frac{\mu_{pred}}{\mu_{obs}} - 1\right)^2}$$

where ρ is the Pearson correlation coefficient between observed and predicted temperatures, σ_{pred} is the standard deviation of the predicted temperatures, σ_{obs} is the standard deviation of the observed temperatures, μ_{pred} is the mean of the predicted temperatures, and μ_{obs} is the mean of the observed temperatures. A KGE score equal to 1 indicates perfect concordance between observed and predicted temperatures, while KGE scores between 0 and 0.5 indicate poor model performance (Rogelis et al., 2016). We chose percent biases to highlight the propensity for the predicted temperatures to be larger or smaller than those measured by the weather stations. Low *pbias* values reflect accurate model prediction; the optimal *pbias* value is 0. We calculated percent biases as follows:

$$pbias = 100 \times \frac{\sum(t_{obs} - t_{pred})}{\sum t_{obs}}$$

where t_{obs} and t_{pred} are observed and predicted temperatures, respectively. Consequently, underestimation corresponds with positive *pbias* values, whereas overestimation with negative *pbias* values. MAE and RMSE are two commonly used validation metrics, and we calculated them as follows:

$$\mathrm{MAE} = \frac{1}{n}\left(\sum |t_{obs} - t_{pred}|\right) \qquad \mathrm{RMSE} = \sqrt{\frac{1}{n}\left(\sum (t_{obs} - t_{pred})^2\right)}$$

where n (= 33) is the number of weather stations.

The predictions of the interpolations and the downscalings were also compared over the entire study area to highlight in which environmental conditions the techniques diverged the most. Hence, we constructed four monthly climate surfaces per month and technique, one for each algorithm. Then, we averaged the surfaces over the algorithms to obtain a monthly climate surface for each month and each technique. These surfaces were then compared by calculating the pairwise differences and inspecting the spatial distribution of these differences across the territory.

Finally, we assessed the impact of environmental extrapolation on the interpolation and downscaling procedures by comparing the local climate estimates of each pair of techniques at increasing degrees of extrapolation. For each month, we extracted the Shape values for each pair of techniques at 100,000 random locations. Then, we correlated these Shape values with the absolute differences between local climate predictions to check whether a joint increase in the degree of environmental extrapolation would lead to a more significant divergence between pairs of techniques.

Results

Methodological comparison

The imputation procedures reliably filled the missing temperatures (average R^2 = 98.017%; average RMSE = 0.72832 °C). Among the three techniques, interpolating weather station data produced estimates that more closely matched the temperatures measured by the weather stations (Fig. A.4 in Appendices). Downscaling WorldClim produced reliable estimates, although they less closely matched the measured temperatures than those predicted by the interpolations (Fig. A.5 in Appendices). On the contrary, downscaling CHELSA produced over-smoothed underestimates of local monthly climates (Fig. A.6 in Appendices). Interpolating weather station data and downscaling WorldClim yielded similarly high average KGE scores. Nevertheless, WorldClim's average KGE scores were noticeably lower during fall, winter, and early spring (Fig. 2a). Interpolating weather station data and downscaling WorldClim also compared in terms of average *pbias*, although mainly from May to October (hereafter referred to as "hot season") when WorldClim's average *pbias* were only slightly positive. During the cold season, WorldClim's average *pbias* decreased towards negative values, while weather stations' average *pbias* remained close to zero (Fig. 2b). Interpolating weather station data yielded slightly lower values of average MAE and RMSE (Fig. 2c and Fig. 2d). Finally, downscaling CHELSA resulted in significantly lower average KGE scores (Fig. 2a), consistently positive average *pbias* (Fig. 2b), and average MAE and RMSE that almost doubled those we obtained from the interpolations and the WorldClim downscaling (Fig. 2c and Fig. 2d). These shortcomings could be partly attributed to the fact that CHELSA data cover a different period (1985-2000) than WorldClim and weather station data (1970-2000).

Downscaling WorldClim produced smoother and less detailed monthly climate surfaces than interpolating weather station data; this was particularly evident during the cold season (Fig. 3c and Fig. 3e) but remained true during the hot season (Fig. 4c and Fig. 4e). During the cold season, downscaling WorldClim also resulted in lower temperatures in valleys and at low altitudes along the coast (Fig. 3f and Fig. 3g). Temperature differences reversed moving along the slopes, where

downscaling WorldClim yielded higher temperatures compared to weather station interpolation (Fig. 3f and Fig. 3g), thus echoing the lower average *pbias* values that emerged in the pointwise cross-validations. During the hot season, downscaling WorldClim led to higher temperatures near the coast and lower temperatures across most of the study area (Fig. 4f and Fig. 4g) compared to interpolating weather station data; these results were in line with WorldClim downscaling scoring higher average *pbias* values during these months. Throughout the year, weather station interpolation and WorldClim downscaling consistently diverged at higher altitudes: interpolating weather station data yielded higher temperatures that exceeded WorldClim's by > 3 °C during the hot season (Fig. 3f and Fig. 4f). Finally, similarly to how it behaved in the pointwise cross-validations, CHELSA downscaling produced heavily over-smoothed monthly climate surfaces (Fig. 3h and Fig. 4h). Consequently, temperature differences between CHELSA downscaling and the other two techniques closely matched the thermal gradients of the study area both during the cold season (Fig. 3b and Fig. 3d) and the hot season (Fig. 4b and Fig. 4d).

At the 100,000 random locations we sampled each month, downscaling WorldClim and interpolating weather station data yielded similar monthly climate estimates (Fig. A.7 in Appendices). Monthly estimates diverged as the Shape values (i.e., degrees of extrapolation) jointly increased but seldom exceeded 2.5 °C. Divergence was highest during the hot season. Monthly climate estimates were far less similar between weather station interpolation and CHELSA downscaling (Fig. A.8 in Appendices) and between WorldClim and CHELSA downscalings (Fig. A.9 in Appendices). No clear divergence at increasing Shape values could be observed for these two pairs of techniques. Finally, the Shape values of weather station interpolation and WorldClim and CHELSA downscalings only moderately correlated ($R^2 \approx 0.30$; Fig. A.7 and A.8 in Appendices); on the contrary, WorldClim and CHELSA downscalings extrapolated nearly identically ($R^2 \approx 0.80$; Fig. A.9 in Appendices).

Weather station interpolation

During the hot season, KGE scores decreased for all the algorithms except ANN. For most of the year, GBM ranked as the least efficient algorithm. Nevertheless, KGE scores remained high (> 0.80; Fig. A.10a in Appendices). Like KGE scores, MAE and RMSE increased for all the algorithms during the hot season, although both metrics showed limited variability (0.4 - 1.3 °C; Fig. A.10c and Fig. A.10d in Appendices). Percent biases were always remarkably close to zero, with little differences between algorithms **(**Fig. A.10b in Appendices). Altitude was the most relevant physiographic descriptor; however, in all algorithms but ANN, its relative importance decreased during the hot

season. In these same months, the relative importance of the remaining descriptors generally increased (Fig. A.11 in Appendices).

Principal component analysis indicated that weather stations sampled moderate amounts of landscape complexity: the study area's distributions of PCA scores and the sampling distributions of the weather stations mostly overlapped, especially along the first two PCs, which accounted for about 55% of the total variance (Table A.2 and Fig. A.14 in Appendices). Most of the unexplained variance, and thus the environmental extrapolation, involved the innermost regions of the study area, which are those at higher altitudes and more heterogeneous topographically. This pattern was especially evident during the cold season but remained consistent throughout the year (Fig. A.15 in Appendices).

WorldClim and CHELSA downscaling

KGE scores did not follow any seasonal trend for WorldClim (Fig. A.10e in Appendices) or CHELSA (Fig. A.10i in Appendices). However, while WorldClim's KGE scores were consistently high (> 0.80), CHELSA's KGE scores indicated poor model performance (< 0.50) all year round and across all algorithms. WorldClim's percent biases were slightly positive during the hot season and negative for the remaining year. In this respect, all the algorithms behaved homogeneously (Fig. A.10f in Appendices). The algorithms behaved homogeneously for CHELSA, too, but always showed significantly positive percent biases (Fig. A.10j in Appendices). Like weather stations, WorldClim's MAE and RMSE increased during the hot season (Fig. A.10g and Fig. A.10h in Appendices). We did not observe this same increase when downscaling CHELSA (Fig. A.10k and Fig. A.10l in Appendices). Altitude was also the most relevant physiographic descriptor for WorldClim and CHELSA downscalings. Contrary to weather station interpolation, its relative importance decreased moderately during the hot season, especially for WorldClim's GAMs and CHELSA's GAMs and RFs. When downscaling macroclimate grids, the relative importance of some other descriptors showed seasonal variation, too, albeit to a far lesser extent than for weather station interpolation. In particular, distance to the coast was the only descriptor whose importance increased when downscaling WorldClim during the hot season; for CHELSA downscaling, the importance of distance to the coast and insolation time displayed reversed seasonal patterns compared to the other techniques, decreasing during the hot season. No seasonal patterns could be observed for WorldClim's and CHELSA's ANNs, as the behavior of these algorithms was remarkably unstable (Fig. A.12 and Fig. A.13 in Appendices).

Compared to the interpolations, WorldClim and CHELSA downscalings extrapolated more diffusely: except for the northwestern lowland region, extrapolation covered the study area almost homogeneously. It also followed no clear seasonal patterns (Fig. A.16 and Fig. A.17 in Appendices).

Discussion

In this study, we aimed to assess how interpolation and downscaling techniques compare in predicting local monthly climates in highly heterogeneous mountain ranges. We interpolated weather station data and downscaled two of the most widely used macroclimate grids – WorldClim and CHELSA – to check if the data source could affect the downscaling performance. Although it was impossible to directly validate the techniques against observed climates over the entire study area, approaching the comparison from different angles allowed us to draw several valuable insights.

Do interpolating weather station data and downscaling macroclimate grids compare in heterogeneous mountain ranges?

Firstly, we compared the interpolation and downscaling techniques by validating them on the only available observed climates, namely the weather stations' measurements. In this context, the interpolation of weather station data ranked as the best-performing technique across all validation metrics (Fig. 2). WorldClim downscaling closely followed, scoring RMSE/MAE values only slightly higher (~ 0.15 °C; Fig. 2c and Fig. 2d) than the interpolations. Downscaling WorldClim also yielded KGE values that rivaled those obtained when interpolating weather station data (Fig. 2a). However, the marginally superior performance of the interpolations should be taken with due caution. Despite capturing good shares of landscape complexity (Table A.2 and Fig. A.14 in Appendices), the weather stations we employed cannot be considered fully independent as they left the most internal and heterogeneous regions above 1250 m asl uncovered. Performing leave-one-out cross-validation in such areas would likely have worsened the interpolations' performance. So, it might be fair to say that interpolating weather station data and downscaling WorldClim emerged, concerning this initial pointwise comparison, as essentially equivalent.

Were then interpolating weather station data and downscaling WorldClim also equivalent over the territory? Here, the answer gets more nuanced. On the one hand, the two techniques produced monthly climate surfaces that were remarkably close, rarely differing by > 2 °C (Fig. 3 and Fig. 4). They demonstrated they were jointly robust against environmental extrapolation since their temperature estimates remained coherent as the algorithms increasingly extrapolated (Fig. A.7 in Appendices). Interpolations and WorldClim downscaling correctly identified altitude as the most

relevant physiographic descriptor (Fig. A.11 and Fig. A.12 in Appendices); at such a high spatial resolution (10 m), we indeed expected the temperature lapse rate to be the predominant driver of local climatic conditions (Joly et al., 2018). More interestingly, both techniques detected decreases in altitude's relative importance during the hot season. They also exhibited more divergent monthly climates during this season (Fig. A.7 in Appendices), lower KGE scores (Fig. 2a), and higher RMSE/MAE values (Fig. 2c and Fig. 2d). These results indicate increased spatial variability in local climates, a phenomenon witnessed in many other geographical contexts (Jones & Briffa, 1992; Caesar et al., 2006; Srivastava et al., 2009; Hopkinson et al., 2012). The reasons for this could be topographical. The proximity of the Aspromonte relief to the sea might affect cloud formation, thereby promoting uneven cloud cover patterns that might induce maximum temperatures to vary more during summer. This phenomenon has, for example, been observed in the Iberian Peninsula (Pena-Angulo et al., 2015). Also, increased evaporation during summer might bolster the formation of precipitation along windward slopes, further enhancing spatial variability in local climates by modifying latent heat fluxes (Martin-Vide, 2004). So, regardless of the reasons explaining them, these shared patterns provided evidence that interpolating weather station data and downscaling WorldClim behaved similarly also over the study area.

On the other hand, the two techniques differed in several crucial aspects. One of the study's premises was that downscaling techniques could have difficulties capturing climate variability in topographically complex landscapes. Our results confirm that these techniques can struggle to account for topographic effects. Indeed, downscaling WorldClim yielded monthly climate surfaces that were smoother than those obtained from the interpolations (Fig. 3 and Fig. 4). Compared to weather station interpolation, this technique also produced consistent underestimates across most of the study area and overestimates along the coast during the hot season (Fig. 4), as well as underestimates in valleys and overestimates along slopes during the cold season (Fig. 3). Importantly, these biases were reflected by the cross-validations, too, namely by consistently negative average *pbias* values (i.e., underestimation) during the hot season and positive average *pbias* values (i.e., overestimation) during the cold season (Fig. 2a). That downscaling techniques could have encountered some difficulties was anticipated. As mentioned, downscaling macroclimate grids cannot catch climate-forcing effects not initially present in the coarse-scale products (Lembrechts et al., 2019). WorldClim's grid values, for instance, are initially derived by interpolating weather station measurements with the help of altitude and distance to the coast as topographical predictors (Fick & Hijmans, 2017); interestingly, these two descriptors were the only relevant ones for this technique (Fig. A.12 in Appendices). In this respect, our results underline that these difficulties can have

practical impacts in highly heterogeneous mountain ranges, introducing biases in local climate estimates and leading to an overall loss of topographical detail.

Despite producing the most detailed and accurate temperature predictions (Fig. A.4 in Appendices), interpolating weather station data also had its share of difficulties. This technique, as expected, extrapolated in the most challenging regions of the study area from a topographical standpoint, namely the innermost high-altitude landscapes (Fig. A.15 in Appendices). While it was impossible to quantify its impact against observed climates directly, such extrapolation affected the technique's performance. Indeed, weather station interpolation produced monthly climates that were several degrees (up to > 3 °C during the hot season; Fig. 4) warmer than those from WorldClim downscaling. Weather stations are not new to this problem; temperature overestimation in high-altitude environments has been witnessed several times (Daly et al., 1994; Bolstad et al., 1998). One possible solution could be limiting the predictors' interactions and the flexibility of their response curves when calibrating the algorithms to prevent them from predicting unrealistic climates in the extrapolations. However, a price for doing this might be paid when trying to keep up with topographic heterogeneity. Too rigid model parameterizations could fail to encompass the locality and complexity of climate-forcing in heterogeneous mountainous landscapes. Temperature lapse rates are notoriously variable in these environments due to local phenomena such as cold-air pools and other topographically induced thermal inversions (Gudiksen et al., 1992; Whiteman et al., 2001). Correctly modeling these lapse rates is critical, as altitude was found to be the most important variable for all the techniques, although less predominantly for the interpolation of weather stations (Fig. A.11, A.12, and A.13 in Appendices). Also, wind fields are affected by the position and topographic conformation of the mountain reliefs, leading to local phenomena like foehn effects that further complicate the thermal gradients of these regions (Dreschel & Mayr, 2008; Ha et al., 2009; Dujardin & Lehning, 2022).

Finally, cross-validations and pairwise spatial comparisons showed that downscaling CHELSA led to over-smoothed and biased temperature estimates. Positive average *pbias* values (Fig. 2b) indicated that the technique systematically underestimated local climates at the weather stations' locations, KGE scores (Fig. 2a) and RMSE/MAE values (Fig. 2c and Fig. 2d) never compared with those of the other two techniques, and monthly climate surfaces displayed severely limited spatial climate variability (Fig. 3 and Fig. 4). We expected that CHELSA, relying on more refined routines integrating small-scale orographic effects, would perform better in highly heterogeneous mountain ranges than WorldClim; instead, it produced monthly climate surfaces that came to differ by > 5 °C from the interpolations and WorldClim downscaling. Most of CHELSA's poor performance results

from a lack of spatial climate variability in the native CHELSA product itself. Indeed, when we compared the empirical temperature lapse rates for the native CHELSA and WorldClim products in January and July, we witnessed much lower temperature range between maxima in lowlands and minima at higher altitudes in CHELSA compared to WorldClim (Fig. A.18 in Appendices). These results were echoed by CHELSA's over-smoothed monthly climate surfaces for both January (Fig. 3h) and July (Fig. 4h). As mentioned earlier, the quality of the downscaling predictions is clearly limited by the quality of the native coarse-grained product. Lembrechts et al. (2019) incurred a similar limitation when they employed CHELSA bioclimatic variables at native (30 arcsecs) and downscaled (30 m) resolutions to model the distribution of 50 plant species, albeit to a far lesser degree. Although they obtained comparable performance between SDMs calibrated with CHELSA and with the topoclimatic interpolation of weather station data from Aalto et al. (2017), they nonetheless gained no substantial benefit from downscaling CHELSA compared to using its coarse-grained version. It is finally worth recalling that CHELSA data covering a different period (1985-2000) than WorldClim and the weather stations (1970-2000) could contribute to CHELSA's lacking performance.

What could be the implications for species conservation under climate change?

Topographically complex territories constitute decisive cornerstones for species conservation under climate change. They house significant variation in microclimatic conditions, which provides microrefugia for vulnerable species to endure warming. Topographically complex territories exhibit greater stability in natural populations, as observed in the case of various British butterfly species (Oliver et al., 2010). Suggitt et al. (2018) showed that, after accounting for anthropogenic pressure, several climate-threatened species across England, including vascular plants, bryophytes, lepidopterans, and coleopterans, have suffered lower population losses in areas exhibiting higher topographic heterogeneity in recent decades. Therefore, failing to account for local topographic effects hinders our ability to locate microrefugia crucial to population survival. For instance, incorporating topographic heterogeneity into SDMs also substantially increased the projected persistence of European tree species (Randin et al., 2009). Similarly, disregarding topographic heterogeneity inflated the projection of future butterfly species losses in mountainous regions (Luoto & Heikkinen, 2008). Finally, including topographically-induced temperature spatial variability improved niche estimates in SDMs calibrated over topographically heterogeneous regions (Karger et al., 2023).

This study compared interpolation and downscaling techniques by predicting monthly average temperatures. However, minima and maxima are equally, if not more, relevant in shaping the niche

of many organisms; weather and climate extremes also contribute to setting the bounds of organisms' range limits (Ummenhofer & Meehl, 2017; Germain & Lutz, 2020). Understanding which techniques to downscale these additional climates with would further boost our modeling capabilities. Due to their complex fine-scale topographic effects, this is especially true for topographically heterogeneous mountain landscapes (Barry & Blanken, 2016).

In vegetated areas with complex topographies, topography interacts with soil characteristics and vegetation structure to generate mosaics of even smaller-scale microclimates. These interactions can take particularly complex forms and delimit the thermal niches most organisms inhabiting forests or other vegetated areas experience (Geiger et al., 2009; Rita et al., 2021). Microclimates can substantially differ from free-air local climates (Barry & Blanken, 2016); as such, interpolations and downscalings like ours failed to capture microclimatic variation at ground level on several occasions (Slavich et al., 2014; Lembrechts et al., 2019). Mapping microclimates is, in fact, the prerogative of specific statistical routines that range from the interpolation of in-situ microclimate measurements (Vanwalleghem & Meentemeyer, 2009; Ashcroft & Gollan, 2012) to the mechanistic modeling of near-the-ground microclimates (Kearney & Porter, 2017; Maclean & Klinges, 2021). As mentioned, some routines require local climates to be estimated before mapping microclimates, which are later derived by modeling the offset between local climates and microclimates directly (Lenoir et al., 2017; Maclean et al., 2019) or by leveraging available maps of temperature offsets like ForestTemp (Haesen et al., 2021). As forest covers will enhance local buffering from future macroclimate warming (De Lombaerde et al., 2022), how to best map forest microclimates is increasingly studied (Zellweger et al., 2019; Maclean et al., 2021). Although deriving local climatic conditions through interpolations and downscalings is often not enough, our results suggest that this step should not be overlooked; indeed, choosing the most suitable technique might significantly improve the temperature estimates and thus prevent statistical uncertainty from propagating down the prediction process.

Conclusions

High topographic heterogeneity severely challenges our attempts to derive high-resolution local climate surfaces. In this respect, are interpolation and downscaling techniques equally performant? Interpolating weather station data managed to capture the fine-scale variability in local climatic conditions; downscaling macroclimatic grids, on the contrary, provided biased and less detailed monthly climate surfaces. Downscaling performance was also found to heavily depend on the choice of the macroclimate grid since downscaling WorldClim yielded far better temperature estimates than CHELSA. Instead, which algorithm to operate with had a lower impact on the accuracy of the

predictions. Given how critical accounting for fine-scale climatic variability is for reliable niche modeling, our study suggests that interpolating weather station data might have the edge over downscaling macroclimate grids in topographically heterogeneous landscapes. However, its advantage was not clear-cut; interpolations suffered from environmental extrapolation in the highest and most heterogeneous landscapes. It is riveting to note how even our simple comparative study elicited far-from-trivial considerations. After all, the stakes are very high: identifying and protecting microrefugia directly depends on us being able to portray the mosaic of fine-grain climatic conditions that topography, vegetation, and soil collectively contribute to creating. In topographically heterogeneous landscapes, such as the Aspromonte mountain range, biodiversity at all levels of organization manages to flourish precisely due to the complexity of these climatic mosaics. Thus, understanding the relationships that natural populations establish with the landscape requires us to carefully select the statistical techniques at our disposal. Only by doing so can we protect those microrefugia that may allow vulnerable mountain communities to endure future climate change.

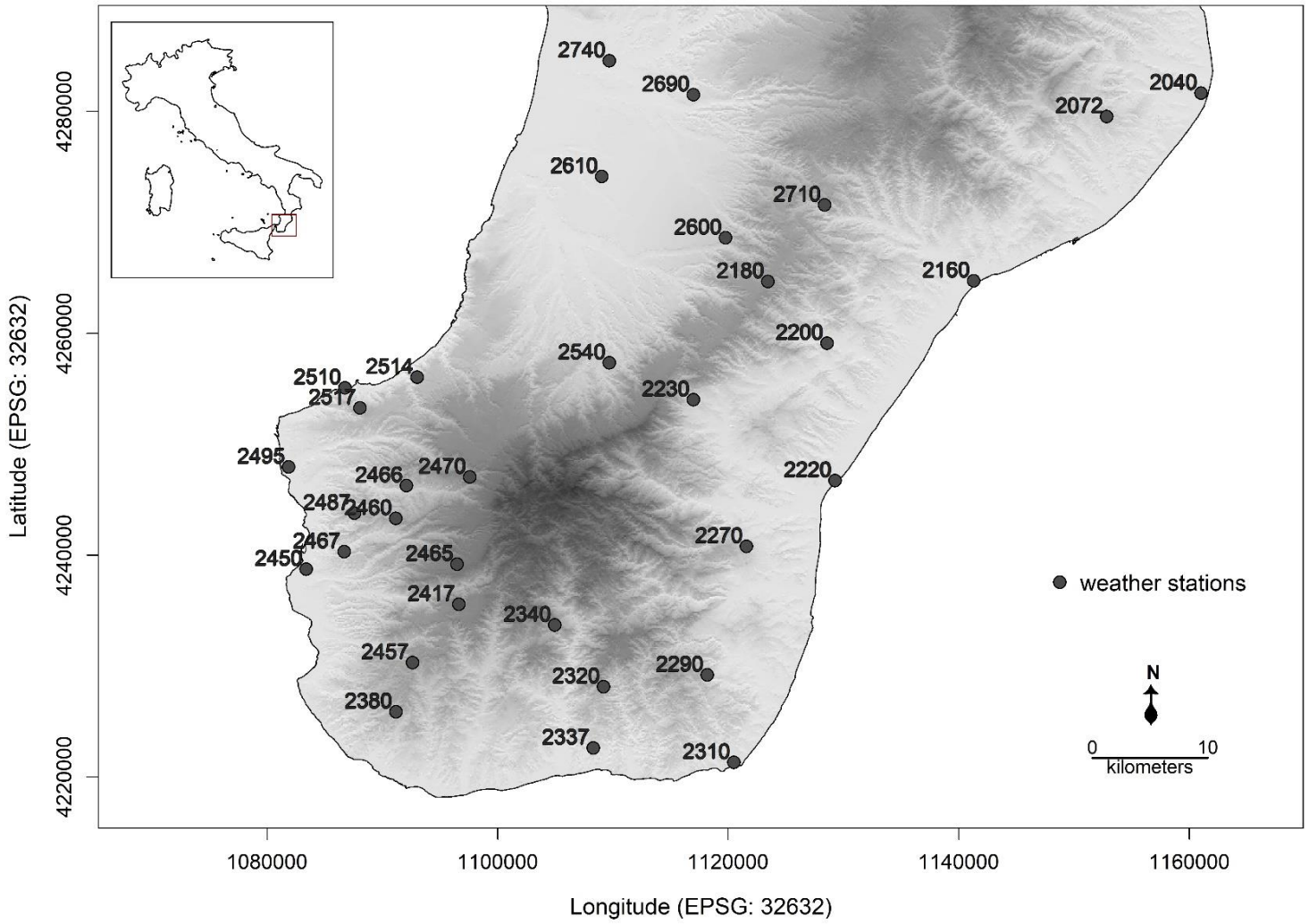

Figure 1. Locations of the weather stations employed in the present study. We indicated the weather station's ID above each location. The inset displays the borders of the Italian peninsula, with those of the study area highlighted in red.

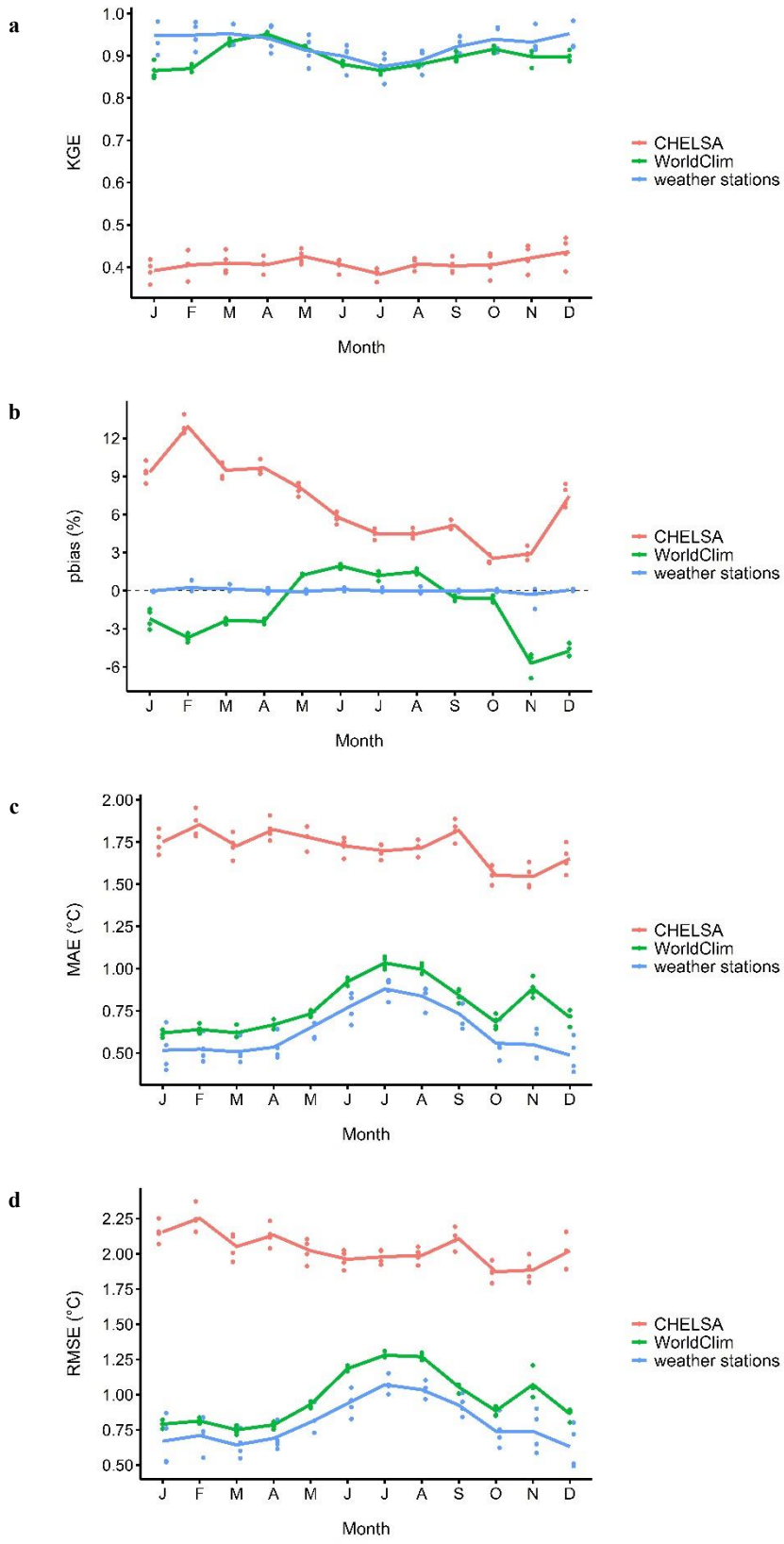

Figure 2. Seasonal patterns in average KGE scores **(a)**, *pbias* **(b)**, MAE **(c)**, and RMSE **(d)** that we obtained when predicting monthly average temperatures using each technique. Lines and points represent average scores and those obtained by each algorithm, respectively.

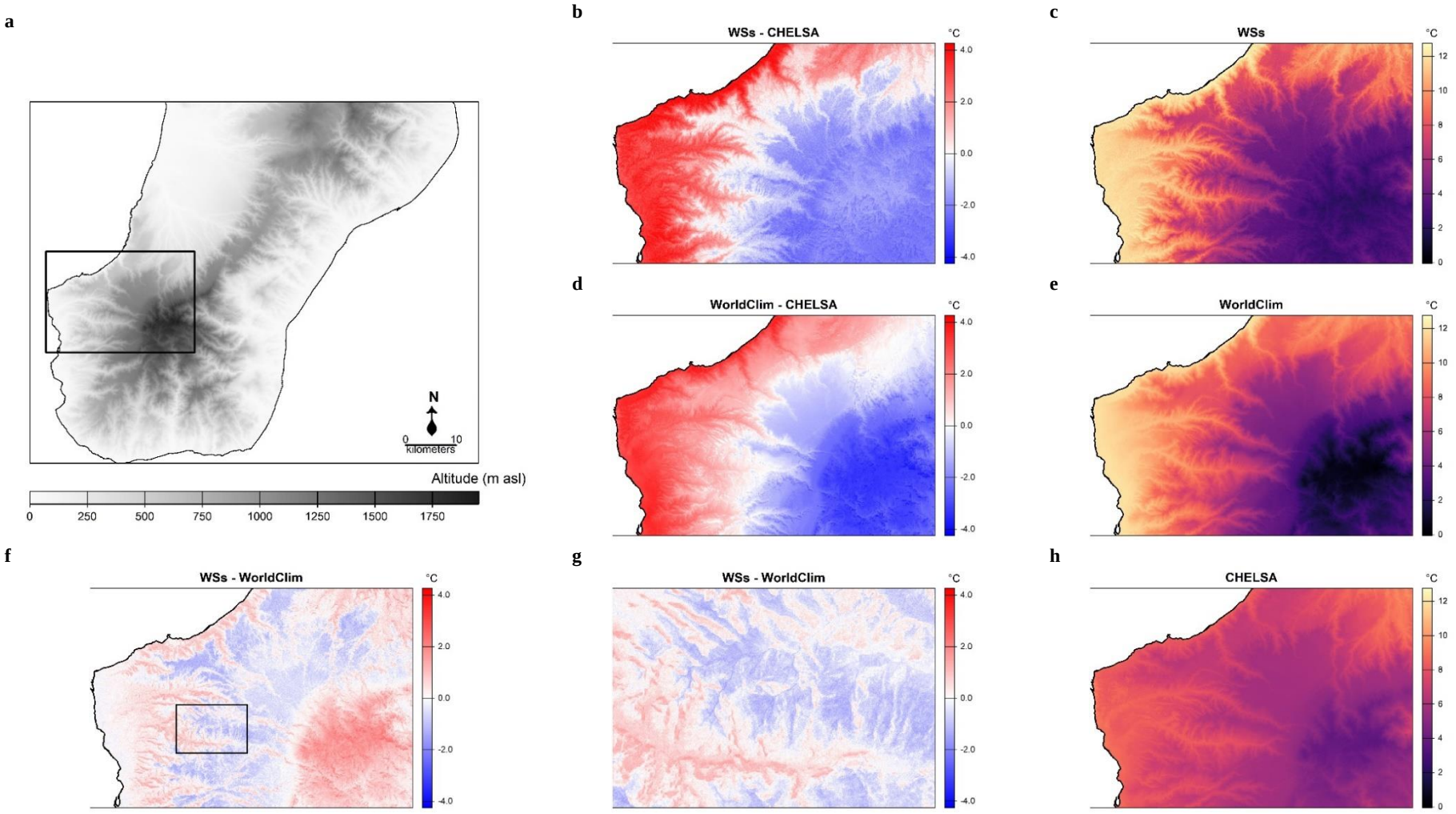

Figure 3. Average January temperatures predicted by interpolating weather station (WS) data and downscaling WorldClim and CHELSA. The contours of the geographical area used for comparison are shown in subplot **(a)**. Subplots **(b)**, **(d)**, and **(f)** display the differences between the temperature surfaces of WSs interpolation and WorldClim downscaling, WSs interpolation and CHELSA downscaling, and WorldClim and CHELSA downscaling, respectively. Subplots **(c)**, **(e)**, and **(h)** display the temperature surfaces predicted by WSs interpolation and WorldClim and CHELSA downscaling, respectively. Subplot **(g)** shows the details of the area contoured in subplot **(f)**.

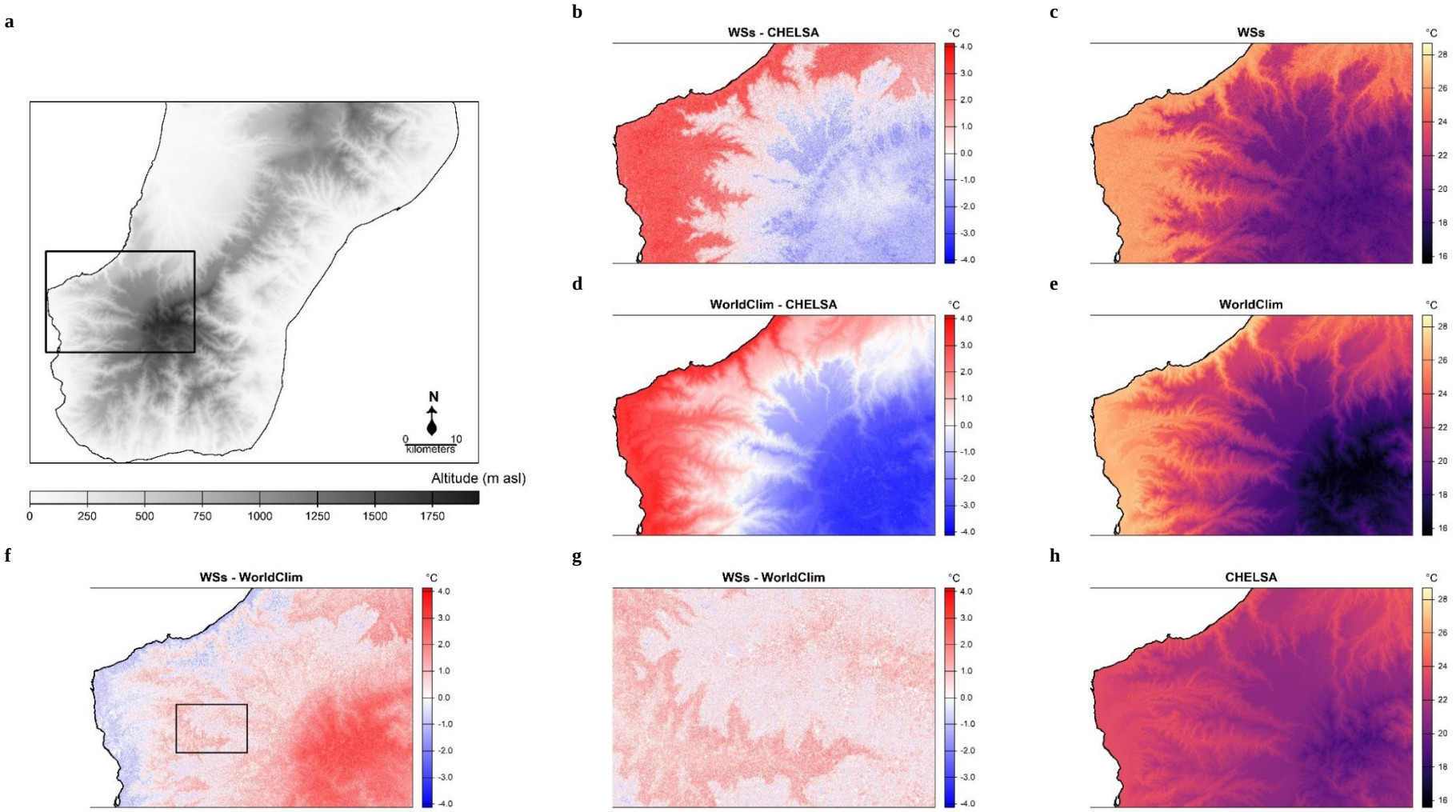

Figure 4. Average July temperatures predicted by interpolating weather station (WS) data and downscaling WorldClim and CHELSA. The contours of the geographical area used for comparison are shown in subplot **(a)**. Subplots **(b)**, **(d)**, and **(f)** display the differences between the temperature surfaces of WSs interpolation and WorldClim downscaling, WSs interpolation and CHELSA downscaling, and WorldClim and CHELSA downscaling, respectively. Subplots **(c)**, **(e)**, and **(h)** display the temperature surfaces predicted by WSs interpolation and WorldClim and CHELSA downscaling, respectively. Subplot **(g)** shows the details of the area contoured in subplot **(f)**.

Authors contributions

Daniele Delle Monache: Data Curation, Investigation, Methodology, Software, Visualization, Writing - Original Draft. **Giuseppe Martino**: Data Curation, Writing - Review & Editing. **Andrea Chiocchio**: Investigation, Supervision, Writing - Review & Editing. **Antonino Siclari**: Funding acquisition, Writing - Review & Editing. **Roberta Bisconti**: Visualization, Writing - Review & Editing. **Luigi Maiorano**: Methodology, Supervision, Validation, Visualization, Writing - Review & Editing. **Daniele Canestrelli**: Conceptualization, Funding acquisition, Supervision, Validation, Writing - Review & Editing.

Acknowledgments

This study is dedicated to the memory of Sergio Tralongo, who supported this research as past director of the Aspromonte National Park.

Funding sources

This work was funded by the Tuscia University and the Aspromonte National Park. Research project implemented under the National Recovery and Resilience Plan (NRRP), Mission 4 Component 2 Investment 1.4 - Call for tender No. 3138 of 16 December 2021, rectified by Decree n.3175 of 18 December 2021 of Italian Ministry of University and Research funded by the European Union - Next Generation EU. Project code CN_00000033, Concession Decree No. 1034 of 17 June 2022 adopted by the Italian Ministry of University and Research, CUP J83C22000860007, Project title “National Biodiversity Future Center - NBFC”, and under the National Recovery and Resilience Plan (NRRP), Mission 4 Component 2 Investment 1.5, funded by the European Union - Next Generation EU, Project code ECS 0000024 Rome Technopole, CUP B83C22002820006.

Data statement

Climate data can be downloaded from the website of the regional environmental agency for Calabria (http://www.arpacal.it/) and from the WorldClim (https://www.worldclim.org/) and CHELSA (https://chelsa-climate.org/) websites.

References

Aalto, J., Riihimäki, H., Meineri, E., Hylander, K., & Luoto, M. (2017). Revealing topoclimatic heterogeneity using meteorological station data. *International Journal of Climatology*, *37*, 544–556.

Ashcroft, M. B. (2010). Identifying refugia from climate change. *Journal of Biogeography*, *37*(8), 1407–1413.

Ashcroft, M. B., & Gollan, J. R. (2012). Fine-resolution (25 m) topoclimatic grids of near-surface (5 cm) extreme temperatures and humidities across various habitats in a large (200× 300 km) and diverse region. *International Journal of Climatology*, *32*(14), 2134–2148.

Barry, R. G., & Blanken, P. D. (2016). *Microclimate and local climate*. Cambridge University Press.

Beck, M. W. (2018). NeuralNetTools: Visualization and analysis tools for neural networks. *Journal of Statistical Software*, *85*(11), 1.

Bolstad, P. V., Swift, L., Collins, F., & Régnière, J. (1998). Measured and predicted air temperatures at basin to regional scales in the southern Appalachian mountains. *Agricultural and Forest Meteorology*, *91*(3-4), 161–176.

Brullo, S., Scelsi, F., & Spampinato, G. (2001). *La Vegetazione dell'Aspromonte. Studio fitosociologico*. Laruffa editore. Reggio Calabria.

Caesar, J., Alexander, L., & Vose, R. (2006). Large-scale changes in observed daily maximum and minimum temperatures: Creation and analysis of a new gridded data set. *Journal of Geophysical Research: Atmospheres*, *111*(D5).

Camacho-Sanchez, M., Quintanilla, I., Hawkins, M. T., Tuh, F. Y., Wells, K., Maldonado, J. E., & Leonard, J. A. (2018). Interglacial refugia on tropical mountains: novel insights from the summit rat (*Rattus baluensis*), a Borneo mountain endemic. *Diversity and Distributions*, *24*(9), 1252–1266.

Canestrelli, D., Bisconti, R., Chiocchio, A., Maiorano, L., Zampiglia, M., & Nascetti, G. (2017). Climate change promotes hybridisation between deeply divergent species. *PeerJ*, *5*, e3072.

Chen, I. C., Hill, J. K., Ohlemüller, R., Roy, D. B., & Thomas, C. D. (2011). Rapid range shifts of species associated with high levels of climate warming. *Science*, *333*(6045), 1024–1026.

Chiocchio, A., Maiorano, L., Pezzarossa, A., Bisconti, R., & Canestrelli, D. (2024). From the mountains to the sea: Rethinking Mediterranean glacial refugia as dynamic entities. *Journal of Biogeography*, *51*(5), 956–967.

Colacino, M., Conte, M., & Piervitali, E. (1997). Elementi di climatologia della Calabria. *IFA-CNR, Rome*.

Daly, C., Neilson, R. P., & Phillips, D. L. (1994). A statistical-topographic model for mapping climatological precipitation over mountainous terrain. *Journal of Applied Meteorology and Climatology*, *33*(2), 140–158.

De Lombaerde, E., Vangansbeke, P., Lenoir, J., Van Meerbeek, K., Lembrechts, J., Rodríguez-Sánchez, F., ... & De Frenne, P. (2022). Maintaining forest cover to enhance temperature buffering under future climate change. *Science of the Total Environment*, *810*, 151338.

Dobrowski, S. Z. (2011). A climatic basis for microrefugia: the influence of terrain on climate. *Global Change Biology*, *17*(2), 1022–1035.

Drechsel, S., & Mayr, G. J. (2008). Objective forecasting of foehn winds for a subgrid-scale Alpine valley. *Weather and Forecasting*, *23*(2), 205–218.

Dujardin, J., & Lehning, M. (2022). Wind-Topo: Downscaling near-surface wind fields to high-resolution topography in highly complex terrain with deep learning. *Quarterly Journal of the Royal Meteorological Society*, *148*(744), 1368–1388.

Elith, J., & Leathwick, J. R. (2009). Species distribution models: ecological explanation and prediction across space and time. *Annual Review of Ecology, Evolution and Systematics*, *40*(1), 677–697.

Fick, S. E., & Hijmans, R. J. (2017). WorldClim 2: new 1-km spatial resolution climate surfaces for global land areas. *International Journal of Climatology*, *37*(12), 4302–4315.

Frey, S. J., Hadley, A. S., Johnson, S. L., Schulze, M., Jones, J. A., & Betts, M. G. (2016). Spatial models reveal the microclimatic buffering capacity of old-growth forests. *Science Advances*, *2*(4), e1501392.

Fridley, J. D. (2009). Downscaling climate over complex terrain: high finescale (< 1000 m) spatial variation of near-ground temperatures in a montane forested landscape (Great Smoky Mountains). *Journal of Applied Meteorology and Climatology*, *48*(5), 1033–1049.

Geiger, R., Aron, R. H., & Todhunter, P. (2009). *The climate near the ground*. Rowman & Littlefield.

Germain, S. J., & Lutz, J. A. (2020). Climate extremes may be more important than climate means when predicting species range shifts. *Climatic Change*, *163*(1), 579–598.

Greenwell, B., Boehmke, B., Cunningham, J., & GBM Developers (2020). gbm: Generalized Boosted Regression Models. *R package version 2.1.8*.

Gudiksen, P. H., Leone, J. M., King, C. W., Ruffieux, D., & Neff, W. D. (1992). Measurements and modeling of the effects of ambient meteorology on nocturnal drainage flows. *Journal of Applied Meteorology and Climatology*, *31*(9), 1023–1032.

Guisan, A., & Zimmermann, N. E. (2000). Predictive habitat distribution models in ecology. *Ecological Modelling*, *135*(2-3), 147–186.

Gupta, H. V., Kling, H., Yilmaz, K. K., & Martinez, G. F. (2009). Decomposition of the mean squared error and NSE performance criteria: Implications for improving hydrological modelling. *Journal of Hydrology*, *377*(1-2), 80–91.

Ha, K. J., Shin, S. H., & Mahrt, L. (2009). Spatial variation of the regional wind field with land–sea contrasts and complex topography. *Journal of Applied Meteorology and Climatology*, *48*(9), 1929–1939.

Haesen, S., Lembrechts, J. J., De Frenne, P., Lenoir, J., Aalto, J., Ashcroft, M. B., ... & Van Meerbeek, K. (2021). ForestTemp–Sub-canopy microclimate temperatures of European forests. *Global Change Biology*, *27*(23), 6307–6319.

Hampe, A., & Jump, A. S. (2011). Climate relicts: past, present, future. *Annual Review of Ecology, Evolution, and Systematics*, *42*, 313–333.

Hopkinson, R. F., Hutchinson, M. F., McKenney, D. W., Milewska, E. J., & Papadopol, P. (2012). Optimizing input data for gridding climate normals for Canada. *Journal of Applied Meteorology and Climatology*, *51*(8), 1508–1518.

Hopper, S. D. (2009). OCBIL theory: towards an integrated understanding of the evolution, ecology and conservation of biodiversity on old, climatically buffered, infertile landscapes. *Plant and Soil*, *322*(1), 49–86.

Honaker, J., King, G., & Blackwell, M. (2011). Amelia II: A program for missing data. *Journal of Statistical Software*, *45*, 1–47.

Joly, D., Castel, T., Pohl, B., & Richard, Y. (2018). Influence of spatial information resolution on the relation between elevation and temperature. *International Journal of Climatology*, *38*(15), 5677–5688.

Jones, P. D., & Briffa, K. R. (1992). Global surface air temperature variations during the twentieth century: Part 1, spatial, temporal and seasonal details. *The Holocene*, *2*(2), 165–179.

Karger, D. N., Saladin, B., Wüest, R. O., Graham, C. H., Zurell, D., Mo, L., & Zimmermann, N. E. (2023). Interannual climate variability improves niche estimates for ectothermic but not endothermic species. *Scientific Reports*, *13*(1), 12538.

Karger, D. N., Conrad, O., Böhner, J., Kawohl, T., Kreft, H., Soria-Auza, R. W., ... & Kessler, M. (2017). Climatologies at high resolution for the Earth's land surface areas. *Scientific Data*, *4*(1), 1–20.

Kearney, M. R., & Porter, W. P. (2017). NicheMapR – an R package for biophysical modelling: the microclimate model. *Ecography*, *40*(5), 664–674.

Lembrechts, J. J., Lenoir, J., Roth, N., Hattab, T., Milbau, A., Haider, S., ... & Nijs, I. (2019). Comparing temperature data sources for use in species distribution models: From in-situ logging to remote sensing. *Global Ecology and Biogeography*, *28*(11), 1578–1596.

Lenoir, J., Graae, B. J., Aarrestad, P. A., Alsos, I. G., Armbruster, W. S., Austrheim, G., ... & Svenning, J. C. (2013). Local temperatures inferred from plant communities suggest strong spatial buffering of climate warming across Northern Europe. *Global Change Biology*, *19*(5), 1470–1481.

Lenoir, J., Hattab, T., & Pierre, G. (2017). Climatic microrefugia under anthropogenic climate change: implications for species redistribution. *Ecography*, *40*(2), 253–266.

Liaw, A., & Wiener, M. (2002). Classification and regression by randomForest. *R news*, *2*(3), 18–22.

Lookingbill, T. R., & Urban, D. L. (2003). Spatial estimation of air temperature differences for landscape-scale studies in montane environments. *Agricultural and Forest Meteorology*, *114*(3-4), 141–151.

Luoto, M., & Heikkinen, R. K. (2008). Disregarding topographical heterogeneity biases species turnover assessments based on bioclimatic models. *Global Change Biology*, *14*(3), 483–494.

Maclean, I. M., & Klinges, D. H. (2021). Microclimc: A mechanistic model of above, below and within-canopy microclimate. *Ecological Modelling*, *451*, 109567.

Maclean, I. M., Mosedale, J. R., & Bennie, J. J. (2019). Microclima: An r package for modelling meso-and microclimate. *Methods in Ecology and Evolution*, *10*(2), 280–290.

Martino, G., Chiocchio, A., Siclari, A., & Canestrelli, D. (2022). Distribution and conservation status of threatened endemic amphibians within the Aspromonte mountain region, a hotspot of Mediterranean biodiversity. *Nature Conservation*, *50*, 1–22.

Martin-Vide, J. (2004). Spatial distribution of a daily precipitation concentration index in peninsular Spain. *International Journal of Climatology: A Journal of the Royal Meteorological Society*, *24*(8), 959–971.

McCullough, I. M., Davis, F. W., Dingman, J. R., Flint, L. E., Flint, A. L., Serra-Diaz, J. M., ... & Franklin, J. (2016). High and dry: high elevations disproportionately exposed to regional climate change in Mediterranean-climate landscapes. *Landscape Ecology*, *31*(5), 1063–1075.

Meineri, E., & Hylander, K. (2017). Fine-grain, large-domain climate models based on climate station and comprehensive topographic information improve microrefugia detection. *Ecography*, *40*(8), 1003–1013.

Milling, C. R., Rachlow, J. L., Olsoy, P. J., Chappell, M. A., Johnson, T. R., Forbey, J. S., ... & Thornton, D. H. (2018). Habitat structure modifies microclimate: An approach for mapping fine-scale thermal refuge. *Methods in Ecology and Evolution*, *9*(6), 1648–1657.

Olden, J. D., Joy, M. K., & Death, R. G. (2004). An accurate comparison of methods for quantifying variable importance in artificial neural networks using simulated data. *Ecological Modelling*, *178*(3-4), 389–397.

Oliver, T., Roy, D. B., Hill, J. K., Brereton, T., & Thomas, C. D. (2010). Heterogeneous landscapes promote population stability. *Ecology Letters*, *13*(4), 473–484.

Parmesan, C. (2006). Ecological and evolutionary responses to recent climate change. *Annual Review of Ecology, Evolution, and Systematics*, 637–669.

Parmesan, C., & Yohe, G. (2003). A globally coherent fingerprint of climate change impacts across natural systems. *Nature*, *421*(6918), 37–42.

Pastore, M., Di Loro, P. A., Mingione, M., & Calcagni, A. (2022). overlapping: Estimation of overlapping in empirical distributions. *R package version 2.1*.

Pena-Angulo, D., Cortesi, N., Brunetti, M., & González-Hidalgo, J. C. (2015). Spatial variability of maximum and minimum monthly temperature in Spain during 1981–2010 evaluated by correlation decay distance (CDD). *Theoretical and Applied Climatology*, *122*(1), 35–45.

Pepin, N., Bradley, R. S., Diaz, H. F., Baraër, M., Caceres, E. B., Forsythe, N., ... & Mountain Research Initiative EDW Working Group. (2015). Elevation-dependent warming in mountain regions of the world. *Nature Climate Change*, *5*(5), 424–430.

Phillips, D. L., Dolph, J., & Marks, D. (1992). A comparison of geostatistical procedures for spatial analysis of precipitation in mountainous terrain. *Agricultural and Forest Meteorology*, *58*(1-2), 119–141.

Potter, K. A., Arthur Woods, H., & Pincebourde, S. (2013). Microclimatic challenges in global change biology. *Global Change Biology*, *19*(10), 2932–2939.

Randin, C. F., Engler, R., Normand, S., Zappa, M., Zimmermann, N. E., Pearman, P. B., ... & Guisan, A. (2009). Climate change and plant distribution: local models predict high-elevation persistence. *Global Change Biology*, *15*(6), 1557–1569.

R Core Team (2022). R: A language and environment for statistical computing. R Foundation for Statistical Computing, Vienna, Austria.

Rita, A., Bonanomi, G., Allevato, E., Borghetti, M., Cesarano, G., Mogavero, V., ... & Saracino, A. (2021). Topography modulates near-ground microclimate in the Mediterranean *Fagus sylvatica* treeline. *Scientific Reports*, *11*(1), 8122.

Rogelis, M. C., Werner, M., Obregón, N., & Wright, N. (2016). Hydrological model assessment for flood early warning in a tropical high mountain basin. *Hydrology and Earth System Sciences Discussions*, 1–36.

Rosenzweig, C., Karoly, D., Vicarelli, M., Neofotis, P., Wu, Q., Casassa, G., ... & Imeson, A. (2008). Attributing physical and biological impacts to anthropogenic climate change. *Nature*, *453*(7193), 353–357.

Rull, V. (2009). Microrefugia. *Journal of Biogeography*, *36*(3), 481–484.

Sandel, B., Arge, L., Dalsgaard, B., Davies, R. G., Gaston, K. J., Sutherland, W. J., & Svenning, J. C. (2011). The influence of Late Quaternary climate-change velocity on species endemism. *Science*, *334*(6056), 660–664.

Scherrer, D., & Körner, C. (2010). Infra-red thermometry of alpine landscapes challenges climatic warming projections. *Global Change Biology*, *16*(9), 2602–2613.

Scherrer, D., & Körner, C. (2011). Topographically controlled thermal-habitat differentiation buffers alpine plant diversity against climate warming. *Journal of Biogeography*, *38*(2), 406–416.

Shoo, L. P., Storlie, C., Williams, Y. M., & Williams, S. E. (2010). Potential for mountaintop boulder fields to buffer species against extreme heat stress under climate change. *International Journal of Biometeorology*, *54*(4), 475–478.

Slavich, E., Warton, D. I., Ashcroft, M. B., Gollan, J. R., & Ramp, D. (2014). Topoclimate versus macroclimate: how does climate mapping methodology affect species distribution models and climate change projections?. *Diversity and Distributions*, *20*(8), 952–963.

Spampinato, G., Cameriere, P., Caridi, D., & Crisafulli, A. (2008). Carta della biodiversità vegetale del Parco Nazionale dell'Aspromonte (Italia meridionale). *Quaderni di Botanica Ambientale e Applicata*, *19*, 3–36.

Stark, J. R., & Fridley, J. D. (2022). Microclimate-based species distribution models in complex forested terrain indicate widespread cryptic refugia under climate change. *Global Ecology and Biogeography*, *31*(3), 562–575.

Stewart, J. R., Lister, A. M., Barnes, I., & Dalén, L. (2010). Refugia revisited: individualistic responses of species in space and time. *Proceedings of the Royal Society B: Biological Sciences*, *277*(1682), 661–671.

Srivastava, A. K., Rajeevan, M., & Kshirsagar, S. R. (2009). Development of a high resolution daily gridded temperature data set (1969–2005) for the Indian region. *Atmospheric Science Letters*, *10*(4), 249–254.

Suggitt, A. J., Wilson, R. J., Isaac, N. J., Beale, C. M., Auffret, A. G., August, T., ... & Maclean, I. (2018). Extinction risk from climate change is reduced by microclimatic buffering. *Nature Climate Change*, *8*(8), 713–717.

Ummenhofer, C. C., & Meehl, G. A. (2017). Extreme weather and climate events with ecological relevance: a review. *Philosophical Transactions of the Royal Society B: Biological Sciences*, *372*(1723), 20160135.

Vanwalleghem, T., & Meentemeyer, R. K. (2009). Predicting forest microclimate in heterogeneous landscapes. *Ecosystems*, *12*, 1158–1172.

Velazco, S. J. E., Rose, M. B., de Andrade, A. F. A., Minoli, I., & Franklin, J. (2022). flexsdm: An r package for supporting a comprehensive and flexible species distribution modelling workflow. *Methods in Ecology and Evolution*, *13*(8), 1661–1669.

Velazco, S. J. E., Rose, M. B., De Marco Jr, P., Regan, H. M., & Franklin, J. (2023). How far can I extrapolate my species distribution model? Exploring shape, a novel method. *Ecography*, e06992.

Venables, W. N., & Ripley, B. D. (2002). Statistics and computing. *Modern applied statistics with S. Springers, New York, USA.*

Vitasse, Y., Ursenbacher, S., Klein, G., Bohnenstengel, T., Chittaro, Y., Delestrade, A., ... & Lenoir, J. (2021). Phenological and elevational shifts of plants, animals and fungi under climate change in the European Alps. *Biological Reviews*, *96*(5), 1816–1835.

Whiteman, C. D., Zhong, S., Shaw, W. J., Hubbe, J. M., Bian, X., & Mittelstadt, J. (2001). Cold pools in the Columbia Basin. *Weather and Forecasting*, *16*(4), 432–447.

Wood, S. N. (2011). Fast stable restricted maximum likelihood and marginal likelihood estimation of semiparametric generalized linear models. *Journal of the Royal Statistical Society: Series B (Statistical Methodology)*, *73*(1), 3–36.

Zampiglia, M., Bisconti, R., Maiorano, L., Aloise, G., Siclari, A., Pellegrino, F., ... & Canestrelli, D. (2019). Drilling down hotspots of intraspecific diversity to bring them into on-ground conservation of threatened species. *Frontiers in Ecology and Evolution*, *7*, 205.

Zellweger, F., De Frenne, P., Lenoir, J., Rocchini, D., & Coomes, D. (2019). Advances in microclimate ecology arising from remote sensing. *Trends in Ecology & Evolution*, *34*(4), 327–341.

3. Fine-scale topoclimatic and habitat heterogeneity are key drivers of genetic variation in a mountain hotspot of biodiversity

Daniele Delle Monache[a], Andrea Chiocchio[a], Giuseppe Martino[a], Roberta Bisconti[a], Antonino Siclari[b,c] & Daniele Canestrelli[a]

[a] Department of Ecological and Biological Sciences, Tuscia University, Viterbo, Italy
[b] Aspromonte National Park, Santo Stefano in Aspromonte, Italy
[c] Città Metropolitana di Reggio Calabria, Piazza Italia, 89100, Reggio Calabria, Italy

Abstract

Mountain regions harbor among the richest hotspots of biodiversity on Earth. Here, heterogeneous topographies create intricate climatic and habitat mosaics, which organisms respond to by local adaptation. At the same time, their ecosystems are critically impacted by anthropogenic climate and land use changes. This results in an interweaving of eco-evolutionary processes that generate and threaten mountain hotspots' biodiversity. Disentangling their contribution is paramount and becomes increasingly challenging as the territory gets heterogeneous.

In this study, we investigated the population genetic structure of the fire salamander (*Salamandra salamandra*) in the Aspromonte mountain region, a highly heterogeneous hotspot of biodiversity in Southern Italy, to identify the drivers of genetic diversity patterns at fine spatial scales. We used 13 microsatellite loci to genotype 189 individuals and employed genetic clustering algorithms to infer the species' population genetic structure. Then, we assessed the influence of high-resolution (10 m) topoclimatic and habitat heterogeneity, hydrographic basins, old-growth forests, and topographic distance on individual differentiation. We also evaluated whether the geographic disposition of old-growth forests could explain the genetic clustering. We finally characterized the species' current connectivity and projected its evolution under increasingly severe climate change scenarios for 2041-2070.

All genetic clustering algorithms suggested a differentiation cline along the region's North-South axis, resulting in three distinct genetic clusters. All landscape predictors correlated with individual differentiation. However, once we ruled out the confounding effect of topographic distance, only topoclimatic and habitat heterogeneity remained relevant. The distribution of old-growth forests significantly associated with genetic clustering. Current connectivity corridors continuously connected individuals; conversely, they were predicted to shrink under climate change, with the shrinking getting worse in increasingly severe scenarios. Also, future connectivity will likely concentrate in the highest areas of the region.

Habitat configuration primarily shapes the intraspecific diversity of the species in the Aspromonte region, closely followed by topoclimatic variation. Old-growth forests might also shelter fire salamanders from recent anthropogenic change. Overall, our study demonstrated that all levels of landscape complexity contribute to biological diversification in mountain hotspots, even at the smallest spatial scales. That said, even such an outstanding complexity might not prevent vulnerable species from being affected by climate change, which should reaffirm the necessity of preserving the precious ecosystems that host them.

Keywords

mountain hotspot of biodiversity, genetic diversity, *Salamandra salamandra*, topoclimate, habitat heterogeneity, old-growth forests.

Introduction

Due to the escalating impact of human activities on global ecosystems, biodiversity hotspots are increasingly becoming focal points for conservation efforts. Biodiversity hotspots, now amounting to 36 regions, concentrate over half of the world's endemic plant species and 42% of endemic terrestrial vertebrates within just 2.4% of the Earth's land surface (CEPF, 2014). They are also inhabited by a significant portion of the global population and play a crucial role in providing ecosystem services that sustain human communities (Cincotta et al., 2000). At the same time, hotspots are exceptionally under threat. Habitat destruction, primarily driven by human activities, is a major driver of many species' extinction (Brooks et al., 2002). Climate change poses a significant threat by altering global climates and exacerbating habitat loss (Thomas et al., 2004; Turner et al., 2010). The introduction of non-native species also contributes to threatening natural populations (Groves & di Castri, 1991; Steadman, 1995), and so do exploitation for trade or meat (van Dijk et al., 2000; Bakarr et al., 2001) and the spread of infections and diseases (Stuart et al., 2004; Wake & Vredenburg, 2008). Given the convergence of biological richness, human-induced pressures, and socioeconomic vulnerabilities in these areas, conservation efforts are paramount (Zachos & Habel, 2011).

Biodiversity hotspots feature some of the most prominent mountain regions worldwide (Myers et al., 2000; Camacho-Sanchez et al., 2018; Noroozi et al., 2018). Similarly, and at broader scales, mountain regions harbor over 87% of the world's amphibian, bird, and mammal species despite covering less than a quarter of the Earth's land surface, excluding Antarctica (Kapos et al., 2000; Rahbek et al., 2019). Large shares of these are endemic, often with ranges restricted to single mountain ranges or mountaintops (Rodgers & Homewood, 1982; Leo, 1995; Körner, 2003; Mutke & Barthlott, 2005). What makes mountains so unique is primarily topographic conformation. Contrasting climatic zones are compressed over short distances by exposure, slope inclination, and steep altitude clines, rivaling the variation observed along much broader elevational or latitudinal gradients (Scherrer & Körner, 2010). At local scales, species with subtly different climatic niches can thus coexist, allowing biological diversity to cumulate (Körner, 2004; Hoorn et al., 2018). Additionally, contrasting microhabitats cause populations to split and diverge despite physical proximity (Särkinen et al., 2012; Stein et al., 2014). Over heterogeneous topographies, extreme day-to-day weather variations interact with seasonality, creating intricate climatic mosaics that further fuel adaptation and specialization (Janzen et al., 1967; Ohlemüller et al., 2008; Chan et al., 2016). During longer-term climate oscillations like the Quaternary shifts, mountains repeatedly enabled susceptible species to endure adverse climatic change (Carnaval et al., 2009; Stewart et al., 2010); in

these instances, mountain species may experience fewer extinctions as they are facilitated in tracking their climatic niche through short-term migrations (Sandel et al., 2011; Scherrer & Körner, 2011).

Mountain biodiversity is severely threatened by anthropogenic change. Accelerated warming rates at higher elevations make mountains vulnerable to temperature shifts (Pepin et al., 2015; McCullough et al., 2016). Changing land management practices and other land cover modifications lead to habitat degradation and fragmentation, severely impacting critical ecosystem services and hindering species from adapting to rapidly shifting climates (Corlett & Westcott, 2013; Pătru-Stupariu et al., 2020). Consequently, preserving mountain hotspots of biodiversity is strategically imperative. Understanding the ecological and evolutionary processes contributing to and sustaining their biodiversity becomes equally essential (Forest et al., 2007). This is one of the prerogatives of landscape genetics, which aims to clarify the interactions between landscape features and the microevolutionary processes that structure biodiversity (Manel et al., 2003). As such, its focus is on the connections between genetic diversity, which relevantly signals the evolvability and adaptive potential of populations (Frankham, 2010; Allendorf et al., 2012), and the processes that contribute to its distribution in space and time; these processes include gene flow, genetic drift, and selection (Holderegger & Wagner, 2006; Storfer et al., 2007). Landscape genetics furthered our understanding of eco-evolutionary processes in the mountains on several occasions, perhaps highlighting source-sink dynamics in metapopulations (Murphy et al., 2010; Klinga et al., 2019) or identifying cryptic barriers and bridges to connectivity in fragmented habitats (Epps et al., 2007; Wasserman et al., 2010; Trense et al., 2021). Still, the discipline can struggle to disentangle the contributions of each landscape feature when topography gets overly complex.

Here, we leveraged an exceptionally heterogeneous region in Southern Italy, the Aspromonte mountain range, to identify which processes shape the genetic diversity patterns of a mountain hotspot at fine spatial scales. The Aspromonte mountain range constitutes a prime candidate. Due to its proximity to the sea and its complex topographic conformation, it harbors widely differentiated climatic and ecological gradients, making it a hotspot of endemisms and genetic diversity at the continental level (Canestrelli et al., 2010). It also forms part of a glacial refuge where many temperate species endured Pleistocene glaciation (Canestrelli et al., 2008; Vega et al., 2010; Canestrelli et al., 2012). Anthropogenic changes add further interest by affecting the Aspromonte region very heterogeneously. On the one hand, the Aspromonte National Park and 57 Natura 2000 sites strictly protect its innermost areas; some of the oldest temperate forests survive there (Piovesan et al., 2020). Conversely, in recent decades, villages and traditional farming practices were abandoned in other internal areas, while urbanization impacted the most populated areas along the coast. We

characterized the population genetic structure of the fire salamander (*Salamandra salamandra gigliolii*) within the Aspromonte region. Then, we investigated how fine-scale topographic conformation, habitat configuration, and topoclimatic variation shaped the species' genetic diversity in the study area. We chose the fire salamander as a candidate species because of its continuous distribution in the region's forested ecosystems (Lanza, 2007). Finally, we evaluated the influence that habitat configuration and topoclimatic variation exert on the current connectivity of the species in the region and projected future connectivity surfaces under increasingly severe climate change scenarios (SSP126, SSP370, SSP585; Karger et al., 2017) for 2041-2070.

Materials & Methods

Study area

The Aspromonte region is a mountainous area situated at the Italian Peninsula's southern boundary and the tip of the Apennines. Owing to its position and orography, the region experiences a broad spectrum of climatic conditions ranging from a Mediterranean rain-seasonal oceanic bioclimate below 1,100 m asl to a temperate oceanic bioclimate above this altitude (Brullo et al., 2001). Rainfall patterns are typically Mediterranean, with more winter rain than summer (Colacino et al., 1997). Most coastal and hilly humid habitats depend on seasonal rains, while mountain streams and brooks are mainly perennial, supplied by abundant autumn, winter, and spring precipitation. Winters in the mountains are cold, often dropping below 0 °C in January and February; conversely, coasts experience scorching summers, with temperatures exceeding 40 °C in July and August. The western and eastern sides have contrasting microclimates, being wetter and cooler on the western side and warmer and drier on the eastern side. The broad spectrum of climatic conditions directly translates into highly varied vegetation and ecological gradients; the Aspromonte region is indeed a hotspot of biodiversity, hosting unique plant and animal species, relict species, and old-growth forests (Spampinato et al., 2008; Zampiglia et al., 2019; Piovesan et al., 2020; Martino et al., 2022).

Sampling and genotyping procedures

We divided the Aspromonte region into hydrographic basins and conducted a grid-based sampling within each basin to minimize the distances between sampling sites. We visited 92 sites, from which we sampled 5 to 10 individuals per site (Fig. 1). To avoid impacting the reproductive population, we sampled the larval stages exclusively and then preserved the collected tissues in 90% ethanol, waiting for molecular investigations.

We extracted, purified, and quantified genomic DNA using the Quick-DNA Miniprep kit (Zymoresearch). For the study of genetic variation, we selected 13 microsatellite loci (SST-A6-I, SST-A6-II, SalE-14, SST-B11, SST-G9, SalE12, SalE2, SST-C3, SalE5, SalE7, Sal29, Sal3, SalE06, SalE8), which proved to be informative at fine geographic scale in this species (Lourenço et al., 2019). Laboratory procedures for microsatellite amplification followed previously described protocols (Steinfartz et al., 2004; Hendrix et al., 2010). We fluorescently labeled forward primers. Then, PCR products were electrophoresed by Macrogen Inc. on an ABI 3730xl genetic analyzer (Applied Biosystems) with a 500-HD size standard. We analyzed microsatellite raw data using GENEMAPPER® 4.1. We excluded individuals with more than 50% of missing data from subsequent analyses. Finally, we excluded null alleles and large-allele drop-out using MICRO-CHECKER 2.2.3 (Van Oosterhout et al., 2004). We computed allelic frequencies with GENETIX 4.05 (Belkhir et al., 2004). We tested for departures from Hardy-Weinberg equilibrium and genotypic linkage disequilibrium with FSTAT (Goudet, 1995) using the Bonferroni correction for multiple tests.

Genetic clustering algorithms

We performed a spatial analysis of principal components (sPCA; Jombart et al., 2008) to evaluate whether genetic variation was structured spatially. We built the connection network using the neighborhood-by-distance criterion (Fig. A.1 in Appendices). We corroborated the spatial pattern by clustering individuals into genetic clusters using a discriminant analysis of principal components (DAPC; Jombart et al., 2010). We selected the most likely number of clusters (K) by visually examining the Bayesian information criterion (BIC) profile with K ranging from 1 to 6. Both sPCA and DAPC are implemented in the ADEGENET R package (Jombart et al., 2008; R Core Team, 2022).

Individuals were also clustered according to the Bayesian algorithm implemented in TESS 2.3.1 (Chen et al., 2007). We allowed for admixture and employed the conditional autoregressive model (CAR) by giving the individuals' geographical coordinates as prior information. We chose to cluster individuals with TESS as it proved to be particularly efficient compared to similar algorithms if the genetic structure is shallow (Chen et al., 2007; François & Durand, 2010). We allowed K to range from 2 to 6 and ran 20 replicates for each value of K, with 70,000 iterations and 20,000 discarded as burn-in. We left the spatial interaction parameter to its default value (0.6) and updated the parameters by enabling the UPDATEPARAMETERS option. To infer the best clustering model, we averaged the deviance information criterion (DIC) over the 20 replicates and inspected the DIC profile, looking for a plateau. Once we selected the optimal K, we finally employed CLUMPP 1.1.2

(Jakobsson & Rosenberg, 2007) to average the estimated admixture proportions of the ten runs that scored the lowest DIC values.

Landscape predictors

We summarized the species' ecological landscape into five landscape predictors, namely 1) the pairwise resistance associated with topoclimatic variation (hereafter TOPOCLIM); 2) the pairwise resistance associated with habitat configuration (HABITAT); 3) the number of hydrographic basins separating each pair of individuals (BASINS); 4) the pairwise distance from a shared old-growth forest (FORESTS); and 5) the pairwise topographic distance (TOPODIST).

TOPOCLIM and HABITAT resistances

We retrieved monthly minimum, average, and maximum temperatures from 33 weather stations in the study area. We then interpolated these temperatures to 10 m resolution by employing geographically weighted regression (GWR) models with fixed bandwidth and by including altitude, slope, northness, eastness, distance to the coast, and monthly average of daily clear-sky insolation time as physiographic descriptors; these are, indeed, known drivers of local climatic conditions (Lenoir et al., 2017). We fitted GWR models using the SPGWR R package (Bivand & Yu, 2020); these models extend the traditional regression framework and are particularly indicated to describe the spatial non-stationarity of free-air temperature's relationship with its physiographic drivers (Li et al., 2010; Su et al., 2012; Tian et al., 2012). Chapter 2 details the weather station data and the interpolation procedure. From the interpolated monthly minimum, average, and maximum temperature surfaces, we calculated seven high-resolution bioclimatic variables, namely BIO1, BIO5, BIO6, BIO10, BIO11, the average temperature of the March-May quarter, and the average temperature of the September-November quarter. We synthesized the bioclimatic variables into a single predictor by taking the first principal component (PC) out of a principal component analysis (PCA).

Next, we modeled the species' distribution using the BIOMOD2 R package, version 4.2-2 (Thuiller et al., 2023). As occurrence data, we integrated our data points with 29 data points from Martino et al. (2022) and 10 data points from museum specimens. We supplemented the previous bioclimatic predictor with the Topographic Wetness Index (TWI), which we considered a reliable proxy for soil moisture (Beven & Kirkby, 1979; Kopecký et al., 2021), and the Terrain Ruggedness Index (TRI) as a measure of topographic heterogeneity. We employed seven algorithms (CTA, FDA, GAM, GBM, GLM, MARS, RF), which we parameterized following the suggestions from Barbet-Massin et al. (2012). We selected the same number of pseudo-absences and occurrences for CTA,

GBM, and RF; 100 pseudo-absences for FDA and MARS; and 1,000 pseudo-absences for GAM and GLM. We set the prevalence to 0.5 for CTA, FDA, GAM, GBM, GLM, and RF and repeated pseudo-absence selection ten times per algorithm. We selected all pseudo-absences randomly. We performed model validation via split sampling, calibrating the algorithms on 80% of the data, and repeated the procedure 20 times per pseudo-absence dataset. We then obtained the TOPOCLIM suitability surface by ensembling the model runs based on their ROC score after discarding runs that scored ROC lower than 0.8. Finally, we converted the suitability surface into pairwise TOPOCLIM resistances with CIRCUITSCAPE, version 4.0.5 (Shah & McRae, 2008).

We obtained the pairwise HABITAT resistances by replicating the previous modeling routine with the following modifications. We modeled the species' distribution using logistic regression models (GLMs), selecting pseudo-absences according to the suggestions of Barbet-Massin et al. (2012): ten runs with 1,000 points selected and prevalence set to 0.5. We employed the land use type at 10 m resolution (De Fioravante et al., 2021) as the sole predictor in GLMs. Again, we converted the suitability surface into pairwise HABITAT resistances with CIRCUITSCAPE, version 4.0.5.

FORESTS and TOPODIST

We considered the pairwise distance from a shared old-growth forest dichotomically, distinguishing pairs of individuals with the same nearest forest from those with different nearest ones. By doing so, we evaluated whether sharing the nearest old-growth forest decreased genetic differentiation, possibly due to sharing a sheltered area. We corrected the geographical distances for topography using the TOPODISTANCE R package, version 1.0.2 (Wang, 2020).

Influence of the landscape predictors on population genetic structure

We quantified individual-based pairwise genetic dissimilarity by performing a PCA on individual genotypes and taking the pairwise Euclidean distance along the first two PCs. This dissimilarity metric is considered more effective than metrics based on relatedness or genetic distance when Hardy-Weinberg equilibrium cannot be assumed (Shirk et al., 2017). Then, we conducted several individual and partial Mantel tests looking for isolation-by-distance (IBD) and isolation-by-resistance (IBR) patterns. Partial Mantel tests are frequently used in landscape genetics studies as they assess the degree of association between two distance matrices (typically, genetic distance and environmental dissimilarity) net of the information contained in a third control matrix (e.g., geographical distance between pairs of individuals or populations; Smouse et al., 1986). In our case, we tested the strength of the association between individual-based pairwise genetic dissimilarity and each landscape

predictor while controlling for pairwise topographic distances. We also tested each combination of independent and control matrices to compare the relative importance of the landscape predictors within a causal modeling analytical framework (Cushman et al., 2006).

Finally, we performed a chi-square test on the contingency table we built by pairing forests with the optimal clustering evidenced by TESS. A significant association between sharing the same nearest forest and the genetic cluster could suggest that old-growth forests sheltered fire salamanders against climatic and environmental changes, thus causing populations to remain isolated and differentiate their gene pools.

Current and future connectivity

We characterized the current connectivity by replicating the previous modeling routine to obtain a TOPOCLIM suitability surface, with the exception that we included the high-resolution monthly climate data for 1981-2010 from CHELSA, version 2.1 (https://chelsa-climate.org/; Karger et al., 2017), as the intercept in the GWR models during the interpolation procedure. We ran the all-to-one algorithm implemented in CIRCUITSCAPE, version 4.0.5, to convert the suitability surface into a cumulative map of the current TOPOCLIM connectivity. Likewise, we ran the CIRCUITSCAPE all-to-one algorithm on the HABITAT suitability surface to obtain the cumulative map of the connectivity associated with habitat configuration.

We projected the GWR models by substituting the intercept with monthly data from different climate change scenarios for 2041-2070. We worked on all the GCM (GFDL-ESM4, IPSL-CM6A-LR, MPI-ESM1-2-HR, MRI-ESM2-0, UKESM1-0-LL) and SSP (SSP126, SSP370, SSP585) combinations currently provided by CHELSA V2 CMIP6 (Karger et al., 2017). For each climate change scenario, we obtained monthly minimum, average, and maximum temperature surfaces for 2041-2070, from which we calculated the same seven high-resolution bioclimatic variables (BIO1, BIO5, BIO6, BIO10, BIO11, the average temperature of the March-May quarter, the average temperature of the September-November quarter). We then replicated the modeling routine to produce a suitability surface for each climate change scenario, which we averaged into three representative SSP126, SSP370, and SSP585 suitability surfaces. Finally, we ran the all-to-one algorithm implemented in CIRCUITSCAPE, version 4.0.5, to convert these suitability surfaces into cumulative maps of the future TOPOCLIM connectivity under SSP126, SSP370, and SSP585.

To assess how TOPOCLIM connectivity might evolve due to climate change, we evaluated current and future connectivity for all climate change scenarios at 100,000 random locations. For each

scenario, we calculated the differences between future and current connectivity at these locations and inspected whether these differences displayed altitudinal patterns indicative of future upslope range shifts.

Results

Genetic population structure

The final microsatellite dataset comprised multilocus genotypes for 189 individuals at 13 loci. MICRO-CHECKER 2.2.3 detected no traces of null alleles and large-allele drop-out. We found no significant deviations from Hardy-Weinberg or linkage equilibria after applying the Bonferroni correction.

The sPCA's global and local tests revealed a significant global structure (max(t) = 0.0347, *p*-value < 0.001) but no significant local structure (max(t) = 0.01524, *p*-value = 0.183). As such, this indicates that most genetic variation was among geographically distant individuals rather than those closer. The eigenvectors' scree plot suggested that only the first two global structures should be interpreted (Fig. A.2 in Appendices). When we plotted these two global structures, the sPCA depicted a pronounced North-South differentiation cline: the scores along the first component gradually increased moving south (Fig. 2d). The second principal component, on the contrary, distinguished a central negative-scored cluster that segregated neatly from northern and southern individuals (Fig. 2e).

The DAPC identified three genetic clusters as the best clustering (Fig. 2a). Optimizing the spline interpolation of the a-scores suggested that only the first 13 PCs, which accounted for 50.1% of the total variance, should be retained in the PCA step (Fig. 2c). The biplot distinguished a well-differentiated northern cluster along the first component (Northern cluster in Fig. 2b) and two other clusters, namely central (Central cluster in Fig. 2b) and southern (Southern cluster in Fig. 2b) clusters, mainly defined by the second component. Both sPCA and DAPC thus highlighted the same genetic differentiation cline along the region's North-South axis, with northern individuals being more differentiated from the rest.

The Bayesian clustering analyses with TESS 2.3.1 further substantiated these results. The DIC profile reached a plateau at K = 3, after which we witnessed only slight decreases in DIC values (Fig. 3b). We should disregard these decreases in DIC values since the bar plots of the individual admixture proportions distinguished three meaningful genetic clusters even at higher values of K (Fig. A.3b-c

in Appendices). Like sPCA and DAPC, TESS identified a northern, central, and southern cluster (Fig. 3a-b). Admixture patterns among the clusters suggested that the northern cluster was well differentiated from the central and southern ones (Fig. 3a). The clustering at K = 2 also clearly distinguished a northern genetic cluster (Fig. A.3a in Appendices). On the contrary, the contributions of the central and southern genetic clusters gradually mix, moving south, indicating significantly higher levels of gene flow (Fig. 3a).

Influence of the landscape predictors on population genetic structure

Individual Mantel tests suggested significant correlations between pairwise genetic dissimilarity, genetic clustering, and all landscape predictors. However, pairwise resistance associated with habitat configuration (HABITAT) was marginally more strongly related to pairwise genetic dissimilarity (Tab. 1). A first partial Mantel test supported an isolation-by-distance (IBD) pattern, as pairwise genetic dissimilarity was more strongly associated with pairwise topographic distance than membership in the same genetic cluster (Tab. 2a). Topographic distance also prevailed over the subdivision of the territory into distinct hydrographic basins (Tab. 2b), as well as over the pairwise distance from a shared old-growth forest (Tab. 2c). Despite pairwise TOPOCLIM ($r = 0.830$) and HABITAT ($r = 0.656$) resistances considerably correlated with topographic distance, both these resistances overcame the influence of TOPODIST (Tab. 2d-e), thus supporting the hypothesis of an isolation-by-resistance (IBR) pattern. In relative terms, HABITAT resistance was moderately more associated with pairwise genetic dissimilarity than TOPOCLIM resistance (Tab. 2f). Habitat configuration also impacts pairwise genetic dissimilarity to a much greater extent than the subdivision of the territory into distinct hydrographic basins (Tab. 2g) and the pairwise distance from a shared old-growth forest (Tab. 2h). Altogether, these results suggested landscape resistances to be primarily responsible for gene flow across the study area.

Finally, the association between genetic clustering and proximity to the same old-growth forest was highly significant ($\chi = 357.8$, df = 6, p-value < 0.001). From the inspection of the contingency table (Tab. 3), the northern genetic cluster almost entirely coincided with the Ferullà forest, the central genetic cluster with the Mancuso and Pollia forests, and the southern genetic cluster with the Tre Limiti forest.

Current and future connectivity

Connectivity corridors associated with habitat configuration connected the bulk of the individuals almost continuously, isolating only the northernmost individuals (Fig. 4a); the same was true for the

current TOPOCLIM connectivity corridors (Fig. 4b). As climate change scenarios increased in severity, the connectivity corridors became thinner and more locally concentrated (Fig. 4c-e). Connectivity corridors also shifted upslope, as evidenced by connectivity losses mainly occurring at low- to mid-altitudes (~ 1000 m asl) in favor of gains at higher altitudes (~ 1500 m asl; Fig. 4c-e and Fig. 5). We witnessed the most significant changes from the present to SSP126 (Fig. 4c). Still, the shrinking and upslope shifting of connectivity corridors continued also moving from SSP126 to SSP370 (Fig. 4b and Fig. 5) and from SSP370 to SSP585 (Fig. 4c and Fig. 5).

Discussion

In this study, we investigated the genetic structure of the fire salamander within the Aspromonte region. Then, we inferred how fine-scale topographic conformation, habitat configuration, and topoclimatic variation shaped the distribution of genetic diversity in the study area. We also evaluated the impact of habitat configuration and topoclimatic variation on population connectivity. Finally, we assessed how connectivity might evolve in the following decades (2014-2070) under different climate change scenarios. We found fire salamander populations highly genetically structured in the Aspromonte region. All the genetic cluster analyses depicted a gradual differentiation cline along the North-South axis of the region, identifying three main genetic clusters. The central and southern clusters were less differentiated than the northern cluster. They also differentiated more gradually (Fig. 2). Such gradual differentiation and the results from our landscape genetics analyses point to an IBD process. Indeed, topographic distances significantly correlated with genetic dissimilarity (Tab. 1), and to a greater degree than did the genetic clustering (Tab. 2a). Also, although all landscape predictors correlated with genetic dissimilarity (Tab. 1), the topographic distances were sufficient to explain the impact of most of them (Tab. 2). HABITAT and TOPOCLIM resistances, nonetheless, remained informative even after ruling out the influence of the topographic distances (Tab. 2d-e), indicating that IBR processes rather than IBD contributed to the differentiation.

The HABITAT resistances were the most strongly associated with genetic dissimilarity (Tab. 2), making fine-scale habitat configuration our predominant driver of recent differentiation in *S. salamandra* populations. Within the Aspromonte region, the species occupies broad-leaved forested environments, followed by oro-Mediterranean mountain pine forests (Martino et al., 2022). These forested environments are confined to the innermost part of the region and are highly heterogeneous, often intertwining with each other and with orchards and arable lands. Mostly, they also fall under the protection of the National Park and are thus relatively free from human disturbance. That heterogeneous habitat configurations affect dispersal and gene flow in natural populations has been

known for decades; indeed, this fact constitutes a core staple in landscape genetics (Keyghobadi, 2007) and is shown for many pond-breeding amphibians (Kolozsvary & Swihart, 1999; Cushman, 2006). While much deserved attention is paid to the effects of heterogeneous habitat configuration in degraded and fragmented environments (Fahrig, 2003; Fischer & Lindenmayer, 2007; Haddad et al., 2015), our findings suggest this landscape feature to be a crucial driver of genetic diversification also in much less anthropized ones. In this light, the clue that populations may be susceptible to even the smallest-scale habitat configurations further reaffirms the necessity of preserving the corridors that functionally connect them.

We found a substantial association between the distribution of old-growth forests and genetic clustering (Tab. 3). Individuals from the northern and southern clusters almost entirely shared the same old-growth forest as their nearest – Ferullà and Tre Limiti, respectively. In contrast, those from the central cluster were split between having Mancuso and Pollia as their nearest old-growth forest. Old-growth forests are topical environments in many respects. For instance, they sequester and store large amounts of carbon, thus serving as global carbon dioxide sinks (Luyssaert et al., 2008). Due to their tall canopies and vertical complexity, old-growth forests display insulating effects that can mitigate climate warming at local scales (Frey et al., 2016; Wolf et al., 2021); as such, they might act as microrefugia for cool-adapted species to cope with increasingly-raising temperatures (Betts et al., 2018; De Frenne et al., 2021; De Lombaerde et al., 2021). Their high structural complexity also translates into rich mosaics of microhabitats that sustain equally rich flora and fauna, making old-growth forests relevant hotspots of biodiversity (Paillet et al., 2010). We add to their importance here by hinting that old-growth forests in the Aspromonte region could have sheltered *S. salamandra* populations from recent anthropogenic change. Although our analyses excluded any contribution of these landscape features to genetic dissimilarity (Tab. 2), the association between their distribution and the genetic clustering might indicate that fire salamanders differentiated their gene pools within forested patches isolated from one another; the four old-growth forests would thus constitute what remains of these patches. This interpretation is in line with the region's contemporary history, which has seen the shrinkage of forest areas due to intense logging (Robb et al., 2021). The species would then have dispersed during the following phase of forest regeneration.

Topoclimatic variation was the second driver of recent differentiation in *S. salamandra* populations, slightly less important than habitat configuration (Tab. 2f). From a topoclimatic viewpoint, populations currently connect through corridors encompassing the internal mid- to high-altitude environments of the study area (Fig. 4b). These are also the most favorable environments habitat-wise, as they are dominated by beech forests (*Fagus sylvatica* L.), constituting the species'

primary habitat in the region (Martino et al., 2022). Accordingly, HABITAT and current TOPOCLIM connectivity corridors substantially overlapped (Fig. 4a and Fig. 4b). Topography is a well-established modulator of many geophysical processes influencing the organisms' ecology. Slope and aspect determine soil moisture (Reid, 1973) and nutrient availability (Singh, 2018) while also controlling the availability of direct and diffuse radiation (Anderson et al., 2014); as a result, the impact of topography on plant microhabitat is hardly overstated (Daws et al., 2002; Gibbons& Newbery, 2002; John et al., 2007). Accordingly, animal movement cannot but be affected by such an array of microclimates and microhabitats (Porter et al., 2002; Sears et al., 2011; Malishev et al., 2018). Its topographic complexity and geographic position distinguish the Aspromonte mountain range; here, we showed that when these two factors combine, even the most detailed topographical tessellation can significantly impact the genetic structure of populations. If sustained over time, such genetic diversification over fine geographic scales may constitute a key factor in establishing hotspots of biodiversity (Trew & Maclean, 2023).

Finally, the species connectivity across the study area will likely suffer from contemporary climate change. Under the most optimistic scenario for 2041-2070 (SSP126), the species was predicted to maintain most of its central and southern connectivity despite an overall shrinking of the corridors. On the contrary, the northern corridors were expected to be lost, leaving the northernmost individuals isolated (Fig. 4c). Corridor shrinkage only got worse in increasingly severe climate change scenarios; at the same time, connectivity tended to concentrate in the central and southern sections (Fig. 4d-e). These are engaging results for a couple of reasons. First, they provide evidence that fire salamanders in the Aspromonte could try redistributing upslope to track their thermal niche; indeed, the central and southern sections where connectivity is expected to concentrate are higher in altitude (Fig. 5). Upslope range shifts are nothing new to science, as they constitute one of the most frequent mechanisms by which organisms cope with changing climates (Parmesan, 2006; Chen et al., 2011). Accordingly, they have been witnessed in many mountain environments (Telwala et al., 2013; Menéndez et al., 2014; Vitasse et al., 2021). Mountains are believed to allow vulnerable taxa to endure warming climates by facilitating isotherm tracking through short-range migration, and this is all the truer as the region is topographically heterogeneous (Sandel et al., 2011). In this light, anticipating that *S. salamandra* could redistribute upslope in a region so topoclimatically diverse adds to the species' sensitivity to climatic alteration. Second, the loss of connectivity in the northern section of the region could lead us to speculate that similar processes might have happened in the past, possibly explaining why the northern cluster appeared more differentiated in the sPCA, DAPC, and TESS analyses.

Conclusions

By investigating the population genetic structure of *S. salamandra* in the Aspromonte mountain region, we demonstrated that habitat configuration and topoclimatic variation comparably shape the diversity of the Aspromonte mountain hotspot at very small spatial scales. Here, landscape complexity at all levels directly connects with the microevolutionary processes instrumental in generating and sustaining outstanding biodiversity. Nonetheless, it does not seem to prevent species from being affected by anthropogenic changes since fire salamanders were predicted to move upslope to track favorable topoclimates. This raises some critical considerations. While we projected how the species would cope with topoclimatic warming, fire salamanders experience ground-level climates that can strongly deviate from free-air ones, especially in forested landscapes (Geiger et al., 2009). On top of topographic complexity, such microclimatic variation further facilitates tracking thermal niches when climate shifts (Scherrer & Körner, 2011). Also, these microclimates are often buffered and decoupled from climate warming, as canopy cover dampens temperature and humidity fluctuations (De Frenne et al., 2019). Buffering and decoupling, however, need structurally dense canopy covers to be established successfully (Ewers & Banks-Leite, 2013). Unfortunately, although logging and other deforestation practices are nowadays less frequent (Robb et al., 2021), the Aspromonte is increasingly plagued by forest fires that lick even its most ancient forests (De Luca & Modica, 2022). Forest fires are a worldwide ecological challenge for forest-dwelling species (McLauchlan et al., 2020) and could severely impact *S. salamandra* and other susceptible species. So, whether our projections should be considered conservative is uncertain. Still, one thing is not. Given the role that old-growth forests seem to play here as contemporary shelters, as well as the global significance of forests as anthropogenic refugia (De Frenne et al., 2021; De Lombaerde, 2021), we should deem the preservation of forested ecosystems in the Aspromonte and other hotspots of biodiversity paramount.

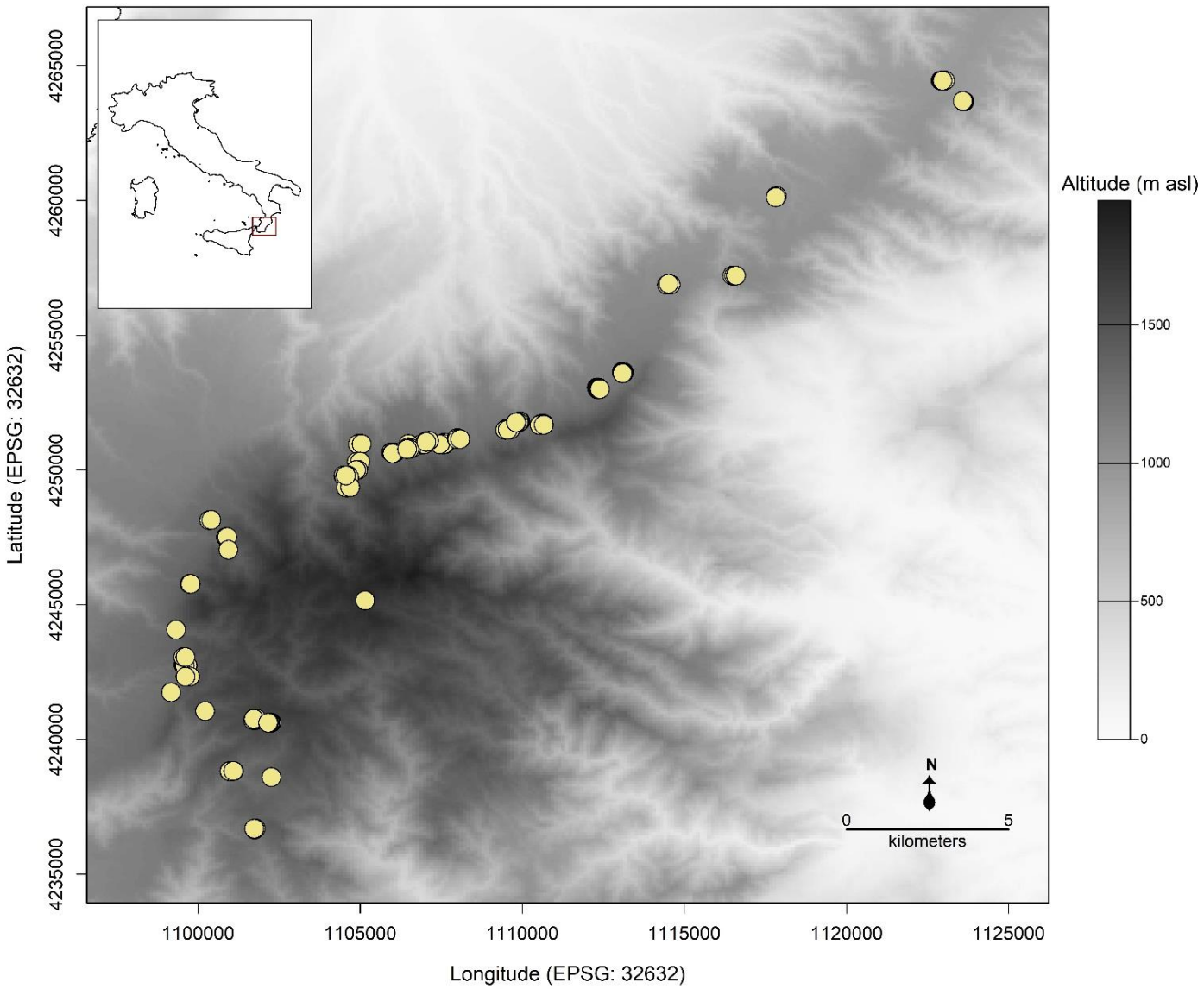

Figure 1. Distribution of the 189 individuals we genotyped for the present study. The inset shows the Italian peninsula's borders, with the study area's borders highlighted in red.

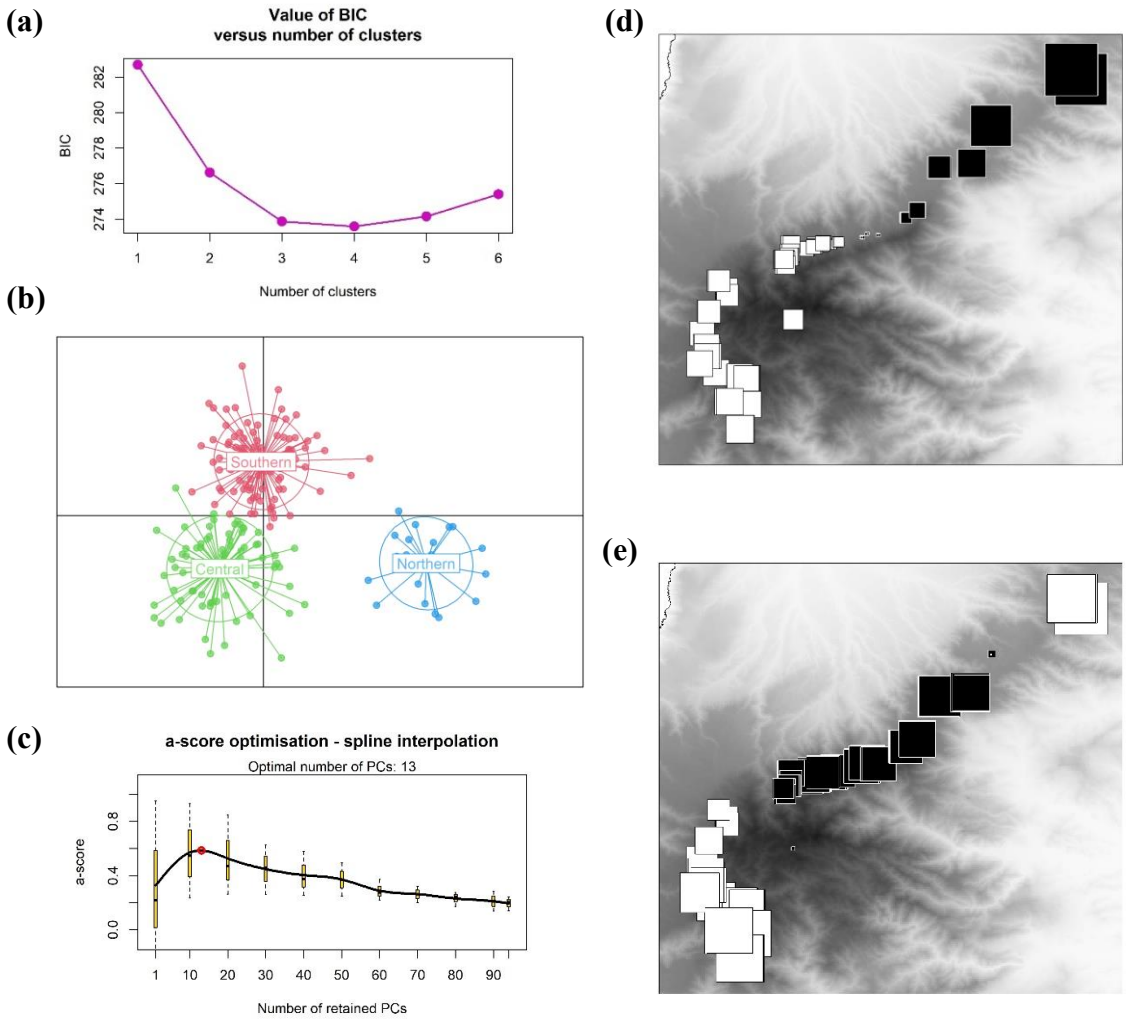

Figure 2. Clustering suggested by the DAPC and sPCA. **(a)** BIC profile of the DAPC with K ranging from 1 to 6. **(b)** Biplot of the first two components of the DAPC, with clusters named according to their geographic location. **(c)** Profile of the spline interpolation of the a-scores of the DAPC, showing the optimal number of informative principal components. **(d)** Distribution of the scores of the first and **(e)** second components identified by the sPCA. Black boxes correspond to negative scores, white ones to positive, and areas of the squares are proportional to the absolute value of the scores.

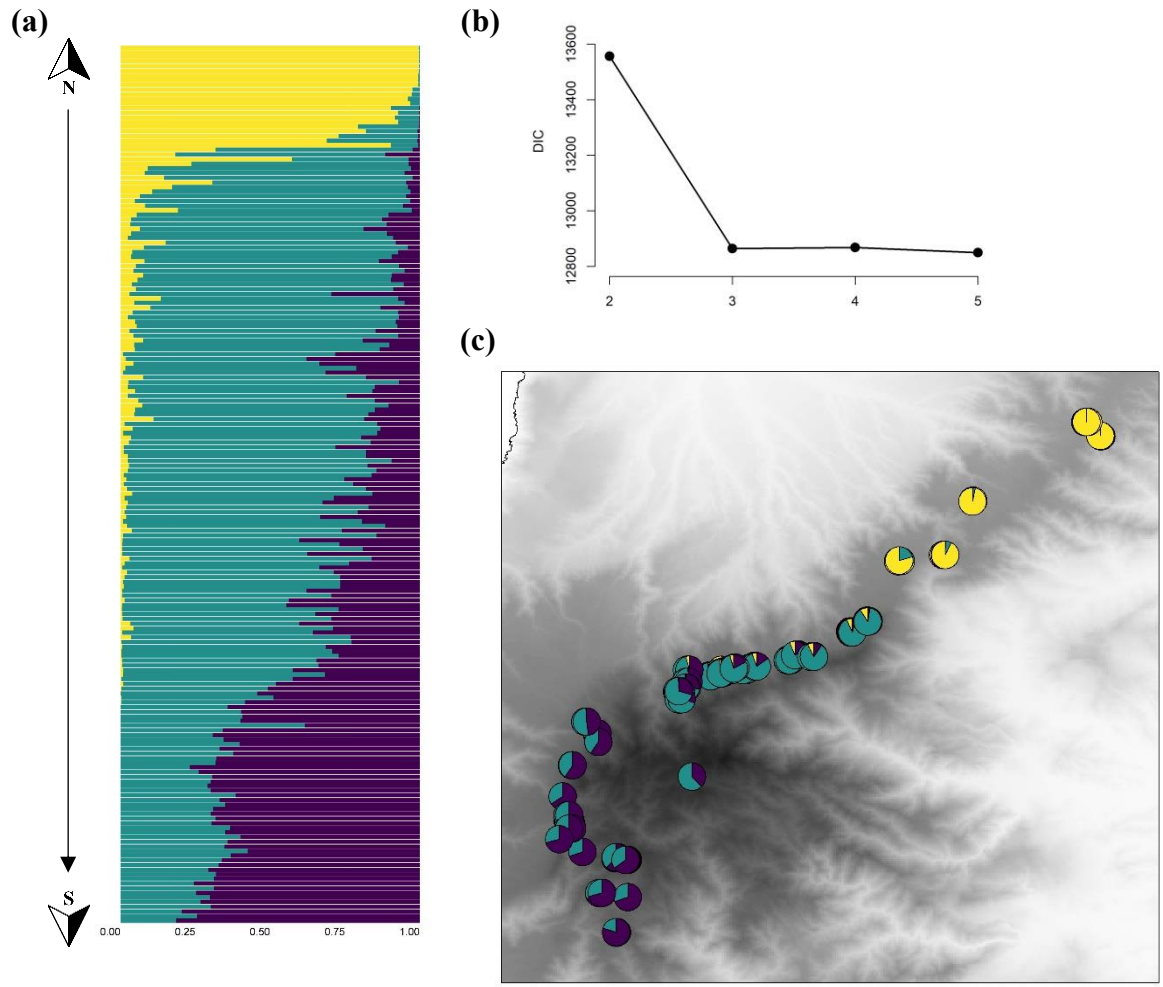

Figure 3. Results of the analysis conducted with TESS. **(a)** The contribution each individual's genotype receives from the three genetic clusters inferred from the study; we sorted individuals according to their position along the North-South axis of the area. **(b)** Profile of the mean DIC values (averaged over 20 replicates) for K ranging from 2 to 5. **(c)** Frequency distributions of each cluster among the individuals.

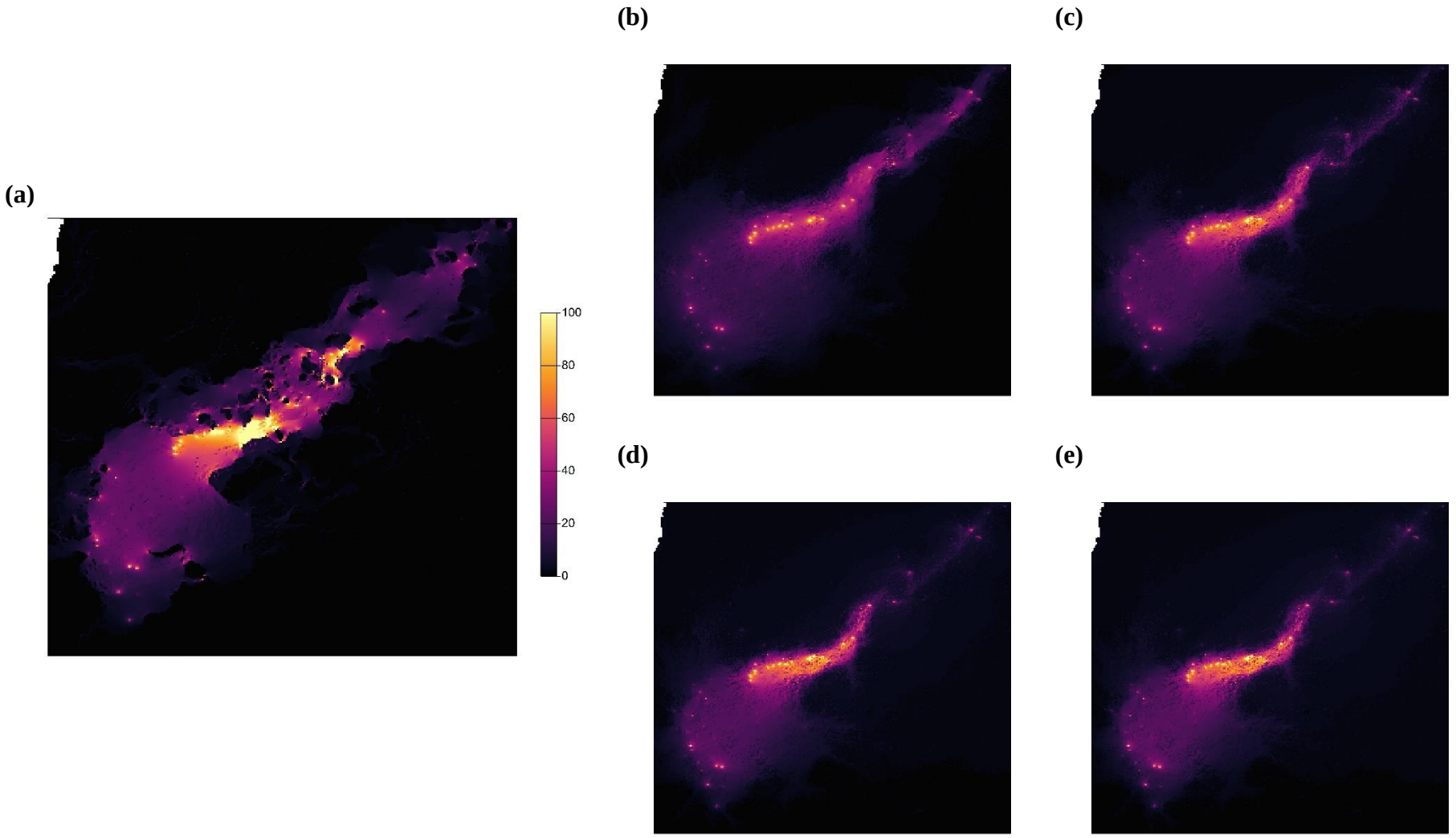

Figure 4. Connectivity corridors of *Salamandra salamandra* in the study area. Maps of the (a) HABITAT connectivity, and **(b)** current and future TOPOCLIM connectivity under **(c)** SSP126, **(d)** SSP370, and **(e)** SSP585 climate change scenarios. For graphical purposes, we capped connectivity values at 100.

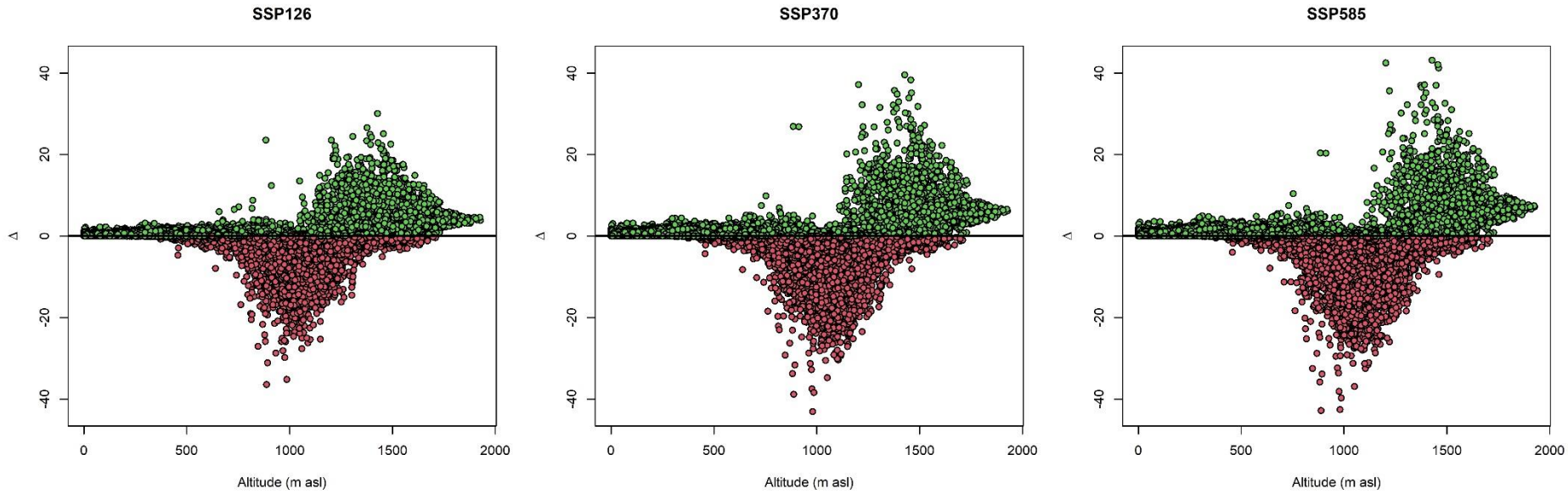

Figure 5. Impact projections of climate change on the connectivity of *Salamandra salamandra* in the study area. We evaluated the current and future connectivity at 100,000 random locations. We then calculated the difference (Δ) between future and current connectivity at these locations for each climate change scenario. Here, connectivity differences are plotted against altitude; future gains are colored in green, while future losses are in red.

Table 1. Mantel tests between individual-based genetic dissimilarity, landscape predictors, and genetic clustering (**TOPOCLIM**: pairwise resistance associated with topoclimatic variation; **HABITAT**: pairwise resistance associated with habitat configuration; **BASINS**: number of hydrographic basins separating each pair of individuals; **FORESTS**: pairwise distance from a shared old-growth forest; **TOPODIST**: pairwise topographic distance).

Variable		**Mantel statistics (*r*)**	***p*-value**
dependent	**independent**		
Individual-based genetic dissimilarity	HABITAT	0.5020	< 0.001
	TOPOCLIM	0.4797	< 0.001
	TOPODIST	0.4253	< 0.001
	Genetic clustering	0.3260	< 0.001
	FORESTS	0.2668	< 0.001
	BASINS	0.1189	0.0019

Table 2. Partial Mantel tests between individual-based genetic dissimilarity, landscape predictors, and genetic clustering. We highlighted in bold the predictor that showed the highest relative weight in each partial Mantel test (**TOPOCLIM**: pairwise resistance associated with topoclimatic variation; **HABITAT**: pairwise resistance associated with habitat configuration; **BASINS**: number of hydrographic basins separating each pair of individuals; **FORESTS**: pairwise distance from a shared old-growth forest; **TOPODIST**: pairwise topographic distance).

Variable			Mantel statistics (*r*)	*p*-value
dependent	**independent**	**control**		
	(a)			
Individual-based genetic dissimilarity	Genetic clustering	**TOPODIST**	0.0157	NS
	TOPODIST	Genetic clustering	0.2892	< 0.001
	(b)			
	BASINS	**TOPODIST**	-0.2572	NS
	TOPODIST	BASINS	0.4734	< 0.001
	(c)			
	FORESTS	**TOPODIST**	0.0201	NS
	TOPODIST	FORESTS	0.3441	< 0.001
	(d)			
	TOPOCLIM	TOPODIST	0.2511	< 0.001
	TOPODIST	**TOPOCLIM**	0.0556	NS
	(e)			
	HABITAT	TOPODIST	0.3264	< 0.001
	TOPODIST	**HABITAT**	0.1468	< 0.001
	(f)			
	TOPOCLIM	**HABITAT**	0.1821	< 0.001
	HABITAT	TOPOCLIM	0.2462	< 0.001
	(g)			
	BASINS	**HABITAT**	-0.0135	NS
	HABITAT	BASINS	0.4913	< 0.001
	(h)			
	FORESTS	**HABITAT**	0.1083	< 0.001
	HABITAT	FORESTS	0.4518	< 0.001

Table 3. Contingency table showing the association between genetic clustering and the geographical distribution of old-growth forest areas. We indicated the expectations under the null hypothesis in parentheses.

	Old-growth forest				
Genetic cluster	**Ferullà**	**Mancuso**	**Pollia**	**Tre Limiti**	
Northern	22 (2.7)	1 (10.2)	0 (3.9)	0 (6.2)	**23**
Central	0 (13.6)	83 (52.0)	32 (19.8)	2 (31.6)	**117**
Southern	0 (5.7)	0 (21.8)	0 (8.3)	49 (13.2)	**49**
	22	**84**	**32**	**51**	**total = 189**

Authors contributions

Daniele Canestrelli conceived the study. **Daniele Canestrelli** and **Antonino Siclari** funded the study. **Giuseppe Martino** collected the tissue samples. **Andrea Chiocchio** and **Roberta Bisconti** performed DNA extraction and sequencing. **Daniele Delle Monache** and **Andrea Chiocchio** performed the genetic analyses. **Daniele Delle Monache** performed the statistical modeling. **Daniele Delle Monache** drafted the manuscript with contributions from **Andrea Chiocchio** and **Daniele Canestrelli**. All the co-authors read and approved the manuscript.

References

Aeschimann, D., Lauber, K., Moser, D. M., & Theurillat, J. P. (2004). *Flora Alpina*. Bern.

Allendorf, F. W., Luikart, G. H., & Aitken, S. N. (2012). *Conservation and the genetics of populations*. John Wiley & Sons.

Anderson, S. P., Hinckley, E. L., Kelly, P., & Langston, A. (2014). Variation in critical zone processes and architecture across slope aspects. *Procedia Earth and Planetary Science*, *10*, 28–33.

Bakarr, M. I., Fonseca, G. A., Mittermeier, R., Rylands, A. B., & Peinemilla, K. W. (2001). Hunting and bushmeat utilization in the African rainforest. *Advances in Applied Biodiversity Science*, *2*, 170.

Barbet-Massin, M., Jiguet, F., Albert, C. H., & Thuiller, W. (2012). Selecting pseudo-absences for species distribution models: How, where and how many?. *Methods in Ecology and Evolution*, *3*(2), 327–338.

Barry, R. G., & Blanken, P. D. (2016). *Microclimate and local climate*. Cambridge University Press.

Barthlott, W., Hostert, A., Kier, G., Kueper, W., Kreft, H., Mutke, J., ... & Sommer, J. H. (2007). Geographic patterns of vascular plant diversity at continental to global scales (Geographische Muster der Gefäßpflanzenvielfalt im kontinentalen und globalen Maßstab). *Erdkunde*, 305–315.

Barthlott, W., Lauer, W., & Placke, A. (1996). Global distribution of species diversity in vascular plants: Towards a world map of phytodiversity. *Erdkunde*, 317–327.

Belkhir, K., Borsa, P., Chikhi, L., Raufaste, N., & Bonhomme, F. (2004). GENETIX 4.05. *Population Genetics Software for Windows TM, University of Montpellier*.

Betts, M. G., Phalan, B., Frey, S. J., Rousseau, J. S., & Yang, Z. (2018). Old-growth forests buffer climate-sensitive bird populations from warming. *Diversity and Distributions*, *24*(4), 439–447.

Beven, K. J., & Kirkby, M. J. (1979). A physically based, variable contributing area model of basin hydrology. *Hydrological Sciences Journal*, *24*(1), 43–69.

Bivand, R., & Yu, D. (2020). spgwr: Geographically weighted regression. *R package version 0.6-34*.

Brooks, T. M., Mittermeier, R. A., Mittermeier, C. G., Da Fonseca, G. A., Rylands, A. B., Konstant, W. R., ... & Hilton-Taylor, C. (2002). Habitat loss and extinction in the hotspots of biodiversity. *Conservation Biology*, *16*(4), 909–923.

Brullo, S., Scelsi, F., & Spampinato, G. (2001). *La Vegetazione dell'Aspromonte. Studio fitosociologico*. Laruffa editore. Reggio Calabria.

Camacho-Sanchez, M., Quintanilla, I., Hawkins, M. T., Tuh, F. Y., Wells, K., Maldonado, J. E., & Leonard, J. A. (2018). Interglacial refugia on tropical mountains: novel insights from the summit rat (*Rattus baluensis*), a Borneo mountain endemic. *Diversity and Distributions*, *24*(9), 1252–1266.

Canestrelli, D., Aloise, G., Cecchetti, S., & Nascetti, G. (2010). Birth of a hotspot of intraspecific genetic diversity: notes from the underground. *Molecular Ecology*, *19*(24), 5432–5451.

Canestrelli, D., Cimmaruta, R., & Nascetti, G. (2008). Population genetic structure and diversity of the Apennine endemic stream frog, *Rana italica*–insights on the Pleistocene evolutionary history of the Italian peninsular biota. *Molecular Ecology*, *17*(17), 3856–3872.

Canestrelli, D., Sacco, F., & Nascetti, G. (2012). On glacial refugia, genetic diversity, and microevolutionary processes: deep phylogeographical structure in the endemic newt *Lissotriton italicus*. *Biological Journal of the Linnean Society*, *105*(1), 42–55.

Carnaval, A. C., Hickerson, M. J., Haddad, C. F., Rodrigues, M. T., & Moritz, C. (2009). Stability predicts genetic diversity in the Brazilian Atlantic forest hotspot. *Science*, *323*(5915), 785–789.

CEPF (Critical Ecosystem Partnership Fund) - The Biodiversity hotspots (2014, November). http://www.cepf.net/resources/hotspots/Pages/default.aspx

Chan, W. P., Chen, I. C., Colwell, R. K., Liu, W. C., Huang, C. Y., & Shen, S. F. (2016). Seasonal and daily climate variation have opposite effects on species elevational range size. *Science*, *351*(6280), 1437–1439.

Chen, C., Durand, E., Forbes, F., & François, O. (2007). Bayesian clustering algorithms ascertaining spatial population structure: a new computer program and a comparison study. *Molecular Ecology Notes*, *7*(5), 747–756.

Chen, I. C., Hill, J. K., Ohlemüller, R., Roy, D. B., & Thomas, C. D. (2011). Rapid range shifts of species associated with high levels of climate warming. *Science*, *333*(6045), 1024–1026.

Cincotta, R. P., Wisnewski, J., & Engelman, R. (2000). Human population in the biodiversity hotspots. *Nature*, *404*(6781), 990–992.

Colacino, M., Conte, M., & Piervitali, E. (1997). Elementi di climatologia della Calabria. *IFA-CNR, Rome*.

Corlett, R. T., & Westcott, D. A. (2013). Will plant movements keep up with climate change?. *Trends in Ecology & Evolution*, *28*(8), 482–488.

Crutzen, P. J., Delany, A. C., Greenberg, J., Haagenson, P., Heidt, L., Lueb, R., ... & Zimmerman, P. (1985). Tropospheric chemical composition measurements in Brazil during the dry season. *Journal of Atmospheric Chemistry*, *2*, 233–256.

Cushman, S. A. (2006). Effects of habitat loss and fragmentation on amphibians: a review and prospectus. *Biological Conservation*, *128*(2), 231–240.

Cushman, S. A., McKelvey, K. S., Hayden, J., & Schwartz, M. K. (2006). Gene flow in complex landscapes: testing multiple hypotheses with causal modeling. *The American Naturalist*, *168*(4), 486–499.

Daws, M. I., Mullins, C. E., Burslem, D. F., Paton, S. R., & Dalling, J. W. (2002). Topographic position affects the water regime in a semideciduous tropical forest in Panama. *Plant and Soil*, *238*, 79–89.

De Fioravante, P., Strollo, A., Assennato, F., Marinosci, I., Congedo, L., & Munafò, M. (2021). High resolution land cover integrating copernicus products: A 2012–2020 map of Italy. *Land*, *11*(1), 35.

De Frenne, P., Lenoir, J., Luoto, M., Scheffers, B. R., Zellweger, F., Aalto, J., ... & Hylander, K. (2021). Forest microclimates and climate change: Importance, drivers and future research agenda. *Global Change Biology*, *27*(11), 2279–2297.

De Frenne, P., Zellweger, F., Rodríguez-Sánchez, F., Scheffers, B. R., Hylander, K., Luoto, M., ... & Lenoir, J. (2019). Global buffering of temperatures under forest canopies. *Nature Ecology & Evolution*, *3*(5), 744–749.

De Lombaerde, E., Vangansbeke, P., Lenoir, J., Van Meerbeek, K., Lembrechts, J., Rodríguez-Sánchez, F., ... & De Frenne, P. (2022). Maintaining forest cover to enhance temperature buffering under future climate change. *Science of the Total Environment*, *810*, 151338.

De Luca, G., & Modica, G. (2022, September). Canopy fire effects estimation using Sentinel-2 imagery and deep learning approach. A case study on the Aspromonte National Park. In *International Conference on Applied Intelligence and Informatics* (pp. 403–417). Cham: Springer Nature Switzerland.

Dobrowski, S. Z. (2011). A climatic basis for microrefugia: the influence of terrain on climate. *Global Change Biology*, *17*(2), 1022–1035.

Epps, C. W., Wehausen, J. D., Bleich, V. C., Torres, S. G., & Brashares, J. S. (2007). Optimizing dispersal and corridor models using landscape genetics. *Journal of Applied Ecology*, *44*(4), 714–724.

Ewers, R. M., & Banks-Leite, C. (2013). Fragmentation impairs the microclimate buffering effect of tropical forests. *PLoS One*, *8*(3), e58093.

Fahrig, L. (2003). Effects of habitat fragmentation on biodiversity. *Annual Review of Ecology, Evolution, and Systematics*, *34*(1), 487–515.

Fischer, J., & Lindenmayer, D. B. (2007). Landscape modification and habitat fragmentation: a synthesis. *Global Ecology and Biogeography*, *16*(3), 265–280.

Forest, F., Grenyer, R., Rouget, M., Davies, T. J., Cowling, R. M., Faith, D. P., ... & Savolainen, V. (2007). Preserving the evolutionary potential of floras in biodiversity hotspots. *Nature, 445*(7129), 757–760.

François, O., & Durand, E. (2010). Spatially explicit Bayesian clustering models in population genetics. *Molecular Ecology Resources, 10*(5), 773–784.

Frankham, R. (2010). Challenges and opportunities of genetic approaches to biological conservation. *Biological Conservation, 143*(9), 1919–1927.

Frey, S. J., Hadley, A. S., Johnson, S. L., Schulze, M., Jones, J. A., & Betts, M. G. (2016). Spatial models reveal the microclimatic buffering capacity of old-growth forests. *Science Advances, 2*(4), e1501392.

Geiger, R., Aron, R. H., & Todhunter, P. (2009). *The climate near the ground*. Rowman & Littlefield.

Gibbons, J. M., & Newbery, D. M. (2003). Drought avoidance and the effect of local topography on trees in the understorey of Bornean lowland rain forest. *Plant Ecology*, 164, 1–18.

Goudet, J. (1995). FSTAT (version 1.2): a computer program to calculate F-statistics. *Journal of Heredity, 86*(6), 485–486.

Groves, R. H., & Di Castri, F. (Eds.). (1991). *Biogeography of Mediterranean invasions*. Cambridge University Press.

Haddad, N. M., Brudvig, L. A., Clobert, J., Davies, K. F., Gonzalez, A., Holt, R. D., ... & Townshend, J. R. (2015). Habitat fragmentation and its lasting impact on Earth's ecosystems. *Science Advances, 1*(2), e1500052.

Hansen, M. C., Potapov, P. V., Moore, R., Hancher, M., Turubanova, S. A., Tyukavina, A., ... & Townshend, J. R. (2013). High-resolution global maps of 21st-century forest cover change. *Science, 342*(6160), 850–853.

Hendrix, R., Susanne Hauswaldt, J., Veith, M., & Steinfartz, S. (2010). Strong correlation between cross-amplification success and genetic distance across all members of 'True Salamanders'(Amphibia: Salamandridae) revealed by *Salamandra salamandra*-specific microsatellite loci. *Molecular Ecology Resources, 10*(6), 1038–1047.

Holderegger, R., & Thiel-Egenter, C. (2009). A discussion of different types of glacial refugia used in mountain biogeography and phylogeography. *Journal of Biogeography, 36*(3), 476–480.

Holderegger, R., & Wagner, H. (2006). A brief guide to landscape genetics. *Landscape Ecology, 21*(6), 793–796.

Hoorn, C., Perrigo, A., & Antonelli, A. (Eds.). (2018). *Mountains, climate and biodiversity*. John Wiley & Sons.

Iannella, M., D'Alessandro, P., & Biondi, M. (2018). Evidences for a shared history for spectacled salamanders, haplotypes and climate. *Scientific Reports*, *8*(1), 16507.

Jakobsson, M., & Rosenberg, N. A. (2007). CLUMPP: a cluster matching and permutation program for dealing with label switching and multimodality in analysis of population structure. *Bioinformatics*, *23*(14), 1801–1806.

Janzen, D. H. (1967). Why mountain passes are higher in the tropics. *The American Naturalist*, *101*(919), 233–249.

John, R., Dalling, J. W., Harms, K. E., Yavitt, J. B., Stallard, R. F., Mirabello, M., ... & Foster, R. B. (2007). Soil nutrients influence spatial distributions of tropical tree species. *Proceedings of the National Academy of Sciences*, *104*(3), 864–869.

Jombart, T., Devillard, S., Dufour, A. B., & Pontier, D. (2008). Revealing cryptic spatial patterns in genetic variability by a new multivariate method. *Heredity*, *101*(1), 92–103.

Jombart, T., Devillard, S., & Balloux, F. (2010). Discriminant analysis of principal components: a new method for the analysis of genetically structured populations. *BMC Genetics*, *11*(1), 1–15.

Kapos, V., Rhind, J., Edwards, M., Price, M. F., & Ravilious, C. (2000). Developing a map of the world's mountain forests. In *Forests in sustainable mountain development: a state of knowledge report for 2000. Task Force on Forests in Sustainable Mountain Development*. (pp. 4–19). Wallingford UK: Cabi Publishing.

Karger, D. N., Conrad, O., Böhner, J., Kawohl, T., Kreft, H., Soria-Auza, R. W., ... & Kessler, M. (2017). Climatologies at high resolution for the Earth's land surface areas. *Scientific Data*, *4*(1), 1–20.

Keyghobadi, N. (2007). The genetic implications of habitat fragmentation for animals. *Canadian Journal of Zoology*, *85*(10), 1049–1064.

Klinga, P., Mikoláš, M., Smolko, P., Tejkal, M., Höglund, J., & Paule, L. (2019). Considering landscape connectivity and gene flow in the Anthropocene using complementary landscape genetics and habitat modelling approaches. *Landscape Ecology*, *34*, 521–536.

Kolozsvary, M. B., & Swihart, R. K. (1999). Habitat fragmentation and the distribution of amphibians: patch and landscape correlates in farmland. *Canadian Journal of Zoology*, *77*(8), 1288–1299.

Kopecký, M., Macek, M., & Wild, J. (2021). Topographic Wetness Index calculation guidelines based on measured soil moisture and plant species composition. *Science of the Total Environment*, *757*, 143785.

Körner, C. (2003). *Alpine plant life: functional plant ecology of high mountain ecosystems; with 47 tables*. Springer Science & Business Media.

Körner, C. (2004). Mountain biodiversity, its causes and function. *AMBIO: A Journal of the Human Environment*, *33*, 11–17.

Körner, C., Jetz, W., Paulsen, J., Payne, D., Rudmann-Maurer, K., & M Spehn, E. (2017). A global inventory of mountains for bio-geographical applications. *Alpine Botany*, *127*, 1–15.

Lanza, B. (2007). *Fauna d'Italia: Amphibia*. Ed. Calderini.

Lenoir, J., Hattab, T., & Pierre, G. (2017). Climatic microrefugia under anthropogenic climate change: implications for species redistribution. *Ecography*, *40*(2), 253–266.

Leo, M. (1995). The importance of tropical montane cloud forest for preserving vertebrate endemism in Peru: the Rio Abiseo National Park as a case study. In *Tropical montane cloud forests* (pp. 198–211). New York, NY: Springer US.

Li, S., Zhao, Z., Miaomiao, X., & Wang, Y. (2010). Investigating spatial non-stationary and scale-dependent relationships between urban surface temperature and environmental factors using geographically weighted regression. *Environmental Modelling & Software*, *25*(12), 1789–1800.

Lourenço, A., Gonçalves, J., Carvalho, F., Wang, I. J., & Velo-Antón, G. (2019). Comparative landscape genetics reveals the evolution of viviparity reduces genetic connectivity in fire salamanders. *Molecular Ecology*, *28*(20), 4573–4591.

Luyssaert, S., Schulze, E. D., Börner, A., Knohl, A., Hessenmöller, D., Law, B. E., ... & Grace, J. (2008). Old-growth forests as global carbon sinks. *Nature*, *455*(7210), 213–215.

Manel, S., Schwartz, M. K., Luikart, G., & Taberlet, P. (2003). Landscape genetics: combining landscape ecology and population genetics. *Trends in Ecology & Evolution*, *18*(4), 189–197.

Malishev, M., Bull, C. M., & Kearney, M. R. (2018). An individual-based model of ectotherm movement integrating metabolic and microclimatic constraints. *Methods in Ecology and Evolution*, *9*(3), 472–489.

Martino, G., Chiocchio, A., Siclari, A., & Canestrelli, D. (2022). Distribution and conservation status of threatened endemic amphibians within the Aspromonte mountain region, a hotspot of Mediterranean biodiversity. *Nature Conservation*, *50*, 1–22.

McCullough, I. M., Davis, F. W., Dingman, J. R., Flint, L. E., Flint, A. L., Serra-Diaz, J. M., ... & Franklin, J. (2016). High and dry: high elevations disproportionately exposed to regional climate change in Mediterranean-climate landscapes. *Landscape Ecology*, *31*, 1063–1075.

McLauchlan, K. K., Higuera, P. E., Miesel, J., Rogers, B. M., Schweitzer, J., Shuman, J. K., ... & Watts, A. C. (2020). Fire as a fundamental ecological process: Research advances and frontiers. *Journal of Ecology*, *108*(5), 2047–2069.

Médail, F., & Diadema, K. (2009). Glacial refugia influence plant diversity patterns in the Mediterranean Basin. *Journal of Biogeography*, *36*(7), 1333–1345.

Médail, F., & Quézel, P. (1997). Hot-spots analysis for conservation of plant biodiversity in the Mediterranean Basin. *Annals of the Missouri Botanical Garden*, 112–127.

Menéndez, R., González-Megías, A., Jay-Robert, P., & Marquéz-Ferrando, R. (2014). Climate change and elevational range shifts: Evidence from dung beetles in two European mountain ranges. *Global Ecology and Biogeography*, *23*(6), 646–657.

Molles, M. C., & Tibbets, T. (2002). *Ecology: concepts and applications* (pp. 186–254). New York: McGraw-Hill.

Murphy, M. A., Dezzani, R., Pilliod, D. S., & Storfer, A. (2010). Landscape genetics of high mountain frog metapopulations. *Molecular Ecology*, *19*(17), 3634–3649.

Mutke, J., & Barthlott, W. (2005). Patterns of vascular plant diversity at continental to global scales. *Biologiske Skrifter*, *55*(4), 521–531.

Myers, N., Mittermeier, R. A., Mittermeier, C. G., Da Fonseca, G. A., & Kent, J. (2000). Biodiversity hotspots for conservation priorities. *Nature*, *403*(6772), 853–858.

Nadeau, C. P., Giacomazzo, A., & Urban, M. C. (2022). Cool microrefugia accumulate and conserve biodiversity under climate change. *Global Change Biology*, *28*(10), 3222–3235.

Noroozi, J., Talebi, A., Doostmohammadi, M., Rumpf, S. B., Linder, H. P., & Schneeweiss, G. M. (2018). Hotspots within a global biodiversity hotspot-areas of endemism are associated with high mountain ranges. *Scientific Reports*, *8*(1), 10345.

Ohlemüller, R., Anderson, B. J., Araujo, M. B., Butchart, S. H., Kudrna, O., Ridgely, R. S., & Thomas, C. D. (2008). The coincidence of climatic and species rarity: high risk to small-range species from climate change. *Biology Letters*, *4*(5), 568–572.

Ozenda, P., & Borel, J. L. (2003). 3.4 The Alpine Vegetation of the Alps. *Alpine Biodiversity in Europe*, *167*, 53.

Paillet, Y., Bergès, L., Hjältén, J., Ódor, P., Avon, C., Bernhardt-Römermann, M., ... & Virtanen, R. (2010). Biodiversity differences between managed and unmanaged forests: Meta-analysis of species richness in Europe. *Conservation Biology*, *24*(1), 101–112.

Parmesan, C. (2006). Ecological and evolutionary responses to recent climate change. *Annual Review of Ecology, Evolution, and Systematics*, 637–669.

Pastore, M. A., Classen, A. T., D'Amato, A. W., Foster, J. R., & Adair, E. C. (2022). Cold-air pools as microrefugia for ecosystem functions in the face of climate change. *Ecology*, *103*(8), e3717.

Pătru-Stupariu, I., Hossu, C. A., Grădinaru, S. R., Nita, A., Stupariu, M. S., Huzui-Stoiculescu, A., & Gavrilidis, A. A. (2020). A review of changes in mountain land use and ecosystem services: From theory to practice. *Land, 9*(9), 336.

Patsiou, T. S., Conti, E., Zimmermann, N. E., Theodoridis, S., & Randin, C. F. (2014). Topo-climatic microrefugia explain the persistence of a rare endemic plant in the Alps during the last 21 millennia. *Global Change Biology*, *20*(7), 2286–2300.

Pauli, H., Gottfried, M., Dirnböck, T., Dullinger, S., & Grabherr, G. (2003). *Assessing the long-term dynamics of endemic plants at summit habitats* (pp. 195–207). Springer Berlin Heidelberg.

Pepin, N., Bradley, R. S., Diaz, H. F., Baraër, M., Caceres, E. B., Forsythe, N., ... & Mountain Research Initiative EDW Working Group. (2015). Elevation-dependent warming in mountain regions of the world. *Nature Climate Change*, *5*(5), 424–430.

Piovesan, G., Baliva, M., Calcagnile, L., D'Elia, M., Dorado-Linan, I., Palli, J., ... & Quarta, G. (2020). Radiocarbon dating of Aspromonte sessile oaks reveals the oldest dated temperate flowering tree in the world. *Ecology*, *101*(12), 1–4.

Porter, W. P., Sabo, J. L., Tracy, C. R., Reichman, O. J., & Ramankutty, N. (2002). Physiology on a landscape scale: plant-animal interactions. *Integrative and Comparative Biology*, *42*(3), 431–453.

R Core Team (2022). R: A language and environment for statistical computing. R Foundation for Statistical Computing, Vienna, Austria.

Rahbek, C., Borregaard, M. K., Colwell, R. K., Dalsgaard, B. O., Holt, B. G., Morueta-Holme, N., ... & Fjeldså, J. (2019). Humboldt's enigma: What causes global patterns of mountain biodiversity?. *Science*, *365*(6458), 1108–1113.

Reid, I. (1973). The influence of slope orientation upon the soil moisture regime, and its hydrogeomorphological significance. *Journal of Hydrology*, *19*(4), 309–321.

Robb, J., Chesson, M. S., Forbes, H., Foxhall, L., Foxhall-Forbes, H., Lazrus, P. K., ... & Yoon, D. (2021). The twentieth century invention of ancient mountains: the archaeology of highland Aspromonte. *International Journal of Historical Archaeology*, *25*, 14–44.

Rodgers, W. A., & Homewood, K. M. (1982). Species richness and endemism in the Usambara mountain forests, Tanzania. *Biological Journal of the Linnean Society*, *18*(3), 197–242.

Sandel, B., Arge, L., Dalsgaard, B., Davies, R. G., Gaston, K. J., Sutherland, W. J., & Svenning, J. C. (2011). The influence of Late Quaternary climate-change velocity on species endemism. *Science*, *334*(6056), 660–664.

Särkinen, T., Pennington, R. T., Lavin, M., Simon, M. F., & Hughes, C. E. (2012). Evolutionary islands in the Andes: persistence and isolation explain high endemism in Andean dry tropical forests. *Journal of Biogeography*, *39*(5), 884–900.

Scherrer, D., & Körner, C. (2010). Infra-red thermometry of alpine landscapes challenges climatic warming projections. *Global Change Biology*, *16*(9), 2602–2613.

Scherrer, D., & Körner, C. (2011). Topographically controlled thermal-habitat differentiation buffers alpine plant diversity against climate warming. *Journal of Biogeography*, *38*(2), 406–416.

Schulte, U., Küsters, D., & Steinfartz, S. (2007). A PIT tag based analysis of annual movement patterns of adult fire salamanders (*Salamandra salamandra*) in a Middle European habitat. *Amphibia-Reptilia*, *28*(4), 531–536.

Sears, M. W., Raskin, E., & Angilletta Jr, M. J. (2011). The world is not flat: defining relevant thermal landscapes in the context of climate change. *Integrative and Comparative Biology*, *51*(5), 666–675.

Shah, V. B., & McRae, B. H. (2008). Circuitscape: a tool for landscape ecology. In *Proceedings of the 7th Python in Science Conference* (Vol. 7, pp. 62–66). Pasadena, California: SciPy.

Shirk, A. J., Landguth, E. L., & Cushman, S. A. (2017). A comparison of individual-based genetic distance metrics for landscape genetics. *Molecular Ecology Resources*, 17(6), 1308–1317.

Singh, S. (2018). Understanding the role of slope aspect in shaping the vegetation attributes and soil properties in Montane ecosystems. *Tropical Ecology*, *59*(3), 417–430.

Smouse, P. E., Long, J. C., & Sokal, R. R. (1986). Multiple regression and correlation extensions of the Mantel test of matrix correspondence. *Systematic Zoology*, *35*(4), 627–632.

Smythies, B. E. (1964). The birds of Mt Kinabalu and their zoogeographical relationships. *Proceedings of the Royal Society B: Biological Sciences*, *161*(982), 75–80.

Spampinato, G., Cameriere, P., Caridi, D., & Crisafulli, A. (2008). Carta della biodiversità vegetale del Parco Nazionale dell'Aspromonte (Italia meridionale). *Quaderni di Botanica Ambientale e Applicata*, *19*, 3–36.

Spehn, E. M., Rudmann-Maurer, K., Körner, C., & Maselli, D. (2010). Mountain Biodiversity and Global Change. Basel, GMBA-DIVERSITAS.

Steadman, D. W. (1995). Prehistoric extinctions of Pacific island birds: biodiversity meets zooarchaeology. *Science*, *267*(5201), 1123–1131.

Stein, A., Gerstner, K., & Kreft, H. (2014). Environmental heterogeneity as a universal driver of species richness across taxa, biomes and spatial scales. *Ecology Letters*, *17*(7), 866–880.

Steinfartz, S., Kuesters, D., & Tautz, D. (2004). Isolation and characterization of polymorphic tetranucleotide microsatellite loci in the Fire salamander *Salamandra salamandra* (Amphibia: Caudata). *Molecular Ecology Notes*, *4*(4), 626–628.

Stewart, J. R., Lister, A. M., Barnes, I., & Dalén, L. (2010). Refugia revisited: individualistic responses of species in space and time. *Proceedings of the Royal Society B: Biological Sciences*, *277*(1682), 661–671.

Storfer, A., Murphy, M. A., Evans, J. S., Goldberg, C. S., Robinson, S., Spear, S. F., ... & Waits, L. P. (2007). Putting the 'landscape' in landscape genetics. *Heredity*, *98*(3), 128–142.

Stuart, S. N., Chanson, J. S., Cox, N. A., Young, B. E., Rodrigues, A. S., Fischman, D. L., & Waller, R. W. (2004). Status and trends of amphibian declines and extinctions worldwide. *Science*, *306*(5702), 1783–1786.

Su, Y. F., Foody, G. M., & Cheng, K. S. (2012). Spatial non-stationarity in the relationships between land cover and surface temperature in an urban heat island and its impacts on thermally sensitive populations. *Landscape and Urban Planning*, *107*(2), 172–180.

Telwala, Y., Brook, B. W., Manish, K., & Pandit, M. K. (2013). Climate-induced elevational range shifts and increase in plant species richness in a Himalayan biodiversity epicentre. *PLoS One*, *8*(2), e57103.

Thomas, C. D., Cameron, A., Green, R. E., Bakkenes, M., Beaumont, L. J., Collingham, Y. C., ... & Williams, S. E. (2004). Extinction risk from climate change. *Nature*, *427*(6970), 145–148.

Thuiller, W., Georges, D., Gueguen, M., Engler, R., Breiner, F., Lafourcade, B., & Patin, R. (2023). biomod2: Ensemble platform for species distribution modeling. *R package version 4.2-2*.

Todisco, V., Gratton, P., Cesaroni, D., & Sbordoni, V. (2010). Phylogeography of *Parnassius apollo*: hints on taxonomy and conservation of a vulnerable glacial butterfly invader. *Biological Journal of the Linnean Society*, *101*(1), 169–183.

Trense, D., Schmidt, T. L., Yang, Q., Chung, J., Hoffmann, A. A., & Fischer, K. (2021). Anthropogenic and natural barriers affect genetic connectivity in an Alpine butterfly. *Molecular Ecology*, *30*(1), 114–130.

Tian, F., Qiu, G. Y., Yang, Y. H., Xiong, Y. J., & Wang, P. (2012). Studies on the relationships between land surface temperature and environmental factors in an inland river catchment based on geographically weighted regression and MODIS data. *IEEE Journal of Selected Topics in Applied Earth Observations and Remote Sensing*, *5*(3), 687–698.

Trew, B. T., & Maclean, I. M. (2021). Vulnerability of global biodiversity hotspots to climate change. *Global Ecology and Biogeography*, *30*(4), 768–783.

Turner, W. R., Bradley, B. A., Estes, L. D., Hole, D. G., Oppenheimer, M., & Wilcove, D. S. (2010). Climate change: helping nature survive the human response. *Conservation Letters*, *3*(5), 304–312.

van Dijk, P. P., Stuart, B. L., & Rhodin, A. G. (2000). Asian turtle trade. *Chelonian Research Monographs*, *2*, 1–164.

Van Oosterhout, C., Hutchinson, W. F., Wills, D. P., & Shipley, P. (2004). MICRO-CHECKER: software for identifying and correcting genotyping errors in microsatellite data. *Molecular Ecology Notes*, *4*(3), 535–538.

Vega, R., Amori, G., Aloise, G., Cellini, S., Loy, A., & Searle, J. B. (2010). Genetic and morphological variation in a Mediterranean glacial refugium: evidence from Italian pygmy shrews, *Sorex minutus* (Mammalia: Soricomorpha). *Biological Journal of the Linnean Society*, *100*(4), 774–787.

Vitasse, Y., Ursenbacher, S., Klein, G., Bohnenstengel, T., Chittaro, Y., Delestrade, A., ... & Lenoir, J. (2021). Phenological and elevational shifts of plants, animals and fungi under climate change in the European Alps. *Biological Reviews*, *96*(5), 1816–1835.

Wake, D. B., & Vredenburg, V. T. (2008). Are we in the midst of the sixth mass extinction? A view from the world of amphibians. *Proceedings of the National Academy of Sciences*, *105*, 11466–11473.

Wang, I. J. (2020). Topographic path analysis for modelling dispersal and functional connectivity: calculating topographic distances using the topoDistance R package. *Methods in Ecology and Evolution*, *11*(2), 265–272.

Wasserman, T. N., Cushman, S. A., Schwartz, M. K., & Wallin, D. O. (2010). Spatial scaling and multi-model inference in landscape genetics: Martes americana in northern Idaho. *Landscape Ecology*, *25*, 1601–1612.

Wolf, C., Bell, D. M., Kim, H., Nelson, M. P., Schulze, M., & Betts, M. G. (2021). Temporal consistency of undercanopy thermal refugia in old-growth forest. *Agricultural and Forest Meteorology*, *307*, 108520.

Zachos, F. E., & Habel, J. C. (Eds.). (2011). *Biodiversity hotspots: distribution and protection of conservation priority areas*. Springer Science & Business Media.

Zampiglia, M., Bisconti, R., Maiorano, L., Aloise, G., Siclari, A., Pellegrino, F., ... & Canestrelli, D. (2019). Drilling down hotspots of intraspecific diversity to bring them into on-ground conservation of threatened species. *Frontiers in Ecology and Evolution*, *7*, 205.

4. Influence of microclimates and forest landscapes on pollinator diversity in a mountain hotspot of biodiversity

Abstract

Pollinating insects are instrumental in the ecosystem services they provide. Here, we present a preliminary analysis exploring whether Aspromonte's microclimatic features and forest landscapes influence its extraordinary pollinator diversity. We found higher pollinator diversity in heterogeneous agricultural areas, while land uses/covers associated with human disturbance had fewer. Interestingly, the proximity to old-growth forests seemingly promoted pollinator diversity, too. In this sense, although far from being statistically robust, we obtained hints that forest microclimates could shape pollinators' species richness. Given our results, deepening the mechanisms driving such influences is necessary.

Keywords

mountain biodiversity hotspot, pollinator diversity, microclimate, forest cover, land use/cover, old-growth forests.

Introduction

Three-quarters of all crops yielding human food worldwide require insect pollination, primarily by bees (Klein et al., 2007). Pollination worldwide was estimated to be worth €153 billion, a good 9.5% of the economic value of Earth's crop production for human food in 2005 (Gallai et al., 2009). Sadly, sudden demographic declines of pollinator populations are increasingly reported, with many resulting in species extinctions (Vanbergen et al., 2013; Potts et al., 2016). According to the latest IPBES report, as many as 40% of wild bee and butterfly species are found to be on the brink of extinction (IPBES, 2016). Most wild plant species (80%) directly depend on insect pollination; many are also pollen-limited (Burd, 1994; Ashman et al., 2004). Declines in pollination services particularly undermine obligate outcrossing animal-pollinated plants. Accordingly, several declined in parallel with their pollinators (Biesmeijer et al., 2006). Evidence of pollinators' decline thus raises well-deserved concerns for biodiversity conservation and decreased crop production's economic and social impacts (Gallai et al., 2009).

Threats to the pollinators' survival are manifold; among them are habitat loss, agricultural intensification, anthropogenic climate change, and the spread of pathogens and non-native species (Potts et al., 2010). These threats lead to the disruption of pollinator communities, and predicting the impact of this disruption on the stability of natural and agroecosystems can be complex. If more

diverse pollinators are expected to promote increased seed sets in plant communities (Fontaine et al., 2006), whether and to what extent this will materialize depends on many features of the pollinator community. Larger sets of variably effective pollinators should be more likely to include the most effective ones. However, these sampling effects, while evidenced by a few (Larsen et al., 2005), fail to consider interactions among co-occurring pollinators that promote emergent properties in pollination function (Petanidou et al., 2008; Miljanic et al., 2019). Facilitation, whereby a pollinator increases the fitness of another pollinator, could explain some of these emergent properties; while well-established as a contributor in other contexts (Hooper et al., 2005), facilitation among pollinators has so far received little attention (but see Reyes-González & Zamudio, 2020). Pollinators' complementarity, on the other hand, has a widely recognized impact on pollination function. Whether it is via functional (Blüthgen & Klein, 2011), temporal (Blüthgen & Klein, 2011), interactive (Klein et al., 2008), or quantitative complementarity (Fontaine et al., 2008), the overlap in the functional niches of pollinators within a network drives the increase in function with pollinator diversity. At one end of the spectrum, when pollinators have no overlap in their functional niches, pollination function increases linearly with pollinator diversity. Conversely, redundancy occurs when pollinators share the same functional niche, making pollination function independent from pollinator diversity. Still, variably redundant pollinator communities may prove more stable when faced with structural and compositional changes (Winfree & Kremen, 2009; Miñarro & García, 2018). Somewhere in between, pollination function can still increase even if functional niches remain overlapping and pollinators interfere. This phenomenon has recently been termed "functional enhancement" (Loy & Brosi, 2022) and happens, for instance, when antagonistic interactions spur pollinators to move more quickly from flower to flower (Greenleaf & Kremen, 2006; Carvalheiro et al., 2011).

As the composition of pollinator communities drives so many ecological outcomes, understanding which landscape and climatic components functionally assemble them becomes paramount. This is where the Aspromonte preposterously comes in. Previous studies identified the region as a prominent hotspot of diversity for pollinating insects both intra- and interspecifically. At the same time, its topographic and microclimatic complexity provides the perfect setting to test many fine-scale topographic, microclimatic, and landscape effects on pollinator diversity in conjunction. Extreme temperature variations are, in fact, sources of stress for the organisms and pose severe threats under climate change (Vasseur et al., 2014). Accordingly, many forest-dwelling species rely on buffered understory microclimates for their survival, performance, and distribution (Scheffers et al., 2014; Greiser et al., 2020). Pollinating insects are no different. More stable understory microclimates allow them to forage longer when temperatures are too high (Corbet et al., 1993; Kwon & Saeed, 2003). Microclimates also impact pollinators indirectly when floral pollination-related traits are

controlled by temperature and humidity (Petanidou & Smets, 1996). In addition, pollinating insects are highly sensitive to habitat alteration and land use/cover changes (Rathcke & Jules, 1993). Likewise, forest cover drives pollinator diversity, with sometimes conflicting results (Winfree et al., 2007; Watson et al., 2011).

Here, we investigated pollinator diversity's ecological determinants in topographically heterogeneous landscapes. Building on samples collected from 20 sites and several microclimate time series, we combined pollinator site diversity with microclimatic and forest features that potentially shape it. Our study laid out key elements that will be explored in further analyses soon.

Materials & Methods

Field data

After reviewing the entomological literature, we decided to work on apoids (*sensu* Sann et al., 2018) and hoverflies. These families possess significant functional importance as obligate pollinators and are often used in bioindication (Tscharntke et al., 1998; Urbini et al., 2006; Vieira et al., 2011). From previous surveys, they also appear to be distributed fragmentedly within the Aspromonte, with geographically isolated populations that might constitute interesting spots of genetic diversity. Finally, from a practical viewpoint, they are generally easy to find and sample.

We sampled pollinator communities from 20 sites (Fig. 1), selected to cover the most representative environments of the Aspromonte region; these included broad-leaved and coniferous forests, old-growth forests, former arable land, pastures, and clearings. We installed a chromotropic trap consisting of three plastic bowls holding approximately 150 cl at each site. Each triplet was fixed about 1.5 m above the ground and colored with three different UV-reflecting paints – white, yellow, and blue – according to the pollinators' color preferences (Westphal et al., 2008; O'Connor, 2019). All traps except 001 and 003 remained active for seven days and then emptied for specimen collection, while those at sites 001 and 003 were left for the entire monitoring season. We also installed a data logger (HOBO Pendant MX Water Temperature; range: -20 °C to 70 °C; accuracy: ±0.5 °C; resolution: 0.04 °C) under each trap to characterize the microclimatic conditions at the sampling sites. These data loggers recorded temperatures at hourly intervals; further information can be found in Table A.1 (Appendices). We carried out additional sweep sampling at each site on the day of trap setting, following linear transects with a fixed duration of 30 minutes. We actively searched for pollinators between 8 a.m. and 5 p.m. in sunny weather with no or weak wind. Additionally, we installed two Malaise traps at sites 001 and 003 to make community sampling as comprehensive as

possible. The sampling activity took place between June and September. We stored the collected specimens in ethanol at 96° until molecular investigations.

Morphological and molecular identification

We screened morphologically the specimens immediately after collection. Most taxa were identified at the genus level, while 80% at the species level. We then performed molecular identification on a subsample of specimens representative of the morphological taxa. In particular, we focused on those taxa that could not be identified morphologically and those whose morphology was the most variable within our collection or at the species level. We also focused on those with a more fragmented distribution. We extracted genomic DNA using the CTAB method (Lienhard & Schäffer, 2019). We amplified the cytochrome oxidase I (COI) barcoding sequence, which allows the identification of most insect species (Wilson, 2012). Sequencing was performed using the Macrogen ABI Prism sequencer. We then compared our sequences with those deposited in GenBank (https://www.ncbi.nlm.nih.gov) and BOLD (https://www.boldsystems.org), i.e., the two largest and most up-to-date international genetic sequence databases. Specimens were identified as belonging to reference species when genetic divergence was less than 3%. When divergence was between 3 and 5%, specimens were attributed to a new lineage of the reference species. In cases of significant genetic divergence exceeding 5% – occasionally, even 10% – specimens were attributed to new taxonomic entities. Finally, we compiled the morphological and molecular identification results into each site's taxa lists, constituting the pollinator diversity (i.e., taxa richness) we employed for subsequent analyses. We also compared morphological and molecular identification results to assess the congruence between the two approaches.

Microclimate data

This study evaluated whether increased microclimatic stability could lead to more diverse pollinator communities by quantifying microclimatic buffering, i.e., the ability of forest canopies to dampen free-air temperature fluctuations, and diurnal temperature ranges (DTRs), which reflect the temperature variation within a day and thus indicate the typical weather stability. We aggregated the data loggers' hourly measurements into daily average temperatures. Then, we interpolated average temperatures from 33 weather stations in the study area to predict the daily average topoclimates at the sampling sites for each day. We performed the interpolations via geographically weighted regression (GWR) models with fixed bandwidth; we included altitude, slope, northness, eastness, distance to the coast, and monthly average of daily clear-sky insolation time as physiographic descriptors, which are known topoclimatic forcing factors (Lenoir et al., 2017). More information regarding the weather station data and interpolation procedures can be found in Chapter 2. We fitted

GWR models using the SPGWR R package (Bivand & Yu, 2020). We quantified buffering effects by modeling the slope parameter introduced by Gril et al. (2023); it represents the coefficient of the linear relationship between microclimate and topoclimate. Accordingly, slope parameters lower than 1 indicate dampened microclimates compared to topoclimates (buffering), while greater than 1 suggest higher temperature fluctuations in microclimates than in topoclimates (amplification; Gril et al., 2023). We calculated slopes by fitting linear regression models (LMs) to microclimates (dependent) and topoclimates (independent variable) at the sampling sites (Fig. A.1 and A.2 in Appendices). We expressed slopes logarithmically (log(β)) so that positive values would indicate amplification and negative values buffering. We considered daily average topoclimates whose local R^2 failed to exceed 0.7 unreliable and excluded them from the LMs. Finally, we calculated DTRs by averaging the differences between daily maxima and minima recorded by each data logger; the respective formula is therefore:

$$\mathrm{DTR} = \frac{1}{n}\sum(t_{max} - t_{min})$$

where n is the length of the daily microclimate time series.

Land use/cover and forest predictors

The heterogeneity of forest landscapes in Aspromonte allowed us to investigate the impact of forest density and vertical structure on pollinating insects' diversification. We also evaluated whether pollinator diversity depended on land use/land cover and the proximity to old-growth forests. We characterized forest density by retrieving the Forest Landscape Integrity Index (FLII; Grantham et al., 2020). This index measures the ecological integrity of Earth's forests as determined by the degree of anthropogenic modification and comes at a 300 m resolution. We supplemented the FLII with the ETH Global Sentinel-2 10m Canopy Height (GCH), which maps global canopy height for 2020 at 10 m resolution (Lang et al., 2023). We aggregated the native 10 m GCH product to 300 m by resampling it to match the extent and pixel size of FLII, thus granting a description of the forest structure and density at the sampling sites' proximity. We also supplemented the FLII with the geographic distance of each site from the nearest old-growth forest (FORESTS). We finally categorized land uses/covers at the sites' locations using the pan-European CORINE Land Cover 2018 inventory (CLC) at 100 m resolution (EEA, 2018). For sample size purposes, we grouped the "Sclerophyllous vegetation" and "Transitional woodland/shrub" categories into "Shrub and/or herbaceous associations."

Multimodel inference and model averaging

We assessed the influence of microclimatic and forest predictors on pollinator diversity by conducting a multimodel inference followed by model averaging. We fitted Poisson-distributed generalized linear models (GLMs) by employing all 64 possible combinations of the six predictors (CLC, DTR, FLII, FORESTS, GCH, log(β)). We ranked models according to their AICc value (Hurvich & Tsai, 1989), then performed "full" model averaging on the best models (ΔAICc ≤ 2) and on a more conservative model set having ΔAICc ≤ 7 (Burnham et al., 2011). "Full" averaging assumes that all variables are included in every model and drops them out by setting to zero their corresponding coefficient and variance; it is thus less biased and more conservative than "subset" averaging (Burnham & Anderson, 2002; Lukacs et al., 2010). We compared each CLC category to broad-leaved forests, as this is the most common category in the study area. We conducted multimodel inference and model averaging using the MuMIn R package (Barton, 2023). All analyses were performed in R, version 4.3.1 (R Core Team, 2023).

Results

Pollinator diversity

Morphological and molecular identification confirmed the prominence of the Aspromonte region as a hotspot of diversity for pollinators, enabling 106 apoid and 23 hoverfly taxa to be identified. Sites 003 and 001 were the richest, corresponding to the two high-altitude meadows where sampling lasted throughout the season; here, as many as 54 and 34 taxa were found, respectively (Fig. A.3 in Appendices). *Bombus* (for apoids) and *Sphaerophoria* (for hoverflies) were the most ubiquitous genera. Bumblebees were also among the most diverse, being represented by 10 species that were frequently syntopic. Interestingly, molecular barcoding revealed two highly divergent (> 10%) DNA sequences, possibly suggesting undescribed species in the region.

Climatic and landscape influences on pollinator diversity

Multimodel inference resulted in the three best models (ΔAICc ≤ 2) cumulating 72.46% of AICc weight, while the most conservative model set (ΔAICc ≤ 7) cumulated 95.89% (Tab. A.2 in Appendices). CLC was present in all the top models and arguably ranked as the most impactful predictor. FORESTS followed closely, appearing in all but one model of the conservative set. DTR and log(β) appeared only in the most conservative model set and displayed positive and negative effects, respectively. Conversely, FLII and GCH featured in the best model set; FLII decreased pollinator diversity, while GCH impacted it positively. Still, the fully-averaged best model only included CLC and FORESTS as significant predictors (Tab. 1); the same is true for the most

conservative one (Tab. 2). Coniferous forests and shrub and/or herbaceous associations were significantly less diverse than broad-leaved forests in both best and conservative model sets (Tab. 1, Tab. 2, and Fig. 2). So was non-irrigated arable land, but its effect size approached significance only in the best models (Tab. 2). Heterogeneous agricultural areas, on the contrary, were found to be significantly more diverse than broad-leaved forests in both fully-averaged best and conservative models (Tab. 1, Tab. 2, and Fig. 2).

Discussion

Understanding how reduced pollinator diversity affects pollination function is paramount for predicting the future stability of natural and agroecosystems (Kremen & Ostfeld, 2005). By examining pollinator communities from a broad perspective, our study showed pollinators' taxa richness depended on land use/cover and proximity to old-growth forests. CORINE Land Cover's heterogeneous agricultural areas span juxtapositions of annual and perennial crops, pastures, meadows, and cultivations under forest trees (EEA, 2018). A significantly positive association between pollinator diversity and such area was to be expected, as pollinator communities were already found to benefit from more spatially heterogeneous semi-natural habitats (Le Féon et al., 2010; Martínez-Núñez et al., 2022) and diverse floral resources (Blaauw & Isaacs, 2014). Likewise, the negative effect of FLII, although not statistically significant, also pointed to less dense forest habitats promoting pollinator diversity, echoing previous evidence (Hanula et al., 2015). Shrub and/or herbaceous associations in the Aspromonte are likely affected by human-mediated naturalization; they also harbor abandoned crops. It is thus plausible that their significantly lower pollinator diversity would result from human disturbance. Likewise, surrounding coniferous forests were found to decrease pollinator diversity, but the sample size makes this conclusion far from robust.

Pollinator diversity decreased as distance from old-growth forests increased. The reasons might be two-fold. On the one hand, distance from old-growth forests could represent a proxy for human disturbance. These areas are least concerned by anthropization; habitats could thus become more pristine as one gets closer, promoting richer pollinator communities. On the other hand, old-growth forests actively governing pollinators' diversification seems more plausible, even in highly forested regions like the Aspromonte. Forests provide many resources to pollinators, ranging from floral (Motten, 1986) and non-floral resources like honeydew and resin (Cameron et al., 2019; Chui et al., 2022) to nesting and overwintering resources (Westerfelt et al., 2015; Mola et al., 2021). The type and abundance of resources vary with forest type and composition, disturbance history, and age; accordingly, old-growth forests provide some that are rare or absent from secondary ones, like large hollow trees, standing dead trees, water-filled tree holes, and decaying logs (Roubik, 1983). These

habitat elements constitute crucial structures for bee nesting (Stockhammer, 1966; Westerfelt et al., 2015) and may thus help older forests in the region support richer pollinator communities.

Besides finding relevant foraging and nesting resources, pollinators benefit from favorable microclimatic conditions within and adjacent to forests. Forest canopies buffer climatic extremes, thus sheltering pollinators from the impact of climate change (Oliver et al., 2013; Ganuza et al., 2022). Cooler and less windy conditions also benefit both nesting and foraging forest-associated pollinators (Mola et al., 2021). Our results echoed these well-known effects. The multimodel inference showed that log(β) primarily had a negative impact, meaning that microclimate buffering increased pollinator diversity. So did more vertically higher forests (i.e., having higher GCH), appearing even in the best model set. Our study, therefore, confirms the forests' relevance for the diversity of pollinating insects, considered here in terms of taxa richness (Ulyshen et al., 2023). These effects could also explain part of the significance of old-growth forests emerged from our study. Old-growth forests typically have complex vertical structures and heterogeneous spatial arrangements, providing many microhabitats and microclimates for forest-dwelling organisms (Franklin & Van Pelt, 2004). They also shelter them more efficiently from climatic extremes (Frey et al., 2016; Betts et al., 2018). Perhaps these older forests' prerogatives could contribute to greater taxa diversity in pollinating insects. While very tempting, it is worth remembering that this hypothesis, so far, remains weakly supported statistically.

The value of forest resources varies among pollinator taxa, with some, like many hoverflies that nest in dead wood, being more associated with forests and others less (Ulyshen, 2018; Smith et al., 2021; Alison et al., 2022). In this light, Aspromonte's old-growth forests might promote specific pollinator assemblages depending on which elements differentiate them from secondary ones in the region. Investigating whether older forests, compared to younger ones, boost the diversity of specific functional groups of pollinating insects would help identify the forest features responsible for the seemingly higher pollinator diversity. It would, likewise, further our understanding regarding the landscape and climatic components that functionally assemble pollinator communities in highly heterogeneous regions, which could prove invaluable for preserving the stability of the natural and agroecosystems they host.

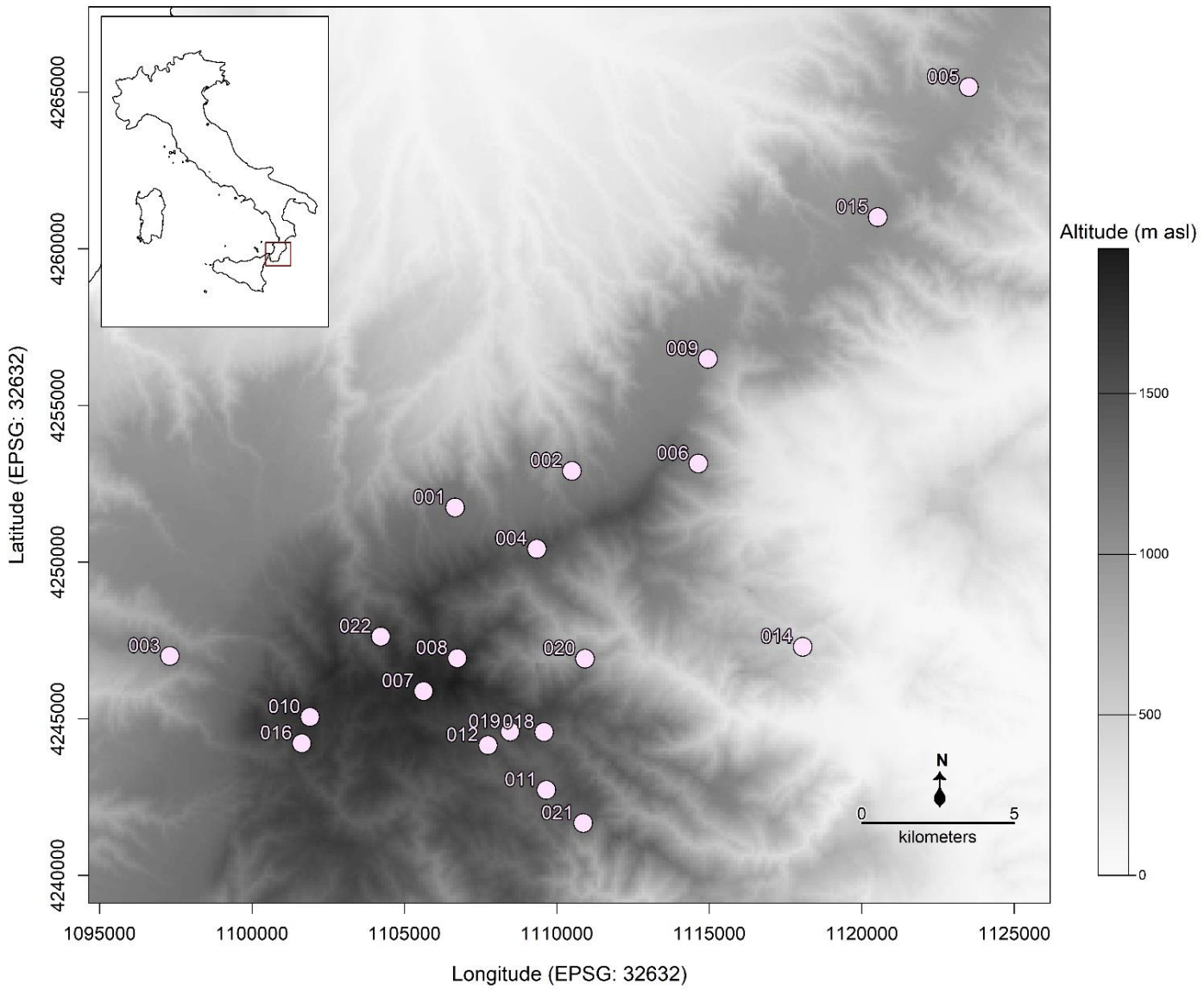

Figure 1. Locations of the 20 data loggers we employed for the study. We added the data logger's ID above each location. The inset displays the Italian peninsula's borders and highlights those of the study area in red.

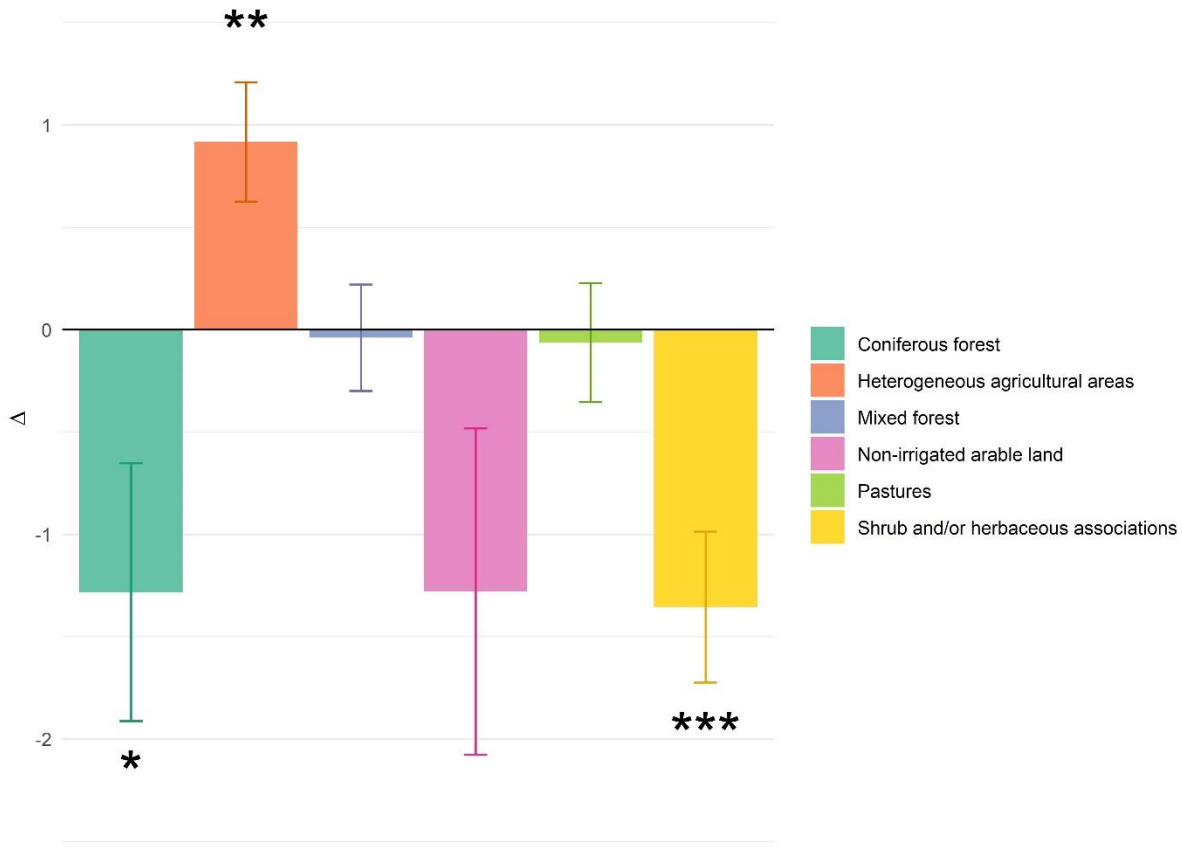

Figure 2. Multimodel inference (ΔAICc ≤ 7) – Estimated differences between the expected taxa richness in broad-leaved forests and the one expected in each other land use/land cover type. Error bars indicate the adjusted standard errors. Differences are on a logarithmic scale.

Significance codes: *p*-value = 0 '***' 0.001 '**' 0.01 '*' 0.05 '·' 0.1 ' ' 1.

Table 1. Multimodel inference (ΔAICc ≤ 2) – Full model-averaged coefficients. Results from the model averaging routine applied on the models having ΔAICc ≤ 2 (**CLC**: CORINE Land Cover; **FORESTS**: distance from the nearest old-growth forest; **FLII**: Forest Landscape Integrity Index; **GCH**: Global Canopy Height).

Significance codes: *p*-value = 0 '***' 0.001 '**' 0.01 '*' 0.05 '·' 0.1 ' ' 1.

		Estimate	Adjusted SE	*z*	*p*-value	
	Intercept	3.46848	1.4603	2.37518	0.01754	*
CLC	Coniferous forest	-1.26073	0.62395	2.02056	0.04333	*
	Heterogeneous agricultural areas	0.90841	0.26884	3.37902	0.00073	***
	Mixed forest	-0.02133	0.26015	0.08198	0.93466	
	Non-irrigated arable land	-1.38719	0.83396	1.66338	0.09624	·
	Pastures	-0.01776	0.2469	0.07192	0.94267	
	Shrub and/or herbaceous vegetation associations	-1.42308	0.35075	4.0572	4.97e-05	***
	FORESTS	-0.07656	0.02147	3.5662	0.00036	***
	FLII	-0.18405	0.12212	1.50713	0.13178	
	GCH	0.04128	0.04963	0.83159	0.40564	

Table 2. Multimodel inference (ΔAICc ≤ 7) – Full model-averaged coefficients. Results from the model averaging routine applied on the models having ΔAICc ≤ 7 (**CLC**: CORINE Land Cover; **FORESTS**: distance from the nearest old-growth forest; **DTR**: diurnal temperature range; **FLII**: Forest Landscape Integrity Index; **GCH**: Global Canopy Height; **log(β)**: logarithm of the buffering slope).

Significance codes: *p*-value = 0 '***' 0.001 '**' 0.01 '*' 0.05 '·' 0.1 ' ' 1.

		Estimate	Adjusted SE	*z*	*p*-value	
	Intercept	3.23554	1.37653	2.35050	0.01875	*
CLC	Coniferous forest	-1.28258	0.62953	2.03736	0.04161	*
	Heterogeneous agricultural areas	0.91635	0.29132	3.14552	0.00166	**
	Mixed forest	-0.04013	0.26008	0.15431	0.87737	
	Non-irrigated arable land	-1.27895	0.79726	1.60418	0.10867	
	Pastures	-0.06356	0.29065	0.21868	0.82690	
	Shrub and/or herbaceous vegetation associations	-1.35556	0.36852	3.67837	0.00023	***
	FORESTS	-0.06662	0.02920	2.28163	0.02251	*
	FLII	-0.14187	0.13198	1.07498	0.28238	
	GCH	0.03119	0.04665	0.66866	0.50371	
	DTR	0.00765	0.02201	0.34763	0.72812	
	log(β)	-0.02862	0.28368	0.10090	0.91963	

References

Alison, J., Botham, M., Maskell, L. C., Garbutt, A., Seaton, F. M., Skates, J., ... & Emmett, B. A. (2022). Woodland, cropland and hedgerows promote pollinator abundance in intensive grassland landscapes, with saturating benefits of flower cover. *Journal of Applied Ecology*, *59*(1), 342–354.

Ashman, T. L., Knight, T. M., Steets, J. A., Amarasekare, P., Burd, M., Campbell, D. R., ... & Wilson, W. G. (2004). Pollen limitation of plant reproduction: ecological and evolutionary causes and consequences. *Ecology*, *85*(9), 2408–2421.

Barton, K. (2023). MuMIn: multi-model inference. *R package version 1.47.5*.

Betts, M. G., Phalan, B., Frey, S. J., Rousseau, J. S., & Yang, Z. (2018). Old-growth forests buffer climate-sensitive bird populations from warming. *Diversity and Distributions*, *24*(4), 439–447.

Biesmeijer, J. C., Roberts, S. P., Reemer, M., Ohlemuller, R., Edwards, M., Peeters, T., ... & Kunin, W. E. (2006). Parallel declines in pollinators and insect-pollinated plants in Britain and the Netherlands. *Science*, *313*(5785), 351–354.

Bivand, R., & Yu, D. (2020). spgwr: Geographically weighted regression. *R package version 0.6-34*.

Blaauw, B. R., & Isaacs, R. (2014). Larger patches of diverse floral resources increase insect pollinator density, diversity, and their pollination of native wildflowers. *Basic and Applied Ecology*, *15*(8), 701–711.

Blüthgen, N., & Klein, A. M. (2011). Functional complementarity and specialisation: the role of biodiversity in plant–pollinator interactions. *Basic and Applied Ecology*, *12*(4), 282–291.

Burd, M. (1994). Bateman's principle and plant reproduction: the role of pollen limitation in fruit and seed set. *The Botanical Review*, *60*, 83–139.

Burnham, K. P., & Anderson, D. R. (Eds.). (2002). *Model selection and multimodel inference: a practical information-theoretic approach*. New York, NY: Springer New York.

Burnham, K. P., Anderson, D. R., & Huyvaert, K. P. (2011). AIC model selection and multimodel inference in behavioral ecology: some background, observations, and comparisons. *Behavioral Ecology and Sociobiology*, *65*, 23–35.

Cameron, S. A., Corbet, S. A., & Whitfield, J. B. (2019). Bumble bees (Hymenoptera: Apidae: *Bombus terrestris*) collecting honeydew from the giant willow aphid (Hemiptera: Aphididae). *Journal of Hymenoptera Research*, *68*, 75–83.

Carvalheiro, L. G., Veldtman, R., Shenkute, A. G., Tesfay, G. B., Pirk, C. W. W., Donaldson, J. S., & Nicolson, S. W. (2011). Natural and within-farmland biodiversity enhances crop productivity. *Ecology Letters*, *14*(3), 251–259.

Chui, S. X., Keller, A., & Leonhardt, S. D. (2022). Functional resin use in solitary bees. *Ecological Entomology*, *47*(2), 115–136.

Corbet, S. A., Fussell, M., Ake, R., Fraser, A., Gunson, C., Savage, A., & Smith, K. (1993). Temperature and the pollinating activity of social bees. *Ecological Entomology*, *18*(1), 17–30.

EEA (2018). Corine Land Cover (CLC) 2018, Version 20b2. Release date: 21-12-2018. European Environment Agency.
Available in: https://land.copernicus.eu/en/products/corine-land-cover/clc2018

Fontaine, C., Collin, C. L., & Dajoz, I. (2008). Generalist foraging of pollinators: diet expansion at high density. *Journal of Ecology*, *96*(5), 1002–1010.

Fontaine, C., Dajoz, I., Meriguet, J., & Loreau, M. (2006). Functional diversity of plant–pollinator interaction webs enhances the persistence of plant communities. *PLoS Biology*, *4*(1), e1.

Franklin, J. F., & Van Pelt, R. (2004). Spatial aspects of structural complexity in old-growth forests. *Journal of Forestry*, *102*(3), 22–28.

Frey, S. J., Hadley, A. S., Johnson, S. L., Schulze, M., Jones, J. A., & Betts, M. G. (2016). Spatial models reveal the microclimatic buffering capacity of old-growth forests. *Science Advances*, *2*(4), e1501392.

Gallai, N., Salles, J. M., Settele, J., & Vaissière, B. E. (2009). Economic valuation of the vulnerability of world agriculture confronted with pollinator decline. *Ecological Economics*, *68*(3), 810–821.

Ganuza, C., Redlich, S., Uhler, J., Tobisch, C., Rojas-Botero, S., Peters, M. K., ... & Steffan-Dewenter, I. (2022). Interactive effects of climate and land use on pollinator diversity differ among taxa and scales. *Science Advances*, *8*(18), eabm9359.

Grantham, H. S., Duncan, A., Evans, T. D., Jones, K. R., Beyer, H. L., Schuster, R., ... & Watson, J. E. M. (2020). Anthropogenic modification of forests means only 40% of remaining forests have high ecosystem integrity. *Nature Communications*, *11*(1), 5978.

Greenleaf, S. S., & Kremen, C. (2006). Wild bees enhance honey bees' pollination of hybrid sunflower. *Proceedings of the National Academy of Sciences*, *103*(37), 13890c13895.

Greiser, C., Ehrlén, J., Meineri, E., & Hylander, K. (2020). Hiding from the climate: Characterizing microrefugia for boreal forest understory species. *Global Change Biology*, *26*(2), 471–483.

Gril, E., Spicher, F., Greiser, C., Ashcroft, M. B., Pincebourde, S., Durrieu, S., ... & Lenoir, J. (2023). Slope and equilibrium: A parsimonious and flexible approach to model microclimate. *Methods in Ecology and Evolution*, *14*(3), 885–897.

Hanula, J. L., Horn, S., & O'Brien, J. J. (2015). Have changing forests conditions contributed to pollinator decline in the southeastern United States?. *Forest Ecology and Management*, *348*, 142–152.

Hooper, D. U., Chapin III, F. S., Ewel, J. J., Hector, A., Inchausti, P., Lavorel, S., ... & Wardle, D. A. (2005). Effects of biodiversity on ecosystem functioning: a consensus of current knowledge. *Ecological Monographs*, *75*(1), 3–35.

Hurvich, C. M., & Tsai, C. L. (1989). Regression and time series model selection in small samples. *Biometrika*, *76*(2), 297–307.

IPBES (2016). Summary for policymakers of the assessment report of the Intergovernmental Science-Policy Platform on Biodiversity and Ecosystem Services on pollinators, pollination and food production. S.G. Potts, V. L. Imperatriz-Fonseca, H. T. Ngo, J. C. Biesmeijer, T. D. Breeze, L. V. Dicks, L. A. Garibaldi, R. Hill, J. Settele, A. J. Vanbergen, M. A. Aizen, S. A. Cunningham, C. Eardley, B. M. Freitas, N. Gallai, P. G. Kevan, A. Kovács-Hostyánszki, P. K. Kwapong, J. Li, X. Li, D. J. Martins, G. Nates-Parra, J. S. Pettis, R. Rader, and B. F. Viana (eds.). Secretariat of the Intergovernmental Science-Policy Platform on Biodiversity and Ecosystem Services, Bonn, Germany. 36 pages.

Klein, A. M., Cunningham, S. A., Bos, M., & Steffan-Dewenter, I. (2008). Advances in pollination ecology from tropical plantation crops. *Ecology*, *89*(4), 935–943.

Klein, A. M., Vaissière, B. E., Cane, J. H., Steffan-Dewenter, I., Cunningham, S. A., Kremen, C., & Tscharntke, T. (2007). Importance of pollinators in changing landscapes for world crops. *Proceedings of the Royal Society B: Biological Sciences*, *274*(1608), 303–313.

Kremen, C., & Ostfeld, R. S. (2005). A call to ecologists: measuring, analyzing, and managing ecosystem services. *Frontiers in Ecology and the Environment*, *3*(10), 540–548.

Kwon, Y. J., & Saeed, S. (2003). Effect of temperature on the foraging activity of *Bombus terrestris* L.(Hymenoptera: Apidae) on greenhouse hot pepper (*Capsicum annuum* L.). *Applied Entomology and Zoology*, *38*(3), 275–280.

Le Féon, V., Schermann-Legionnet, A., Delettre, Y., Aviron, S., Billeter, R., Bugter, R., ... & Burel, F. (2010). Intensification of agriculture, landscape composition and wild bee communities: a large scale study in four European countries. *Agriculture, Ecosystems & Environment*, *137*(1-2), 143–150.

Lang, N., Jetz, W., Schindler, K., & Wegner, J. D. (2023). A high-resolution canopy height model of the Earth. *Nature Ecology & Evolution*, *7*(11), 1778–1789.

Larsen, T. H., Williams, N. M., & Kremen, C. (2005). Extinction order and altered community structure rapidly disrupt ecosystem functioning. *Ecology Letters*, *8*(5), 538–547.

Lenoir, J., Hattab, T., & Pierre, G. (2017). Climatic microrefugia under anthropogenic climate change: implications for species redistribution. *Ecography*, *40*(2), 253–266.

Lienhard, A., & Schäffer, S. (2019). Extracting the invisible: obtaining high quality DNA is a challenging task in small arthropods. *PeerJ*, *7*, e6753.

Loy, X., & Brosi, B. J. (2022). The effects of pollinator diversity on pollination function. *Ecology*, *103*(4), e3631.

Lukacs, P. M., Burnham, K. P., & Anderson, D. R. (2010). Model selection bias and Freedman's paradox. *Annals of the Institute of Statistical Mathematics*, *62*, 117–125.

Martínez-Núñez, C., Kleijn, D., Ganuza, C., Heupink, D., Raemakers, I., Vertommen, W., & Fijen, T. P. (2022). Temporal and spatial heterogeneity of semi-natural habitat, but not crop diversity, is correlated with landscape pollinator richness. *Journal of Applied Ecology*, *59*(5), 1258–1267.

Miljanic, A. S., Loy, X., Gruenewald, D. L., Dobbs, E. K., Gottlieb, I. G., Fletcher, R. J., & Brosi, B. J. (2019). Bee communities in forestry production landscapes: interactive effects of local-level management and landscape context. *Landscape Ecology*, *34*, 1015–1032.

Miñarro, M., & García, D. (2018). Complementarity and redundancy in the functional niche of cider apple pollinators. *Apidologie*, *49*, 789–802.

Mola, J. M., Hemberger, J., Kochanski, J., Richardson, L. L., & Pearse, I. S. (2021). The importance of forests in bumble bee biology and conservation. *Bioscience*, *71*(12), 1234–1248.

Motten, A. F. (1986). Pollination ecology of the spring wildflower community of a temperate deciduous forest. *Ecological Monographs*, *56*(1), 21–42.

O'Connor, R. S., Kunin, W. E., Garratt, M. P., Potts, S. G., Roy, H. E., Andrews, C., ... & Carvell, C. (2019). Monitoring insect pollinators and flower visitation: The effectiveness and feasibility of different survey methods. *Methods in Ecology and Evolution*, *10*(12), 2129–2140.

Oliver, T. H., Brereton, T., & Roy, D. B. (2013). Population resilience to an extreme drought is influenced by habitat area and fragmentation in the local landscape. *Ecography*, *36*(5), 579–586.

Petanidou, T., Kallimanis, A. S., Tzanopoulos, J., Sgardelis, S. P., & Pantis, J. D. (2008). Long-term observation of a pollination network: fluctuation in species and interactions, relative invariance of network structure and implications for estimates of specialization. *Ecology Letters*, *11*(6), 564–575.

Petanidou, T., & Smets, E. (1996). Does temperature stress induce nectar secretion in Mediterranean plants?. *New Phytologist*, *133*(3), 513–518.

Potts, S. G., Biesmeijer, J. C., Kremen, C., Neumann, P., Schweiger, O., & Kunin, W. E. (2010). Global pollinator declines: trends, impacts and drivers. *Trends in Ecology & Evolution*, *25*(6), 345–353.

Potts, S. G., Imperatriz-Fonseca, V., Ngo, H. T., Aizen, M. A., Biesmeijer, J. C., Breeze, T. D., ... & Vanbergen, A. J. (2016). Safeguarding pollinators and their values to human well-being. *Nature*, *540*(7632), 220–229.

Rathcke, B. J., & Jules, E. S. (1993). Habitat fragmentation and plant–pollinator interactions. *Current Science*, 273–277.

R Core Team (2023). R: A language and environment for statistical computing. R Foundation for Statistical Computing, Vienna, Austria.

Reyes-González, A., & Zamudio, F. (2020). Competition interactions among stingless bees (Apidae: Meliponini) for *Croton yucatanensis* Lundell resins. *International Journal of Tropical Insect Science*, *40*(4), 1099–1104.

Roubik, D. W. (1983). Nest and colony characteristics of stingless bees from Panama (Hymenoptera: Apidae). *Journal of the Kansas Entomological Society*, 327–355.

Sann, M., Niehuis, O., Peters, R. S., Mayer, C., Kozlov, A., Podsiadlowski, L., ... & Ohl, M. (2018). Phylogenomic analysis of Apoidea sheds new light on the sister group of bees. *BMC Evolutionary Biology*, *18*, 1–15.

Scheffers, B. R., Edwards, D. P., Diesmos, A., Williams, S. E., & Evans, T. A. (2014). Microhabitats reduce animal's exposure to climate extremes. *Global Change Biology*, *20*(2), 495–503.

Smith, C., Harrison, T., Gardner, J., & Winfree, R. (2021). Forest-associated bee species persist amid forest loss and regrowth in eastern North America. *Biological Conservation*, *260*, 109202.

Stockhammer, K. A. (1966). Nesting habits and life cycle of a sweat bee, *Augochlora pura* (Hymenoptera: Halictidae). *Journal of the Kansas Entomological Society*, 157–192.

Tscharntke, T., Gathmann, A., & Steffan-Dewenter, I. (1998). Bioindication using trap-nesting bees and wasps and their natural enemies: community structure and interactions. *Journal of Applied Ecology*, *35*(5), 708–719.

Ulyshen, M. D. (2018). *Saproxylic Insects: Diversity, Ecology and Conservation*. Springer, Cham.

Ulyshen, M., Urban-Mead, K. R., Dorey, J. B., & Rivers, J. W. (2023). Forests are critically important to global pollinator diversity and enhance pollination in adjacent crops. *Biological Reviews*, *98*(4), 1118–1141.

Urbini, A., Sparvoli, E., & Turillazzi, S. (2006). Social paper wasps as bioindicators: a preliminary research with *Polistes dominulus* (Hymenoptera Vespidae) as a trace metal accumulator. *Chemosphere*, *64*(5), 697–703.

Vanbergen, A. J., & the Insect Pollinators Initiative (2013). Threats to an ecosystem service: pressures on pollinators. *Frontiers in Ecology and the Environment*, *11*(5), 251–259.

Vasseur, D. A., DeLong, J. P., Gilbert, B., Greig, H. S., Harley, C. D., McCann, K. S., ... & O'Connor, M. I. (2014). Increased temperature variation poses a greater risk to species than climate warming. *Proceedings of the Royal Society B: Biological Sciences*, *281*(1779), 20132612.

Vieira, L. C., Oliveira, N. G., & Gayubo, S. F. (2011). On the use of Apiformes and Spheciformes (Insecta: Hymenoptera) populations as a management tool. *Biodiversity and Conservation*, *20*, 519-530.

Watson, J. C., Wolf, A. T., & Ascher, J. S. (2011). Forested landscapes promote richness and abundance of native bees (Hymenoptera: Apoidea: Anthophila) in Wisconsin apple orchards. *Environmental Entomology*, *40*(3), 621–632.

Westerfelt, P., Widenfalk, O., Lindelöw, Å., Gustafsson, L., & Weslien, J. (2015). Nesting of solitary wasps and bees in natural and artificial holes in dead wood in young boreal forest stands. *Insect Conservation and Diversity*, *8*(6), 493–504.

Westphal, C., Bommarco, R., Carré, G., Lamborn, E., Morison, N., Petanidou, T., ... & Steffan-Dewenter, I. (2008). Measuring bee diversity in different European habitats and biogeographical regions. *Ecological Monographs*, *78*(4), 653–671.

Wilson, J. J. (2012). DNA barcodes for insects. *DNA barcodes: Methods and Protocols*, 17–46.

Winfree, R., & Kremen, C. (2009). Are ecosystem services stabilized by differences among species? A test using crop pollination. *Proceedings of the Royal Society B: Biological Sciences*, *276*(1655), 229–237.

5. Conclusions

In this thesis, I aimed to identify the climatic and landscape determinants that structure the biodiversity of highly heterogeneous mountain hotspots. First, I had to assess the best way to characterize the fine-scale heterogeneity of mountain climates; as we saw, climate variability is a major driver of mountains' eco-evolutionary processes. Once I selected the most suitable technique, I studied the climatic and landscape determinants from two distinct angles, looking at biological diversity from intraspecific and community viewpoints. The Aspromonte, with its highly heterogeneous environments and outstanding biodiversity, proved the perfect candidate for the task. Let us now frame the results of this thesis from a conservation perspective.

Deriving high-resolution local climatic surfaces in the Aspromonte region posed multiple challenges. The interpolation of weather stations emerged as the most suitable technique but struggled with topographic heterogeneity in the innermost areas of the region. On the other hand, downscaling macroclimate grids, at best, visibly over-smoothed the fine-scale climate variability. We can draw a stimulating consideration from this. Interpolation and downscaling techniques have hesitated to derive high-resolution conditions of monthly climatologies, which are very aggregated climates. Since the Aspromonte region is affected by very volatile atmospheric currents (Prete et al., 2023), going into more detail by looking at daily or monthly weather would probably have been impractical. However, day-to-day weather variations are those with the most direct impact on the life of mountain organisms. We are making ever greater strides in climate modeling, including downscaling atmospheric precipitation (Abdollahipour et al., 2022); results from our methodological comparison perhaps help us realize how much room for improvement we still have.

Investigating the population genetic structure of *Salamandra salamandra* showed that the species could suffer topoclimatic warming even under the mildest climate change scenario (SSP126). This begs the question: How does the current zonation of the Aspromonte National Park fare with the projected connectivity shifts? To get an answer, we differentiated the impact projections of climate change on connectivity by functional zones (Fig. 1). Against expectations, despite the highest areas of the Park occurring within Zone A, most of the upslope shift will benefit Zone B: the highest concentrations of green points (i.e., connectivity gains), indeed, can be found in Zone B under the worst climate change scenarios (SSP370 and SSP585). That is because the central to southern areas where connectivity is predicted to concentrate and brightly colored in Chapter 3, Figure 5, fall within these zones. Hence, we

found evidence that the current zonation of the Park could prove suboptimal for conserving *S. salamandra* under climate change, perhaps even for preserving other forest-dwelling organisms. But there might be a catch. As mentioned, Zone A is the least impacted by anthropization, meaning that forest buffering/decoupling here could be enhanced by denser and more structurally complex canopy covers (Ewers & Banks-Leite, 2013). Would these effects outbalance the predicted topoclimatic warming? Some studies suggest so (De Frenne et al., 2021; De Lombaerde et al., 2022), but until microclimates in the Aspromonte are modeled in all their complexity, the question remains open for debate. It also remains even more open, given the forest fires increasingly affecting the Park (De Luca & Modica, 2022).

Can we also draw considerations about the current functional zonation from the analysis of pollinator diversity? Only partially. Figure 2 shows that frequency distributions for the CORINE Land Cover categories vary significantly between functional zones (Fig. 2). This prevented us from including zonation in our multimodel inference, as we may not have disentangled the effects of zonation and land cover on pollinators' taxa richness. So, we could not directly test whether increased protection levels promoted pollinator diversity. Perhaps one solution could be to cover the land cover categories more equally by increasing the number of sampling sites in the most unbalanced ones. However, doing that might prove impractical in a topographically challenging context like the Aspromonte.

On the other hand, patterns of pollinator diversity suggest that, like in the genetic differentiation of *S. salamandra*, old-growth forests play a role in pollinators' diversification. Forest characteristics also seemed to affect diversification, albeit non-significantly, while habitat heterogeneity affected the genetic structure of *S. salamandra* and taxa richness in pollinator communities. Such similarities validate this thesis' integrated framework and answer our central question: the same landscape elements can influence biodiversity distribution at different hierarchical levels. These are comforting results for the Aspromonte National Park and similar institutions because resources can be channeled to preserve specific landscape elements and simultaneously benefit several levels of biological diversity.

More generally, our results underline how landscape and climatic heterogeneity on the finest geographic scales are crucial in generating and maintaining high levels of diversity at all biological levels. In this sense, they echo the shift we witnessed in the biogeographical studies of the last few decades as we transitioned from a "southern richness, northern purity" paradigm – with its strong emphasis on major postglacial recolonization events from southern glacial

refugia (Hewitt, 2000) – to a "refugia within refugia" paradigm where topographic complexity drives complex patterns of glacial survival in smaller pockets of suitable landscapes and microclimates (Gómez & Lunt, 2007; Abellán & Svenning, 2014). By providing insights on how to best account for extreme levels of topoclimatic variability and on how to disentangle the influence that landscape and climate heterogeneity exert on biodiversity distribution at different hierarchical levels, we hope that this thesis will make its contribution to this very contemporary and vitally important field for species conservation under anthropogenic change.

In the light of all these considerations, we thus deem our integrated framework worthy of further investigation. To mention a few perspectives in close continuity with this thesis' content, one could assess whether the internal and most heterogeneous sections of the Park are also crucial for the connectivity of pollinating insects by investigating how beta diversity links to habitat resistance or which habitat configurations foster genetic differentiation in widespread taxa like wild bees and bumblebees. These investigations would give the National Park vital tools to optimize its conservation strategies. They would also bring us closer to understanding whether populations and communities respond similarly to anthropogenic change in topographically heterogeneous mountain hotspots. Given the outstanding biodiversity these hotspots harbor, this could constitute a turning point for future species conservation.

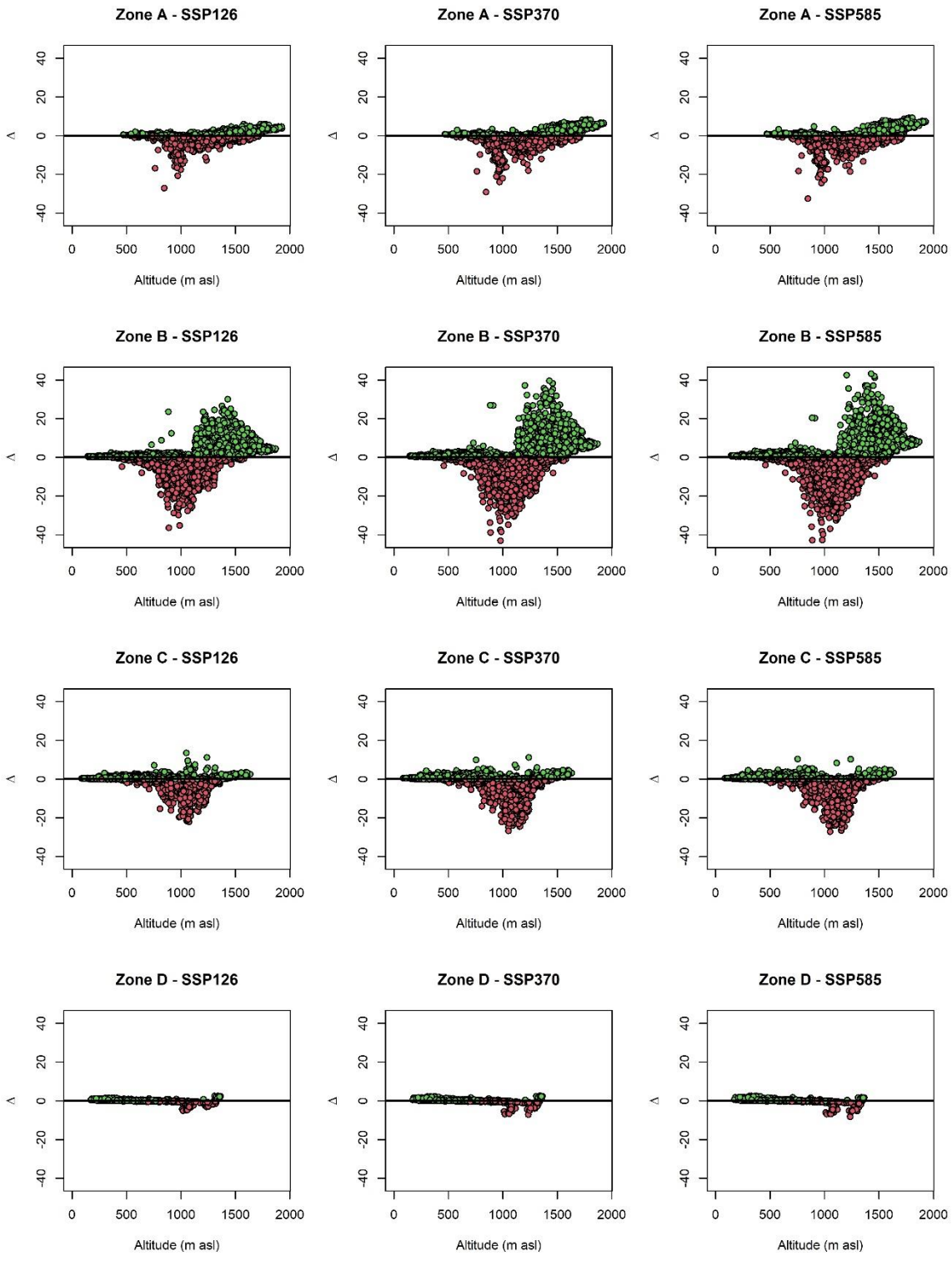

Figure 1. Impact projections of climate change on the connectivity of *Salamandra salamandra* in each Aspromonte National Park functional zone. We evaluated the current and future connectivity at 100,000 random locations. We then calculated the difference (Δ) between future and current connectivity at these locations for each climate change scenario. Here, connectivity differences are plotted against altitude; future gains are colored in green, while future losses are in red. Contrary to Fig. 5 in Chapter 3, we differentiated the subplots by functional zones: the first row shows Zone A, the second Zone B, the third Zone C, and the fourth Zone D.

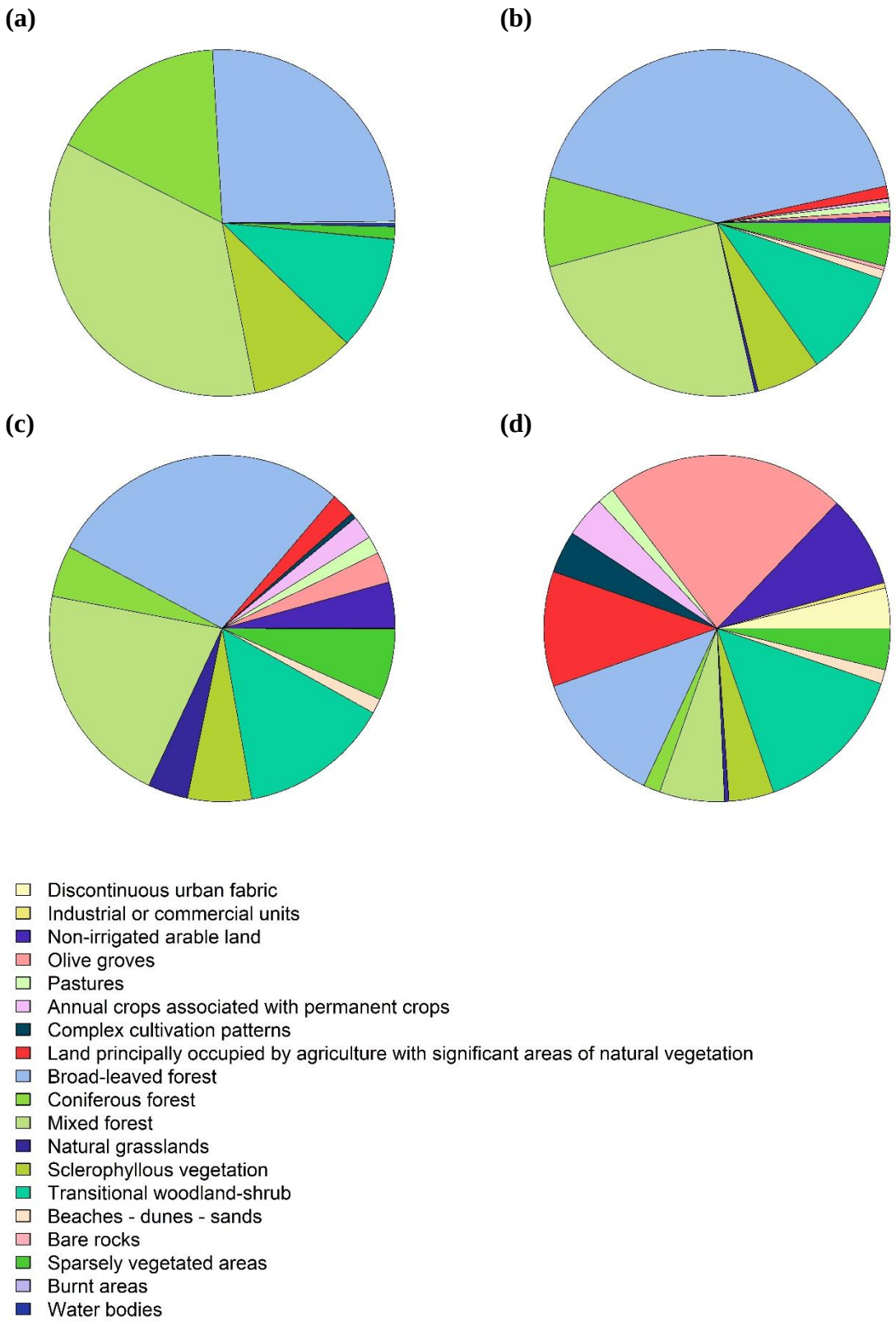

Figure 2. Frequency distributions of CORINE Land Cover categories for **(a)** Zone A, **(b)** Zone B, **(c)** Zone C, and **(d)** Zone D.

References

Abdollahipour, A., Ahmadi, H., & Aminnejad, B. (2022). A review of downscaling methods of satellite-based precipitation estimates. *Earth Science Informatics*, *15*(1), 1–20.

Abellán, P., & Svenning, J. C. (2014). Refugia within refugia–patterns in endemism and genetic divergence are linked to Late Quaternary climate stability in the Iberian Peninsula. *Biological Journal of the Linnean Society*, *113*(1), 13–28.

Aeschimann, D., Lauber, K., Moser, D. M., & Theurillat, J. P. (2004). *Flora Alpina*. Bern.

Antonelli, A., Kissling, W. D., Flantua, S. G., Bermúdez, M. A., Mulch, A., Muellner-Riehl, A. N., ... & Hoorn, C. (2018). Geological and climatic influences on mountain biodiversity. *Nature Geoscience*, *11*(10), 718–725.

Bakarr, M. I., Fonseca, G. A., Mittermeier, R., Rylands, A. B., & Peinemilla, K. W. (2001). Hunting and bushmeat utilization in the African rainforest. *Advances in Applied Biodiversity Science*, *2*, 170.

Barry, R. G., & Blanken, P. D. (2016). *Microclimate and local climate*. Cambridge University Press.

Barthlott, W., Hostert, A., Kier, G., Kueper, W., Kreft, H., Mutke, J., ... & Sommer, J. H. (2007). Geographic patterns of vascular plant diversity at continental to global scales (Geographische Muster der Gefäßpflanzenvielfalt im kontinentalen und globalen Maßstab). *Erdkunde*, 305–315.

Barthlott, W., Lauer, W., & Placke, A. (1996). Global distribution of species diversity in vascular plants: Towards a world map of phytodiversity. *Erdkunde*, 317–327.

Benito Garzón, M., Alía, R., Robson, T. M., & Zavala, M. A. (2011). Intra-specific variability and plasticity influence potential tree species distributions under climate change. *Global Ecology and Biogeography*, *20*(5), 766–778.

Brooks, T. M., Mittermeier, R. A., Mittermeier, C. G., Da Fonseca, G. A., Rylands, A. B., Konstant, W. R., ... & Hilton-Taylor, C. (2002). Habitat loss and extinction in the hotspots of biodiversity. *Conservation Biology*, *16*(4), 909–923.

Camacho-Sanchez, M., Quintanilla, I., Hawkins, M. T., Tuh, F. Y., Wells, K., Maldonado, J. E., & Leonard, J. A. (2018). Interglacial refugia on tropical mountains: novel insights from the summit rat (*Rattus baluensis*), a Borneo mountain endemic. *Diversity and Distributions*, *24*(9), 1252–1266.

Chan, W. P., Chen, I. C., Colwell, R. K., Liu, W. C., Huang, C. Y., & Shen, S. F. (2016). Seasonal and daily climate variation have opposite effects on species elevational range size. *Science*, *351*(6280), 1437–1439.

Canestrelli, D., Aloise, G., Cecchetti, S., & Nascetti, G. (2010). Birth of a hotspot of intraspecific genetic diversity: notes from the underground. *Molecular Ecology*, *19*(24), 5432–5451.

Carnaval, A. C., Hickerson, M. J., Haddad, C. F., Rodrigues, M. T., & Moritz, C. (2009). Stability predicts genetic diversity in the Brazilian Atlantic forest hotspot. *Science*, *323*(5915), 785–789.

CEPF (Critical Ecosystem Partnership Fund) - The Biodiversity hotspots (2014, November). http://www.cepf.net/resources/hotspots/Pages/default.aspx

Chiocchio, A., Colangelo, P., Aloise, G., Amori, G., Bertolino, S., Bisconti, R., ... & Canestrelli, D. (2019). Population genetic structure of the bank vole *Myodes glareolus* within its glacial refugium in peninsular Italy. *Journal of Zoological Systematics and Evolutionary Research*, *57*(4), 959–969.

Cincotta, R. P., Wisnewski, J., & Engelman, R. (2000). Human population in the biodiversity hotspots. *Nature*, *404*(6781), 990–992.

De Frenne, P., Lenoir, J., Luoto, M., Scheffers, B. R., Zellweger, F., Aalto, J., ... & Hylander, K. (2021). Forest microclimates and climate change: Importance, drivers and future research agenda. *Global Change Biology*, *27*(11), 2279–2297.

De Lombaerde, E., Vangansbeke, P., Lenoir, J., Van Meerbeek, K., Lembrechts, J., Rodríguez-Sánchez, F., ... & De Frenne, P. (2022). Maintaining forest cover to enhance temperature buffering under future climate change. *Science of the Total Environment*, *810*, 151338.

De Luca, G., & Modica, G. (2022, September). Canopy fire effects estimation using Sentinel-2 imagery and deep learning approach. A case study on the Aspromonte National Park. In *International Conference on Applied Intelligence and Informatics* (pp. 403–417). Cham: Springer Nature Switzerland.

Dobrowski, S. Z. (2011). A climatic basis for microrefugia: the influence of terrain on climate. *Global Change Biology*, *17*(2), 1022–1035.

Ewers, R. M., & Banks-Leite, C. (2013). Fragmentation impairs the microclimate buffering effect of tropical forests. *PLoS One*, *8*(3), e58093.

Favre, A., Päckert, M., Pauls, S. U., Jähnig, S. C., Uhl, D., Michalak, I., & Muellner-Riehl, A. N. (2015). The role of the uplift of the Qinghai-Tibetan Plateau for the evolution of Tibetan biotas. *Biological Reviews*, *90*(1), 236–253.

Flantua, S. G., O'Dea, A., Onstein, R. E., Giraldo, C., & Hooghiemstra, H. (2019). The flickering connectivity system of the north Andean páramos. *Journal of Biogeography*, *46*(8), 1808–1825.

Gallai, N., Salles, J. M., Settele, J., & Vaissière, B. E. (2009). Economic valuation of the vulnerability of world agriculture confronted with pollinator decline. *Ecological Economics*, *68*(3), 810–821.

Gómez, A., & Lunt, D. H. (2007). Refugia within refugia: patterns of phylogeographic concordance in the Iberian Peninsula. *Phylogeography of Southern European Refugia: Evolutionary perspectives on the origins and conservation of European biodiversity*, 155–188.

Groves, R. H., & Di Castri, F. (Eds.). (1991). *Biogeography of Mediterranean invasions*. Cambridge University Press.

Hansen, M. C., Potapov, P. V., Moore, R., Hancher, M., Turubanova, S. A., Tyukavina, A., ... & Townshend, J. R. (2013). High-resolution global maps of 21st-century forest cover change. *Science*, *342*(6160), 850–853.

Hewitt, G. (2000). The genetic legacy of the Quaternary ice ages. *Nature*, *405*(6789), 907–913.

Holderegger, R., & Thiel-Egenter, C. (2009). A discussion of different types of glacial refugia used in mountain biogeography and phylogeography. *Journal of Biogeography*, *36*(3), 476–480.

Hoorn, C., Guerrero, J., Sarmiento, G. A., & Lorente, M. A. (1995). Andean tectonics as a cause for changing drainage patterns in Miocene northern South America. *Geology*, *23*(3), 237–240.

Hoorn, C., Perrigo, A., & Antonelli, A. (Eds.). (2018). *Mountains, climate and biodiversity*. John Wiley & Sons.

Iannella, M., D'Alessandro, P., & Biondi, M. (2018). Evidences for a shared history for spectacled salamanders, haplotypes and climate. *Scientific Reports*, *8*(1), 16507.

Janzen, D. H. (1967). Why mountain passes are higher in the tropics. *The American Naturalist*, *101*(919), 233–249.

Kapos, V., Rhind, J., Edwards, M., Price, M. F., & Ravilious, C. (2000). Developing a map of the world's mountain forests. In *Forests in sustainable mountain development: a state of knowledge report for 2000. Task Force on Forests in Sustainable Mountain Development*. (pp. 4–19). Wallingford UK: Cabi Publishing.

Klein, A. M., Vaissière, B. E., Cane, J. H., Steffan-Dewenter, I., Cunningham, S. A., Kremen, C., & Tscharntke, T. (2007). Importance of pollinators in changing landscapes for world crops. *Proceedings of the Royal Society B: Biological Sciences*, *274*(1608), 303–313.

Körner, C. (2003). *Alpine plant life: functional plant ecology of high mountain ecosystems; with 47 tables*. Springer Science & Business Media.

Körner, C. (2004). Mountain biodiversity, its causes and function. *AMBIO: A Journal of the Human Environment*, *33*, 11–17.

Körner, C., Jetz, W., Paulsen, J., Payne, D., Rudmann-Maurer, K., & M Spehn, E. (2017). A global inventory of mountains for bio-geographical applications. *Alpine Botany*, *127*, 1–15.

Kremen, C., & Ostfeld, R. S. (2005). A call to ecologists: measuring, analyzing, and managing ecosystem services. *Frontiers in Ecology and the Environment*, *3*(10), 540–548.

Lanza, B. (2007). *Fauna d'Italia: Amphibia*. Ed. Calderini.

Lembrechts, J. J., & Lenoir, J. (2020). Microclimatic conditions anywhere at any time!. *Global Change Biology*, *26*(2), 337–339.

Leo, M. (1995). The importance of tropical montane cloud forest for preserving vertebrate endemism in Peru: the Rio Abiseo National Park as a case study. In *Tropical montane cloud forests* (pp. 198–211). New York, NY: Springer US.

Luoto, M., & Heikkinen, R. K. (2008). Disregarding topographical heterogeneity biases species turnover assessments based on bioclimatic models. *Global Change Biology*, *14*(3), 483–494.

Martino, G., Chiocchio, A., Siclari, A., & Canestrelli, D. (2022). Distribution and conservation status of threatened endemic amphibians within the Aspromonte mountain region, a hotspot of Mediterranean biodiversity. *Nature Conservation*, *50*, 1–22.

Médail, F., & Diadema, K. (2009). Glacial refugia influence plant diversity patterns in the Mediterranean Basin. *Journal of Biogeography*, *36*(7), 1333–1345.

Médail, F., & Quézel, P. (1997). Hot-spots analysis for conservation of plant biodiversity in the Mediterranean Basin. *Annals of the Missouri Botanical Garden*, 112–127.

Molles, M. C., & Tibbets, T. (2002). *Ecology: concepts and applications* (pp. 186–254). New York: McGraw-Hill.

Mutke, J., & Barthlott, W. (2005). Patterns of vascular plant diversity at continental to global scales. *Biologiske Skrifter*, *55*(4), 521–531.

Myers, N., Mittermeier, R. A., Mittermeier, C. G., Da Fonseca, G. A., & Kent, J. (2000). Biodiversity hotspots for conservation priorities. *Nature*, *403*(6772), 853–858.

Nadeau, C. P., Giacomazzo, A., & Urban, M. C. (2022). Cool microrefugia accumulate and conserve biodiversity under climate change. *Global Change Biology*, *28*(10), 3222–3235.

Nevado, B., Contreras-Ortiz, N., Hughes, C., & Filatov, D. A. (2018). Pleistocene glacial cycles drive isolation, gene flow and speciation in the high-elevation Andes. *New Phytologist*, *219*(2), 779–793.

Noroozi, J., Talebi, A., Doostmohammadi, M., Rumpf, S. B., Linder, H. P., & Schneeweiss, G. M. (2018). Hotspots within a global biodiversity hotspot-areas of endemism are associated with high mountain ranges. *Scientific Reports*, *8*(1), 10345.

Ohlemüller, R., Anderson, B. J., Araujo, M. B., Butchart, S. H., Kudrna, O., Ridgely, R. S., & Thomas, C. D. (2008). The coincidence of climatic and species rarity: high risk to small-range species from climate change. *Biology Letters*, *4*(5), 568–572.

Ozenda, P., & Borel, J. L. (2003). 3.4 The Alpine Vegetation of the Alps. *Alpine Biodiversity in Europe*, *167*, 53.

Pastore, M. A., Classen, A. T., D'Amato, A. W., Foster, J. R., & Adair, E. C. (2022). Cold-air pools as microrefugia for ecosystem functions in the face of climate change. *Ecology*, *103*(8), e3717.

Patsiou, T. S., Conti, E., Zimmermann, N. E., Theodoridis, S., & Randin, C. F. (2014). Topo-climatic microrefugia explain the persistence of a rare endemic plant in the Alps during the last 21 millennia. *Global Change Biology*, *20*(7), 2286–2300.

Pauli, H., Gottfried, M., Dirnböck, T., Dullinger, S., & Grabherr, G. (2003). *Assessing the long-term dynamics of endemic plants at summit habitats* (pp. 195–207). Springer Berlin Heidelberg.

Piovesan, G., Baliva, M., Calcagnile, L., D'Elia, M., Dorado-Linan, I., Palli, J., ... & Quarta, G. (2020). Radiocarbon dating of Aspromonte sessile oaks reveals the oldest dated temperate flowering tree in the world. *Ecology*, *101*(12), 1–4.

Potts, S. G., Biesmeijer, J. C., Kremen, C., Neumann, P., Schweiger, O., & Kunin, W. E. (2010). Global pollinator declines: trends, impacts and drivers. *Trends in Ecology & Evolution*, *25*(6), 345–353.

Prete, G., Avolio, E., Capparelli, V., Lepreti, F., & Carbone, V. (2023). Daily Precipitation and Temperature Extremes in Southern Italy (Calabria Region). *Atmosphere*, *14*(3), 553.

Rahbek, C., Borregaard, M. K., Colwell, R. K., Dalsgaard, B. O., Holt, B. G., Morueta-Holme, N., ... & Fjeldså, J. (2019). Humboldt's enigma: What causes global patterns of mountain biodiversity?. *Science*, *365*(6458), 1108–1113.

Sandel, B., Arge, L., Dalsgaard, B., Davies, R. G., Gaston, K. J., Sutherland, W. J., & Svenning, J. C. (2011). The influence of Late Quaternary climate-change velocity on species endemism. *Science*, *334*(6056), 660–664.

Schulte, U., Küsters, D., & Steinfartz, S. (2007). A PIT tag based analysis of annual movement patterns of adult fire salamanders (*Salamandra salamandra*) in a Middle European habitat. *Amphibia-Reptilia, 28*(4), 531–536.

Spehn, E. M., Rudmann-Maurer, K., Korner, C., & Maselli, D. (2010). Mountain Biodiversity and Global Change. Basel, GMBA-DIVERSITAS.

Steinbauer, M. J., Field, R., Grytnes, J. A., Trigas, P., Ah-Peng, C., Attorre, F., ... & Beierkuhnlein, C. (2016). Topography-driven isolation, speciation and a global increase of endemism with elevation. *Global Ecology and Biogeography, 25*(9), 1097–1107.

Stewart, J. R., Lister, A. M., Barnes, I., & Dalén, L. (2010). Refugia revisited: individualistic responses of species in space and time. *Proceedings of the Royal Society B: Biological Sciences, 277*(1682), 661–671.

Rodgers, W. A., & Homewood, K. M. (1982). Species richness and endemism in the Usambara mountain forests, Tanzania. *Biological Journal of the Linnean Society*, *18*(3), 197–242.

Särkinen, T., Pennington, R. T., Lavin, M., Simon, M. F., & Hughes, C. E. (2012). Evolutionary islands in the Andes: persistence and isolation explain high endemism in Andean dry tropical forests. *Journal of Biogeography*, *39*(5), 884–900.

Scherrer, D., & Körner, C. (2010). Infra-red thermometry of alpine landscapes challenges climatic warming projections. *Global Change Biology*, *16*(9), 2602–2613.

Scherrer, D., & Körner, C. (2011). Topographically controlled thermal-habitat differentiation buffers alpine plant diversity against climate warming. *Journal of Biogeography*, *38*(2), 406–416.

Smythies, B. E. (1964). The birds of Mt Kinabalu and their zoogeographical relationships. *Proceedings of the Royal Society of London. Series B. Biological Sciences*, *161*(982), 75–80.

Steadman, D. W. (1995). Prehistoric extinctions of Pacific island birds: biodiversity meets zooarchaeology. *Science*, *267*(5201), 1123–1131.

Stein, A., Gerstner, K., & Kreft, H. (2014). Environmental heterogeneity as a universal driver of species richness across taxa, biomes and spatial scales. *Ecology Letters*, *17*(7), 866–880.

Stuart, S. N., Chanson, J. S., Cox, N. A., Young, B. E., Rodrigues, A. S., Fischman, D. L., & Waller, R. W. (2004). Status and trends of amphibian declines and extinctions worldwide. *Science*, *306*(5702), 1783–1786.

Thomas, C. D., Cameron, A., Green, R. E., Bakkenes, M., Beaumont, L. J., Collingham, Y. C., ... & Williams, S. E. (2004). Extinction risk from climate change. *Nature*, *427*(6970), 145–148.

Todisco, V., Gratton, P., Cesaroni, D., & Sbordoni, V. (2010). Phylogeography of Parnassius apollo: hints on taxonomy and conservation of a vulnerable glacial butterfly invader. *Biological Journal of the Linnean Society*, *101*(1), 169–183.

Turner, W. R., Bradley, B. A., Estes, L. D., Hole, D. G., Oppenheimer, M., & Wilcove, D. S. (2010). Climate change: helping nature survive the human response. *Conservation Letters*, *3*(5), 304–312.

van Dijk, P. P., Stuart, B. L., & Rhodin, A. G. (2000). Asian turtle trade. *Chelonian Research Monographs*, *2*, 1–164.

Vasconcelos, T. N., Alcantara, S., Andrino, C. O., Forest, F., Reginato, M., Simon, M. F., & Pirani, J. R. (2020). Fast diversification through a mosaic of evolutionary histories characterizes the endemic flora of ancient Neotropical mountains. *Proceedings of the Royal Society B*, *287*(1923), 20192933.

Wake, D. B., & Vredenburg, V. T. (2008). Are we in the midst of the sixth mass extinction? A view from the world of amphibians. *Proceedings of the National Academy of Sciences*, *105*, 11466–11473.

Zachos, F. E., & Habel, J. C. (Eds.). (2011). *Biodiversity hotspots: distribution and protection of conservation priority areas*. Springer Science & Business Media.

Zampiglia, M., Bisconti, R., Maiorano, L., Aloise, G., Siclari, A., Pellegrino, F., ... & Canestrelli, D. (2019). Drilling down hotspots of intraspecific diversity to bring them into on-ground conservation of threatened species. *Frontiers in Ecology and Evolution*, *7*, 205.

Zellweger, F., De Frenne, P., Lenoir, J., Rocchini, D., & Coomes, D. (2019). Advances in microclimate ecology arising from remote sensing. *Trends in Ecology & Evolution*, *34*(4), 327–341.

Appendices of Chapter 2

Table A.1. Coordinates, altitude, daily average time series length, and proportion of missing data for 1970-2000 for each weather station employed in the present study.

ID	Coordinates (EPSG: 32632)		Altitude	Daily average time series		Missing data
	longitude	latitude	(m a.s.l.)	start	end	for 1970-2000
2040	1161029	4281649	74.97	1989-01-19	2021-01-31	62.06 %
2072	1152849	4279535	393.49	2004-10-14	2021-01-31	100 %
2160	1141307	4264722	13.03	1999-05-06	2021-01-31	94.65 %
2180	1123456	4264655	944.89	1963-01-01	2021-01-31	22.38 %
2200	1128582	4259092	163.40	1992-03-25	2021-01-31	73.05 %
2220	1129293	4246703	8.97	2005-01-01	2021-01-31	100 %
2230	1116979	4254000	309.00	1992-03-25	2021-01-31	72.52 %
2270	1121600	4240769	406.67	1992-03-24	2021-01-31	72.53%
2290	1118187	4229187	456.32	1992-03-24	2021-01-31	71.79 %
2310	1120507	4221293	102.96	1988-06-10	2021-01-31	61.90 %
2320	1109195	4228125	960.13	2005-01-01	2021-01-31	100 %
2337	1108304	4222600	202.55	2014-05-01	2021-01-31	100 %
2340	1104962	4233682	972.76	1992-04-10	2021-01-31	71.84 %
2380	1091178	4225861	708.85	2001-12-04	2021-01-31	100 %
2417	1096637	4235553	1124.54	2014-05-01	2021-01-31	100 %
2450	1083389	4238723	67.11	1924-01-01	2021-01-31	14.09 %
2457	1092630	4230294	902.05	2014-05-01	2021-01-31	100 %
2460	1091155	4243293	758.06	2014-05-01	2021-01-31	100 %
2465	1096479	4239176	1238.84	1999-05-08	2021-01-31	94.94 %
2466	1092099	4246248	547.11	2004-10-14	2021-01-31	100 %
2467	1086702	4240290	387.55	2014-05-01	2021-01-31	100 %
2470	1097587	4247042	1157.10	1939-04-26	2021-01-31	42.71 %
2487	1087578	4243767	551.72	2014-05-01	2021-01-31	100 %
2495	1081864	4247930	21.45	2005-01-01	2021-01-31	100 %
2510	1086756	4255067	68.64	1988-09-08	2021-01-31	60.66 %
2514	1093014	4256028	555.04	2005-11-01	2021-01-31	100 %
2517	1088060	4253266	660.75	2014-05-01	2021-01-31	100 %
2540	1109687	4257321	454.58	1988-07-15	2021-01-31	61.55 %
2600	1119769	4268599	484.03	1924-01-01	2021-01-31	10.10 %
2610	1109031	4274130	85.70	2005-01-01	2021-01-31	100 %
2690	1116977	4281494	175.47	1988-10-01	2021-01-31	61.01 %
2710	1128374	4271555	701.19	1992-03-26	2021-01-31	71.97 %
2740	1109681	4284554	25.31	1940-05-16	2021-01-31	46.06 %

Table A.2. Proportions of overlap between the study area's distribution of PCA scores and the sampling distribution of the weather stations, and proportions of variance (i.e., landscape complexity) explained by the PC axes.

		PC 1	PC 2	PC 3	PC 4	PC 5
January	**overlap**	84.74 %	79.05 %	73.02 %	59.50 %	64.51 %
	variance	35.39 %	19.94 %	19.25 %	19.19 %	6.22 %
February	**overlap**	85.51 %	93.25 %	78.50 %	87.29 %	63.33 %
	variance	35.54 %	19.48 %	19.37 %	19.33 %	6.26 %
March	**overlap**	83.97 %	83.18 %	71.61 %	71.69 %	63.02 %
	variance	35.90 %	19.72 %	19.65 %	18.39 %	6.34 %
April	**overlap**	83.94 %	83.37 %	71.36 %	73.47 %	63.02 %
	variance	36.05 %	19.97 %	19.90 %	17.68 %	6.40 %
May	**overlap**	84.49 %	83.49 %	71.35 %	74.88 %	62.50 %
	variance	36.06 %	19.99 %	19.93 %	17.63 %	6.39 %
June	**overlap**	84.28 %	83.49 %	71.33 %	74.13 %	62.08 %
	variance	36.17 %	20.28 %	20.21 %	16.86 %	6.48 %
July	**overlap**	84.36 %	83.49 %	71.23 %	74.66 %	62.53 %
	variance	36.04 %	20.05 %	19.98 %	17.53 %	6.40 %
August	**overlap**	84.25 %	83.43 %	71.42 %	74.12 %	62.45 %
	variance	36.10 %	20.02 %	19.95 %	17.52 %	6.41 %
September	**overlap**	83.83 %	83.27 %	71.26 %	72.32 %	63.21 %
	variance	36.00 %	19.89 %	19.82 %	17.90 %	6.38 %
October	**overlap**	85.69 %	83.57 %	71.74 %	69.60 %	62.97 %
	variance	35.69 %	19.61 %	19.54 %	18.85 %	6.32 %
November	**overlap**	85.03 %	80.18 %	73.05 %	58.61 %	63.98 %
	variance	35.41 %	19.89 %	19.27 %	19.21 %	6.23 %
December	**overlap**	83.83 %	81.97 %	70.30 %	56.78 %	64.68 %
	variance	35.43 %	20.48 %	19.00 %	18.94 %	6.14 %

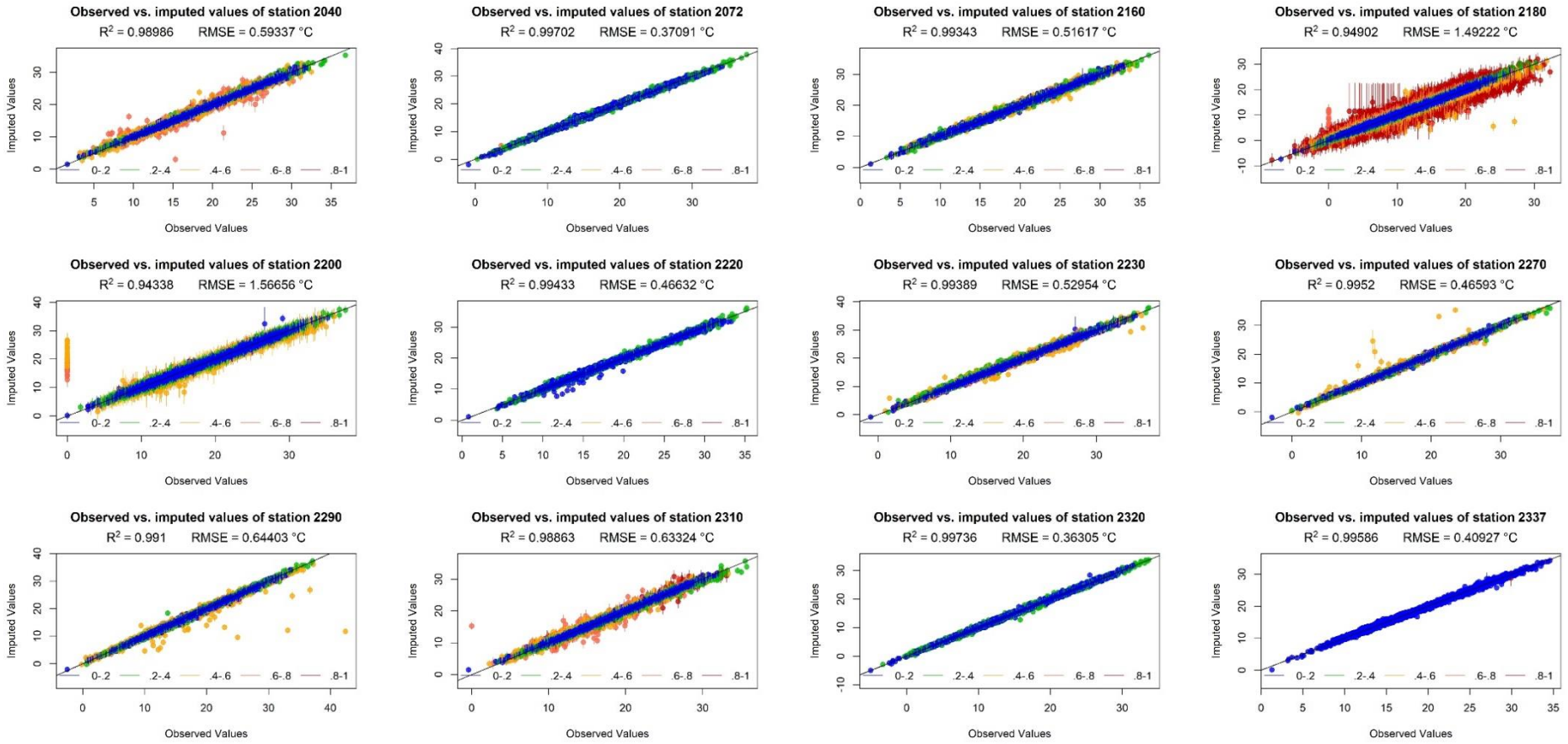

Figure A.1. Overimputation diagnostic plots for stations 2040 to 2337. For each weather station, we treated each observed temperature as missing and drew 20 imputed replicas for each: dots represent the mean of these replicas, while the vertical lines are their 90% confidence intervals. The diagonal line indicates perfect concordance between observed and imputed temperatures; the dots would all fall on the line if the imputations were perfect. For each observed temperature of a weather station, the color of dots and vertical lines displays the proportion of measurements that are missing from other weather stations; the legend reports this information in decimals. As expected, imputations get more precise as the proportion of missing measurements from other weather stations decreases. R^2 and RMSE values measure the degree of association between observed and imputed temperatures.

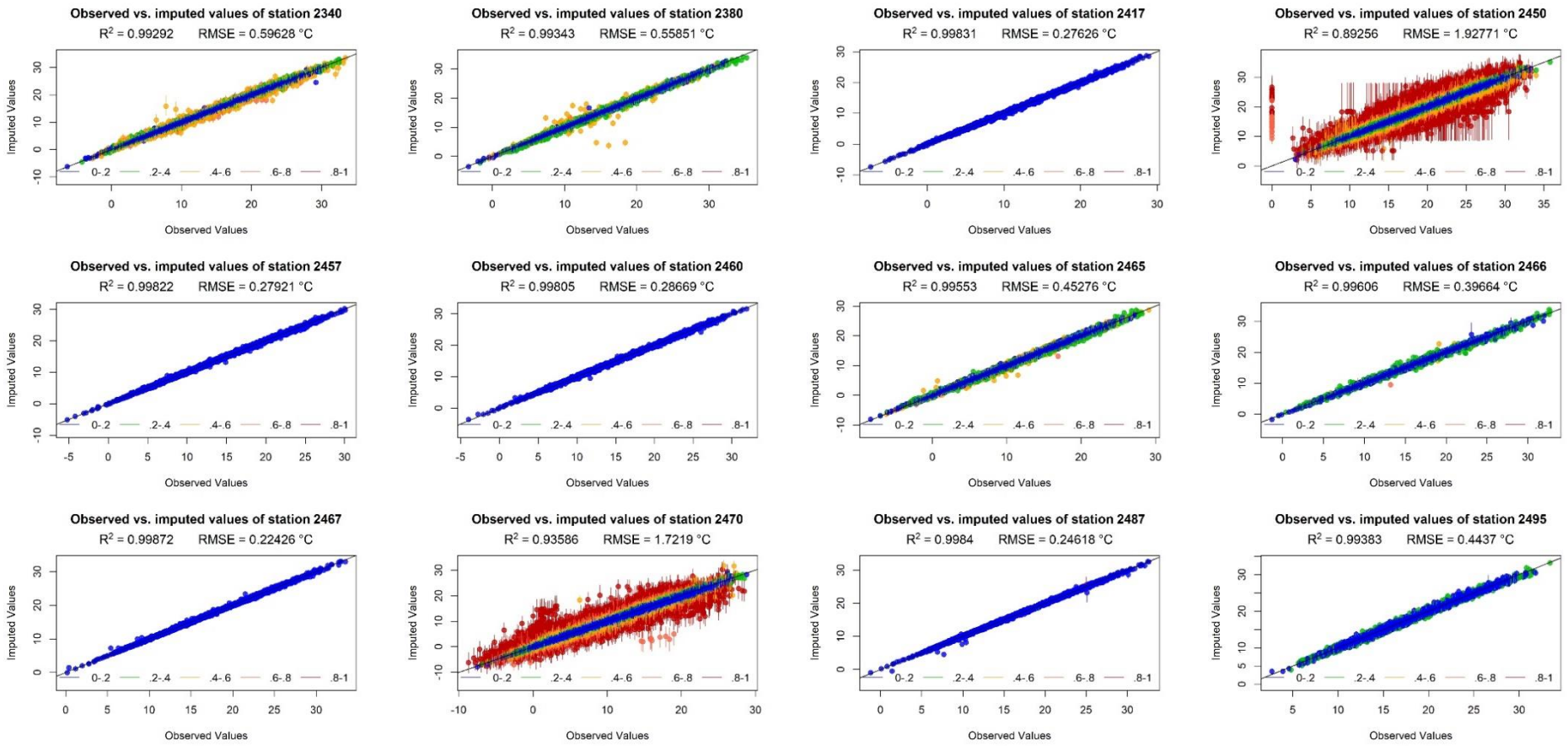

Figure A.2. Overimputation diagnostic plots for stations 2340 to 2495. For each weather station, we treated each observed temperature as missing and drew 20 imputed replicas for each: dots represent the mean of these replicas, while the vertical lines are their 90% confidence intervals. The diagonal line indicates perfect concordance between observed and imputed temperatures; the dots would all fall on the line if the imputations were perfect. For each observed temperature of a weather station, the color of dots and vertical lines displays the proportion of measurements that are missing from other weather stations; the legend reports this information in decimals. As expected, imputations get more precise as the proportion of missing measurements from other weather stations decreases. R^2 and RMSE values measure the degree of association between observed and imputed temperatures.

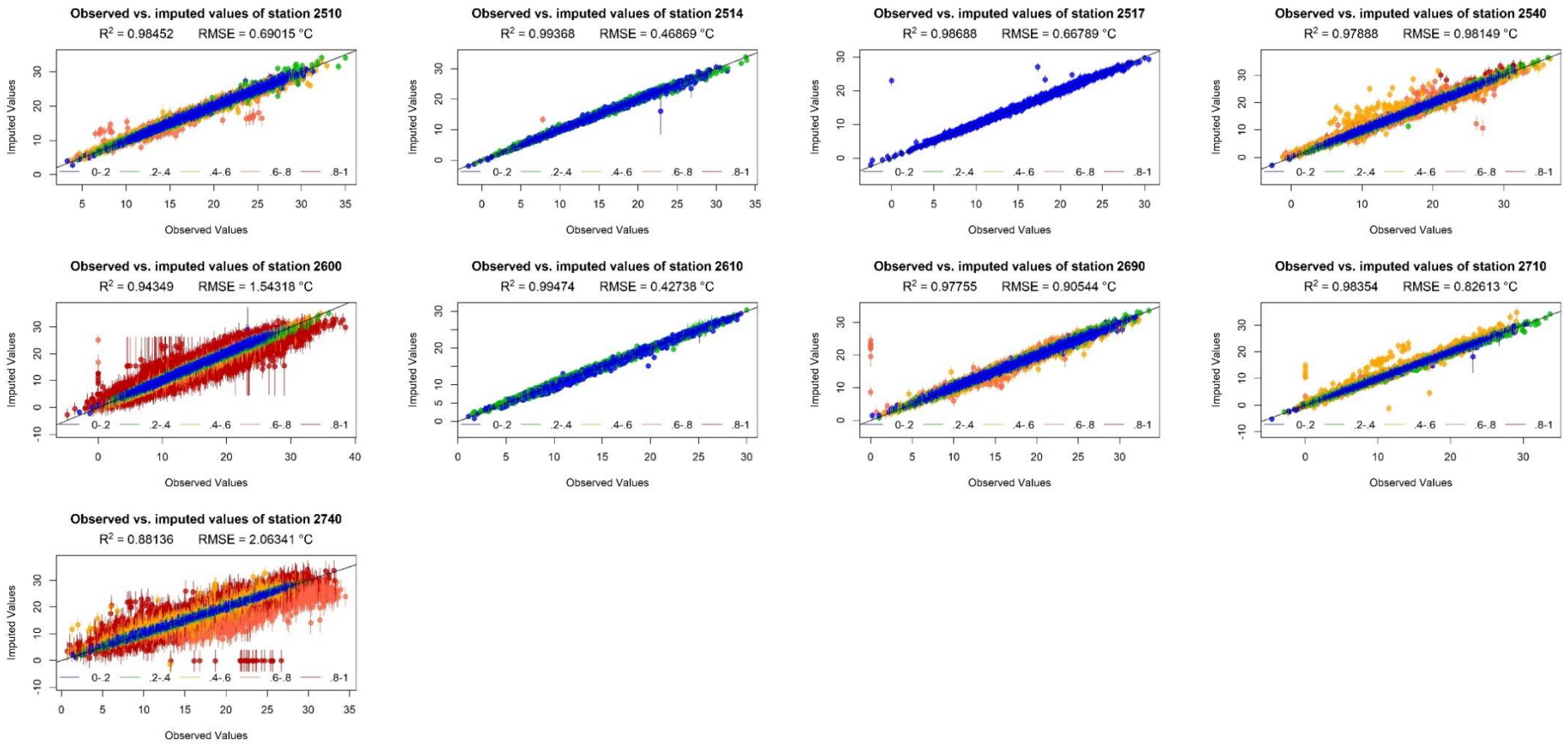

Figure A.3. Overimputation diagnostic plots for stations 2510 to 2740. For each weather station, we treated each observed temperature as missing and drew 20 imputed replicas for each: dots represent the mean of these replicas, while the vertical lines are their 90% confidence intervals. The diagonal line indicates perfect concordance between observed and imputed temperatures; the dots would all fall on the line if the imputations were perfect. For each observed temperature of a weather station, the color of dots and vertical lines displays the proportion of measurements that are missing from other weather stations; the legend reports this information in decimals. As expected, imputations get more precise as the proportion of missing measurements from other weather stations decreases. R^2 and RMSE values measure the degree of association between observed and imputed temperatures.

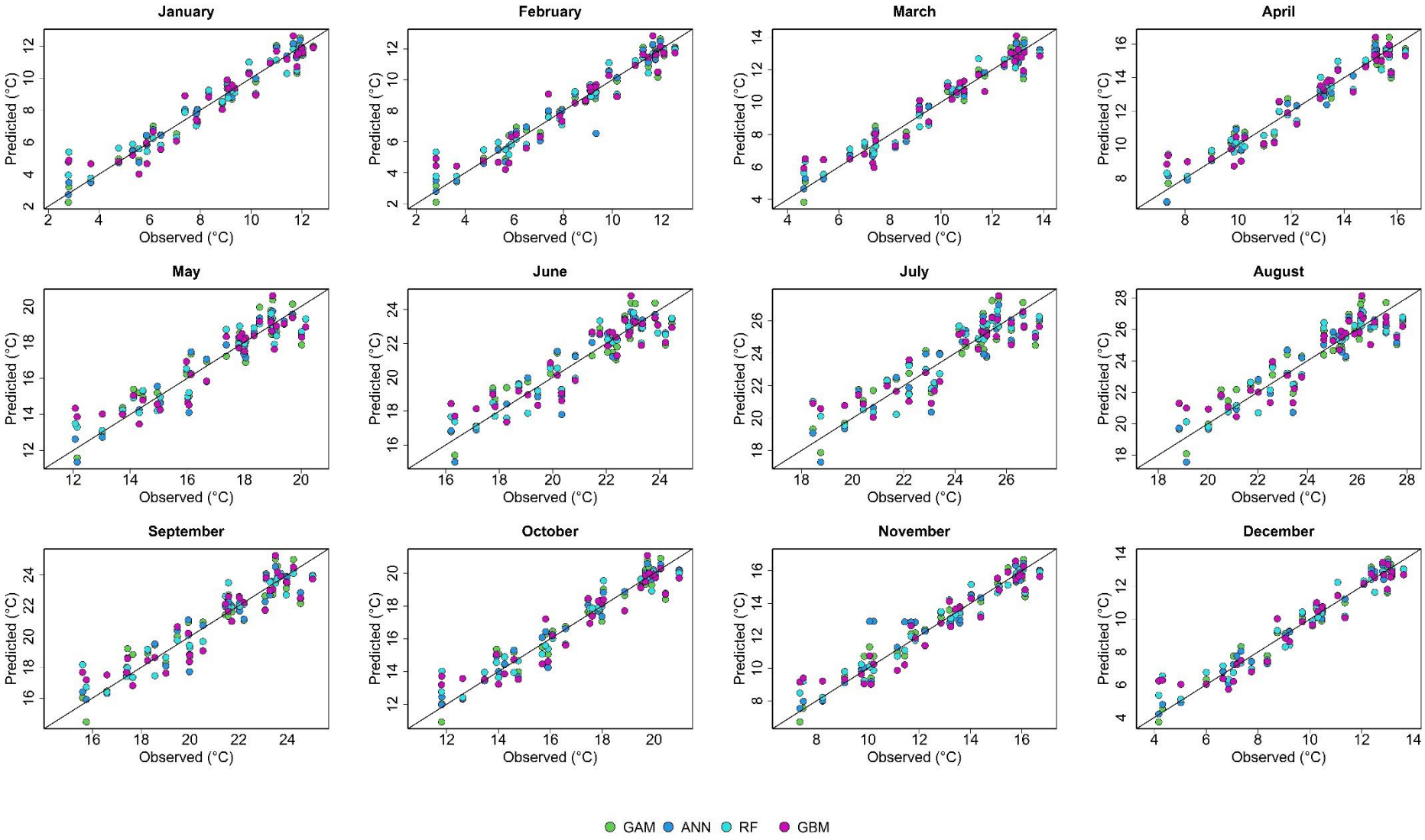

Figure A.4. Observed monthly climates at the weather stations' locations and those predicted when interpolating weather station data.

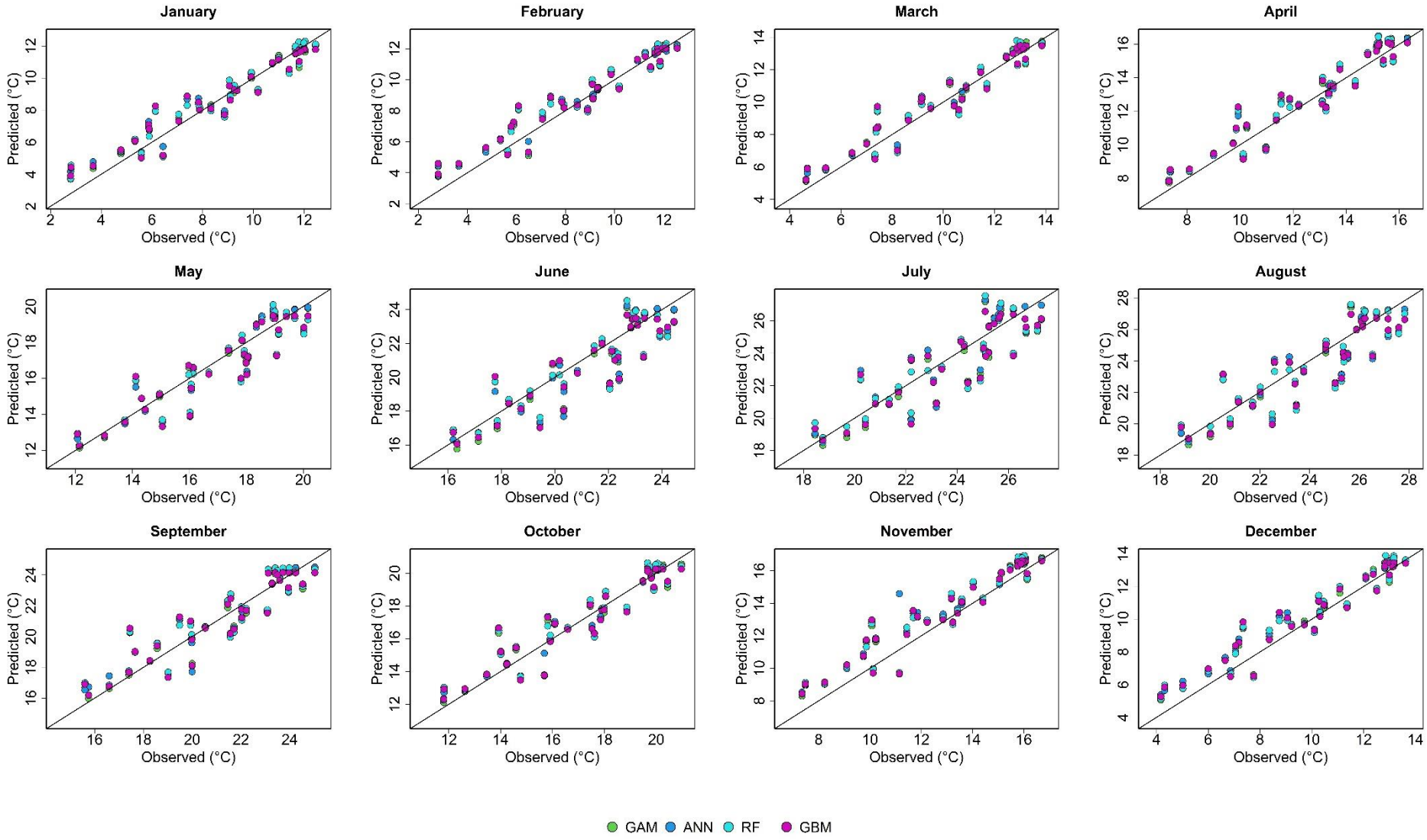

Figure A.5. Observed monthly climates at the weather stations' locations and those predicted when downscaling WorldClim.

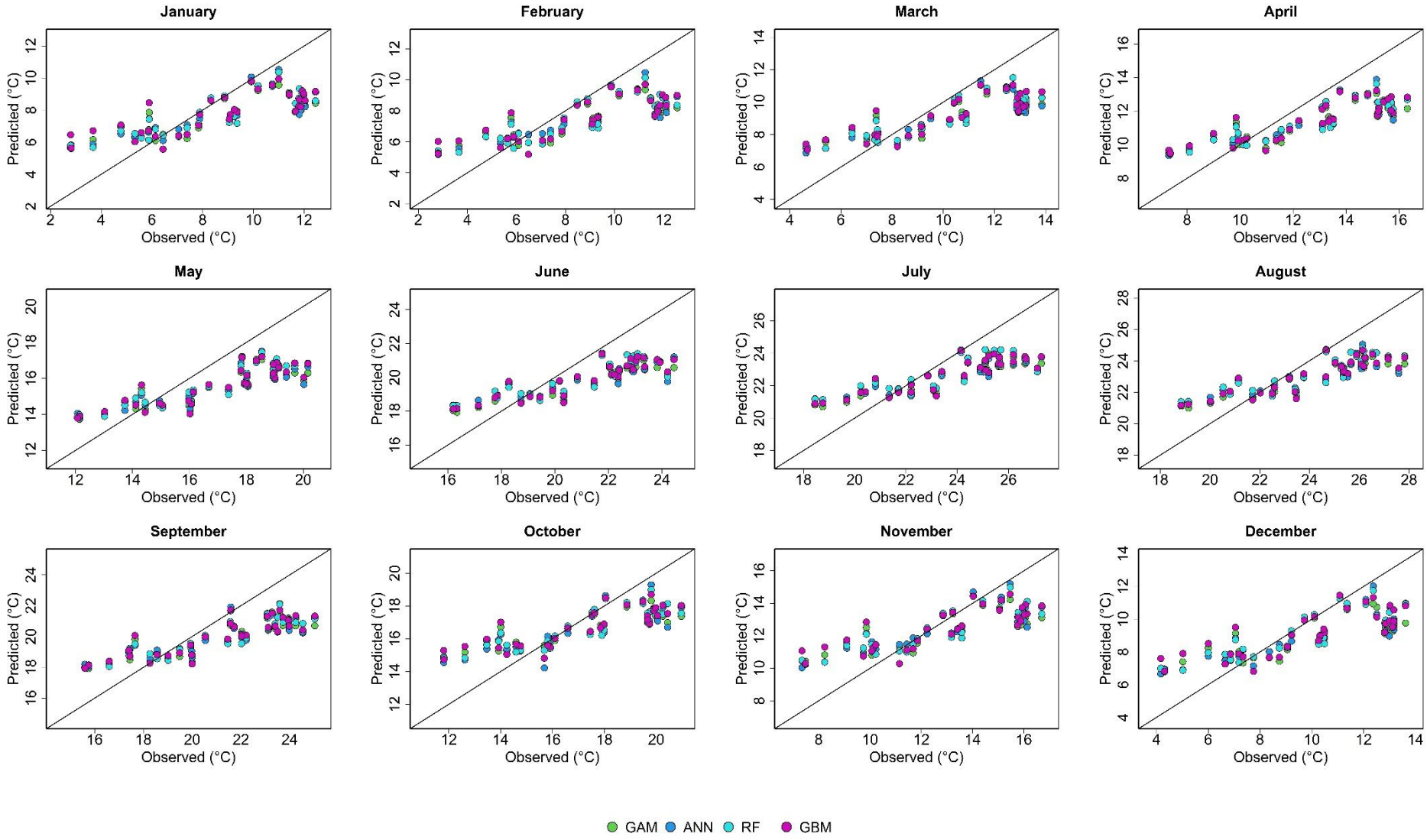

Figure A.6. Observed monthly climates at the weather stations' locations and those predicted when downscaling CHELSA.

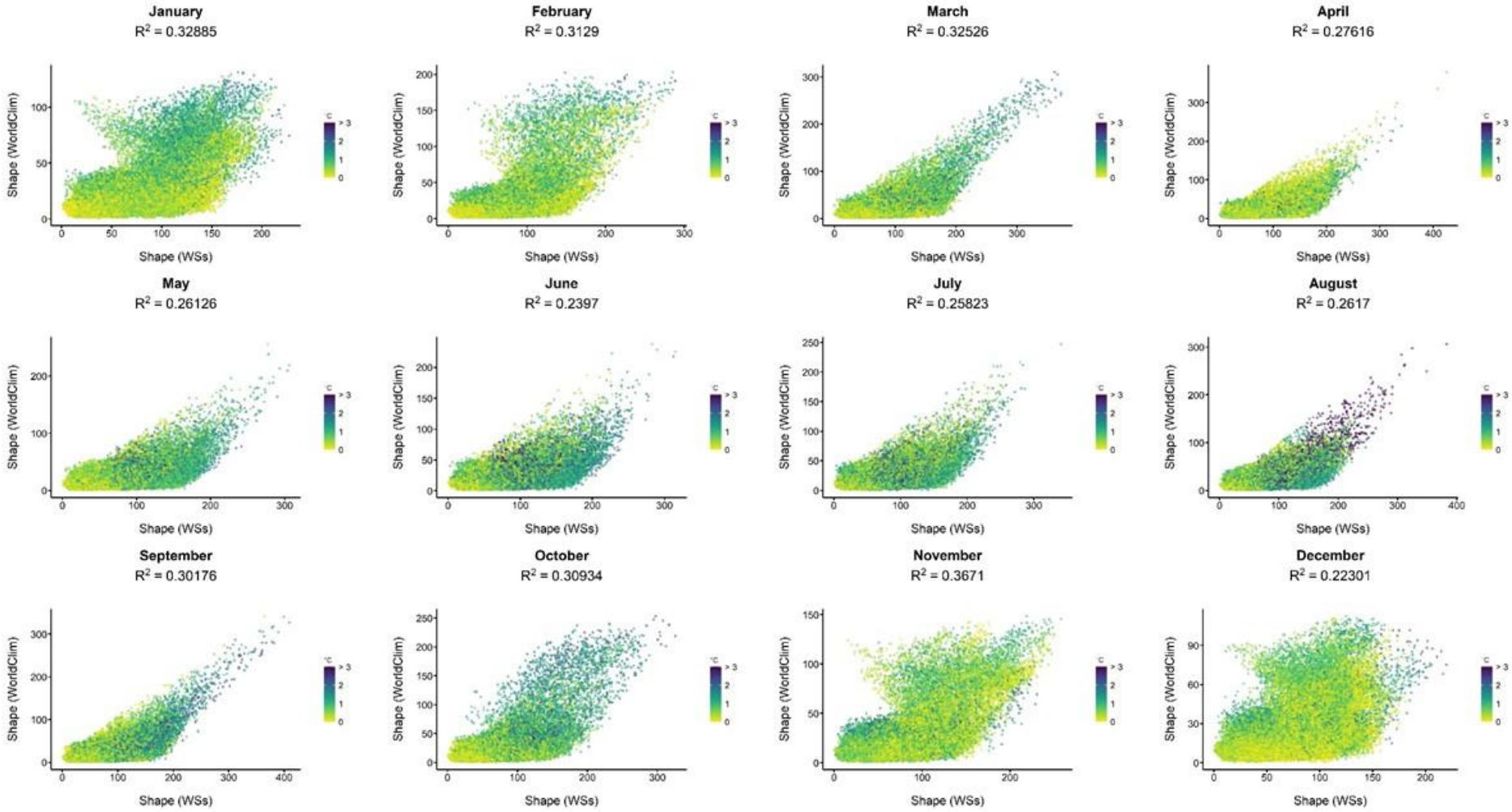

Figure A.7. Coherence of monthly climate estimates when interpolating weather station (WS) data and downscaling WorldClim, with respect to the degree of environmental extrapolation. We quantified environmental extrapolation by calculating the Shape metric at 100,000 random points; higher Shape values indicate higher extrapolation degrees. Color gradients indicate the absolute differences between predictions under WSs interpolation and WorldClim downscaling at those 100,000 points; lighter colors indicate stronger coherence of monthly climate estimates. We capped temperature absolute differences at 3 °C for graphical purposes. R^2 values measure the degree of association between the Shape values of WSs and WorldClim.

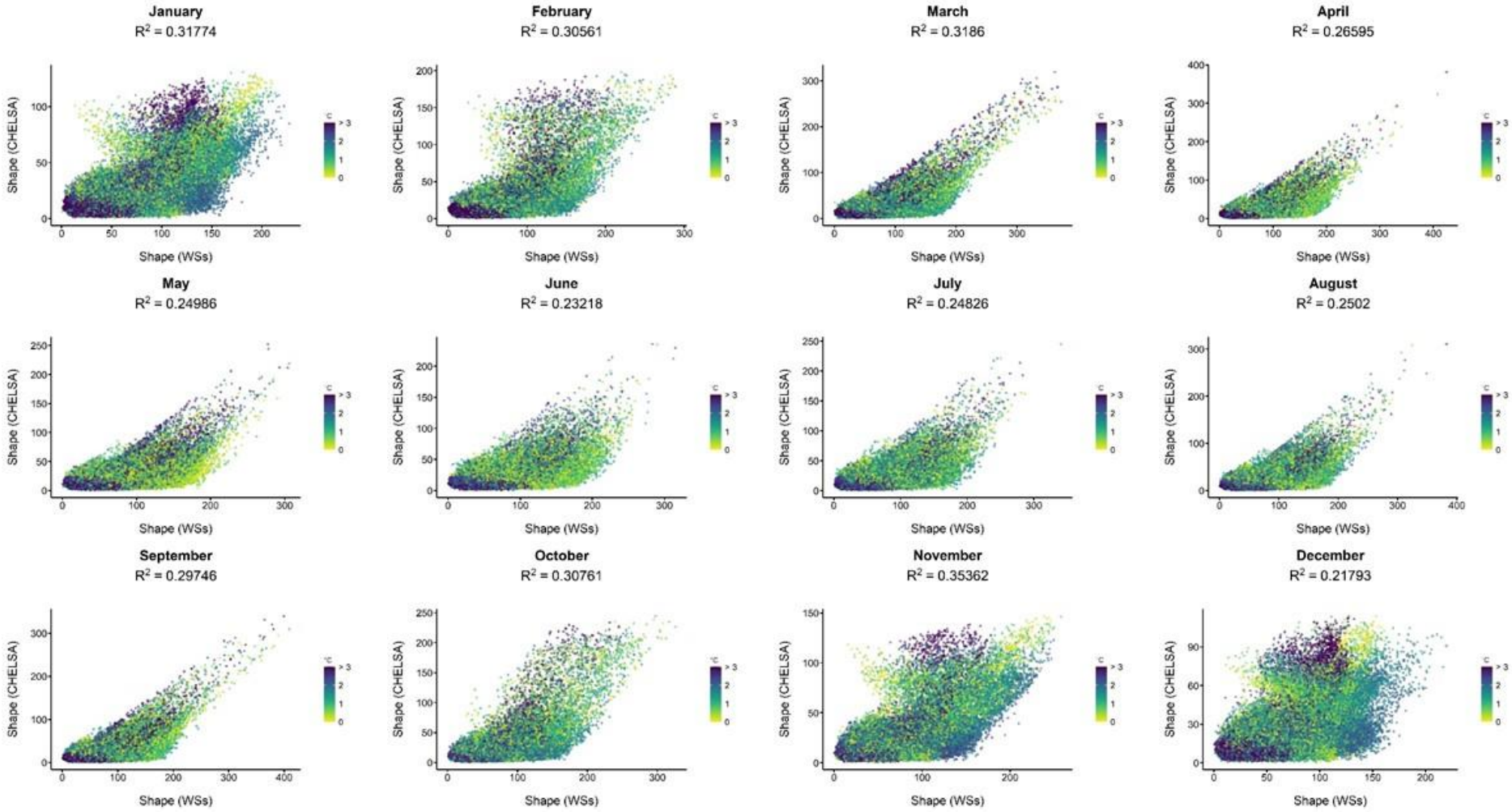

Figure A.8. Coherence of monthly climate estimates when interpolating weather station (WS) data and downscaling CHELSA, with respect to the degree of environmental extrapolation. We quantified environmental extrapolation by calculating the Shape metric at 100,000 random points; higher Shape values indicate higher extrapolation degrees. Color gradients indicate the absolute differences between predictions under WSs interpolation and CHELSA downscaling at those 100,000 points; lighter colors indicate stronger coherence of monthly climate estimates. We capped temperature absolute differences at 3 °C for graphical purposes. R^2 values measure the degree of association between the Shape values of WSs and CHELSA.

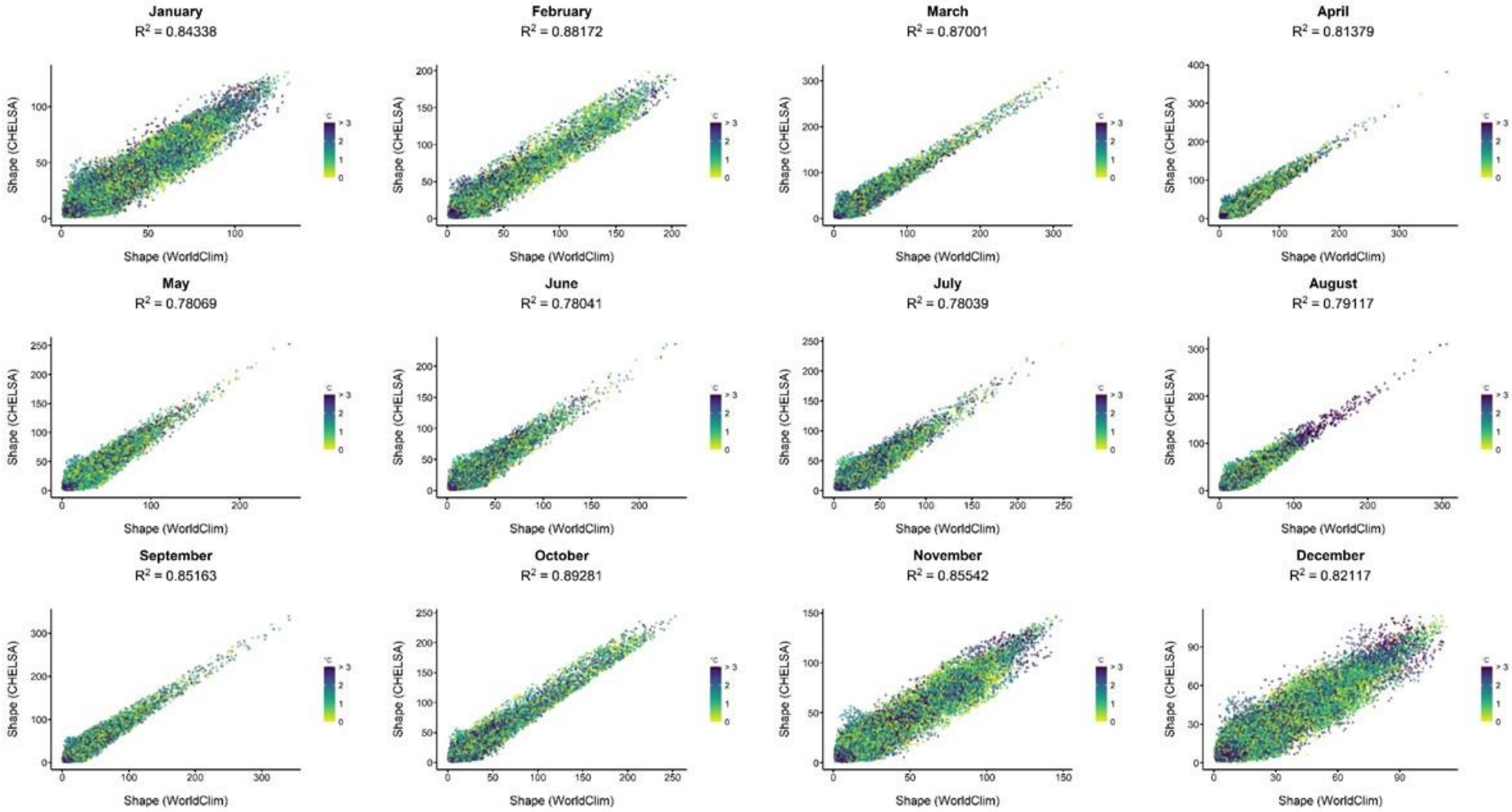

Figure A.9. Coherence of monthly climate estimates when downscaling WorldClim and CHELSA, with respect to the degree of environmental extrapolation. We quantified environmental extrapolation by calculating the Shape metric at 100,000 random points; higher Shape values indicate higher extrapolation degrees. Color gradients indicate the absolute differences between predictions under WorldClim and CHELSA downscaling at those 100,000 points; lighter colors indicate stronger coherence of monthly climate estimates. We capped temperature absolute differences at 3 °C for graphical purposes. R^2 values measure the degree of association between the Shape values of WorldClim and CHELSA.

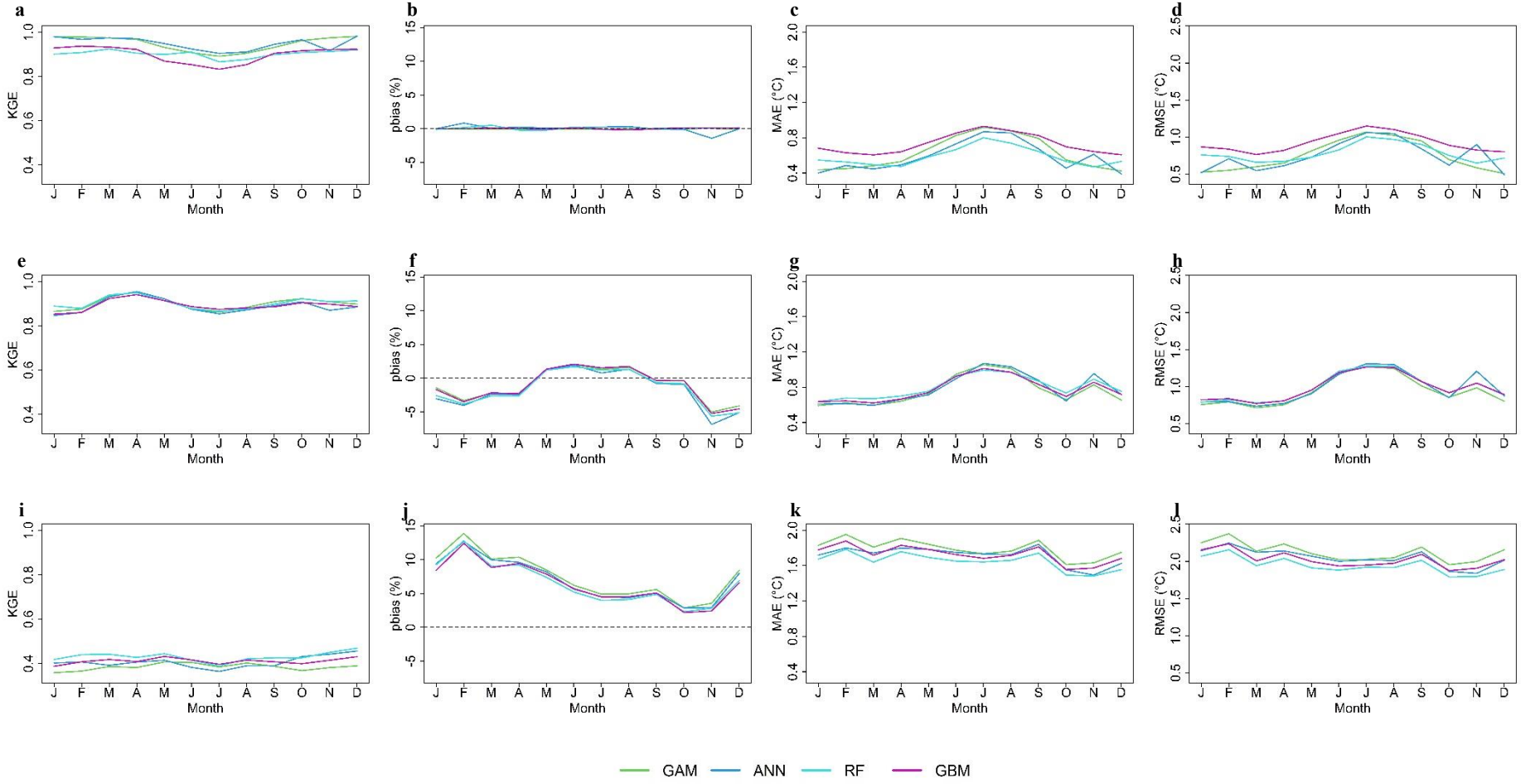

Figure A.10. Seasonal patterns in KGE scores (first column), *pbias* (second column), MAE (third column), and RMSE (fourth column) that we obtained in the cross-validations when employing each algorithm to interpolate weather station data (top row) and downscale WorldClim (middle row) and CHELSA (bottom row). Model performance improves as KGE values approach 1; KGE values between 0 and 0.5 indicate poor model performance. Low *pbias* values reflect accurate model prediction; the optimal *pbias* value is 0. Model performance increases as MAE and RMSE values decrease.

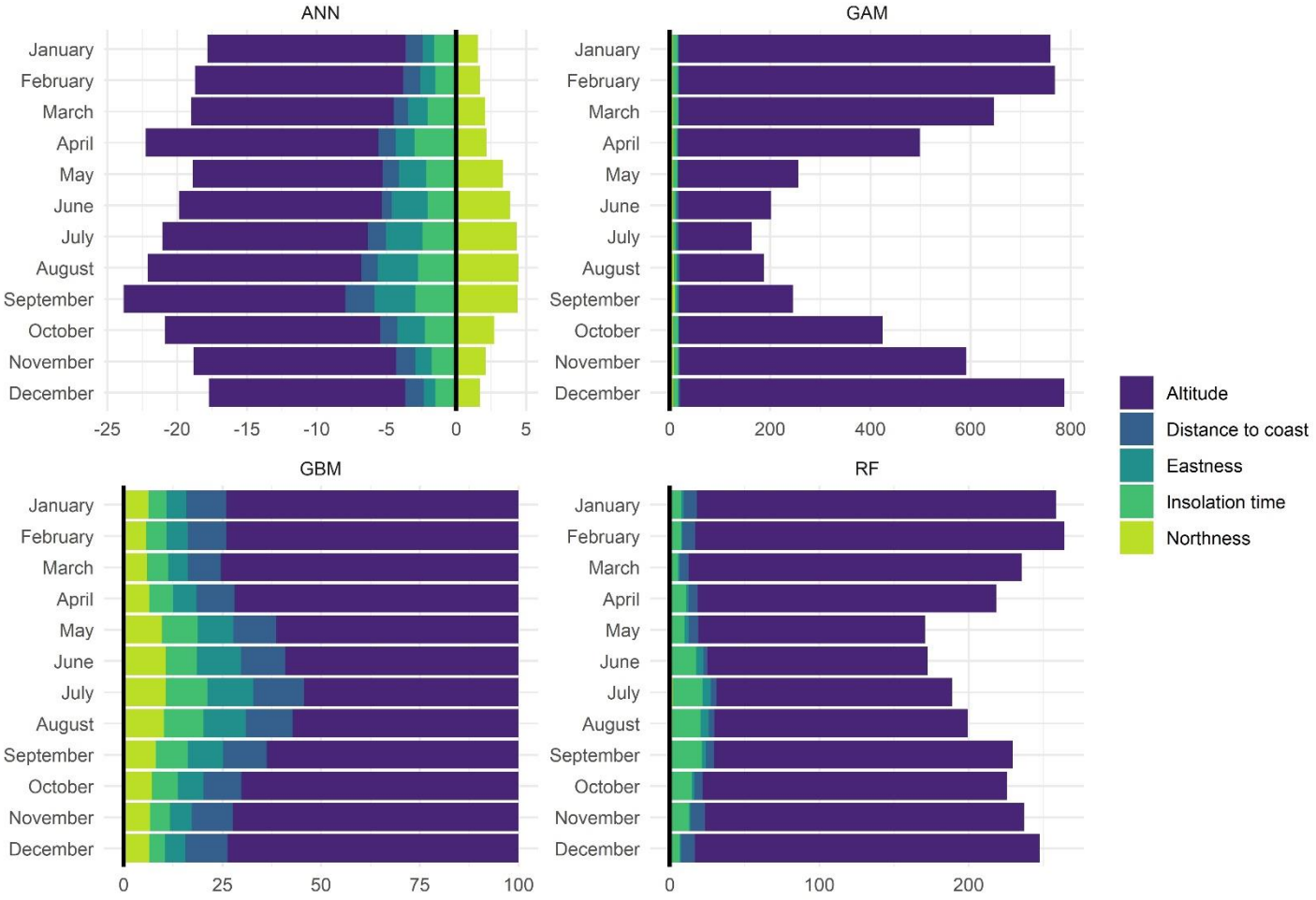

Figure A.11. Variable importance plots for the interpolation of weather station data. ANN's top-left subplot displays the Olden relative variable importance, GAM's top-right subplot the F statistic for each predictor, GBM's bottom-left subplot the computed relative influences, normalized to sum to 100, and RF's bottom-right subplot the increase in node purity associated with each predictor.

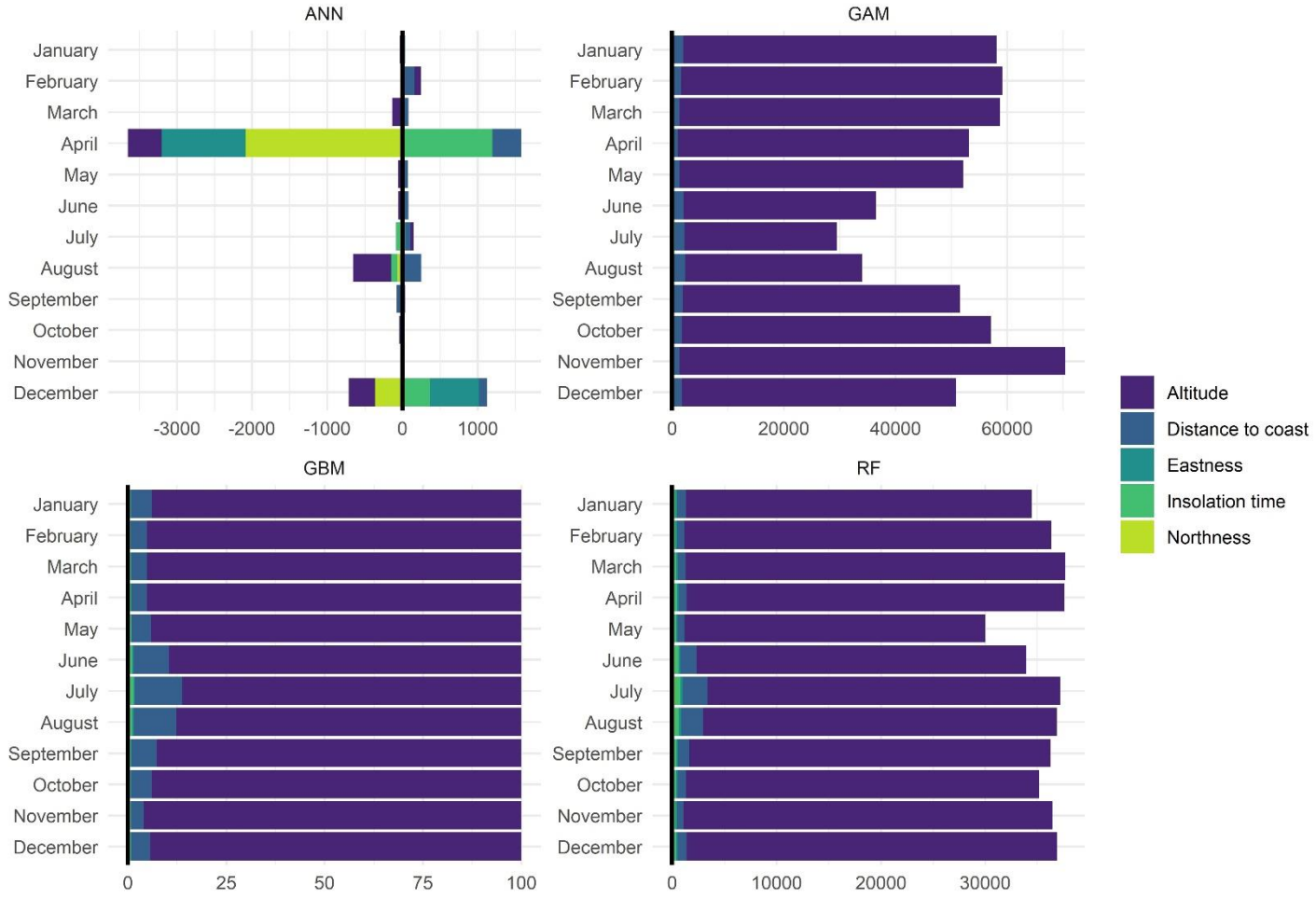

Figure A.12. Variable importance plots for the WorldClim downscaling. ANN's top-left subplot displays the Olden relative variable importance, GAM's top-right subplot the F statistic for each predictor, GBM's bottom-left subplot the computed relative influences, normalized to sum to 100, and RF's bottom-right subplot the increase in node purity associated with each predictor.

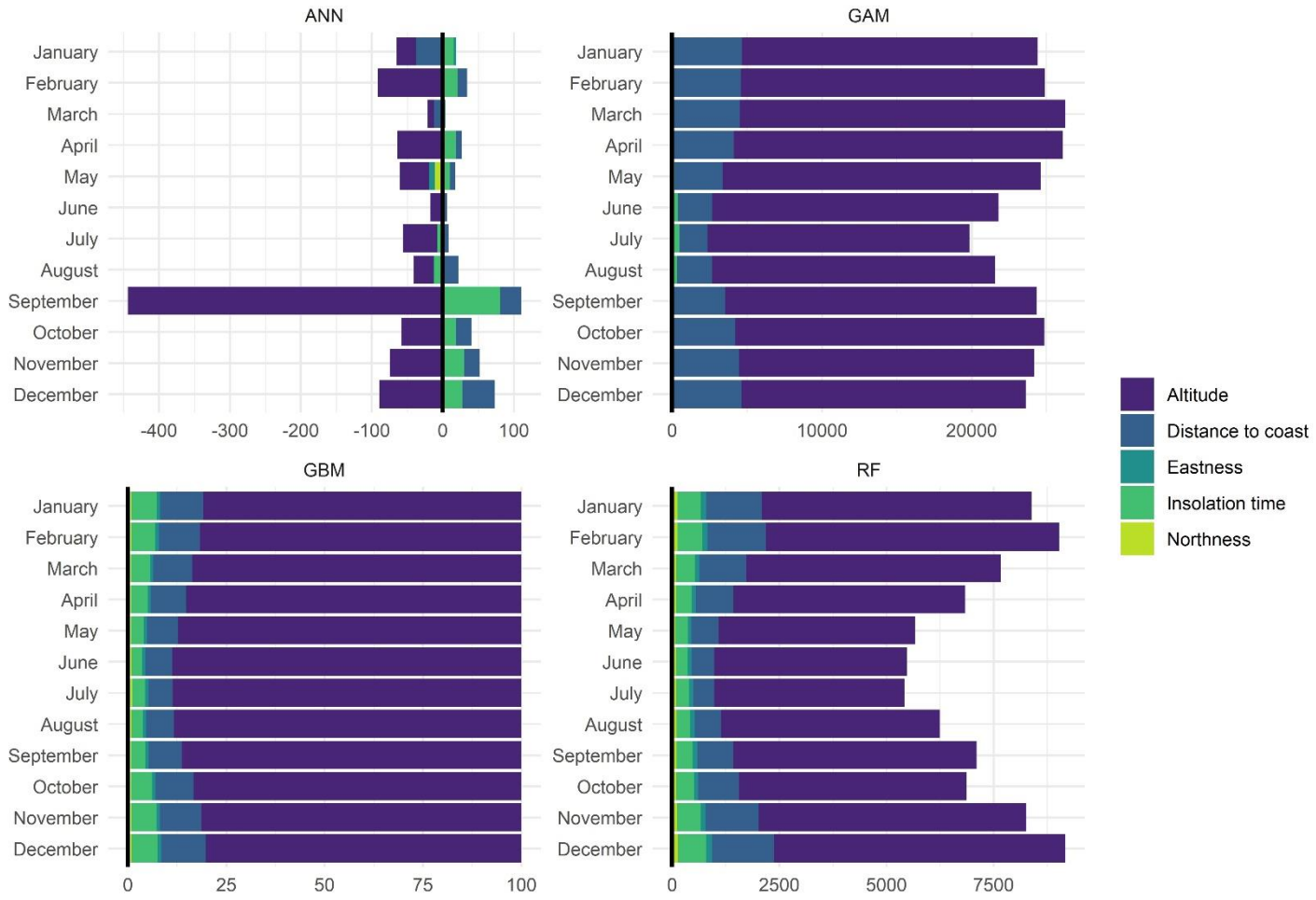

Figure A.13. Variable importance plots for the CHELSA downscaling. ANN's top-left subplot displays the Olden relative variable importance, GAM's top-right subplot the F statistic for each predictor, GBM's bottom-left subplot the computed relative influences, normalized to sum to 100, and RF's bottom-right subplot the increase in node purity associated with each predictor.

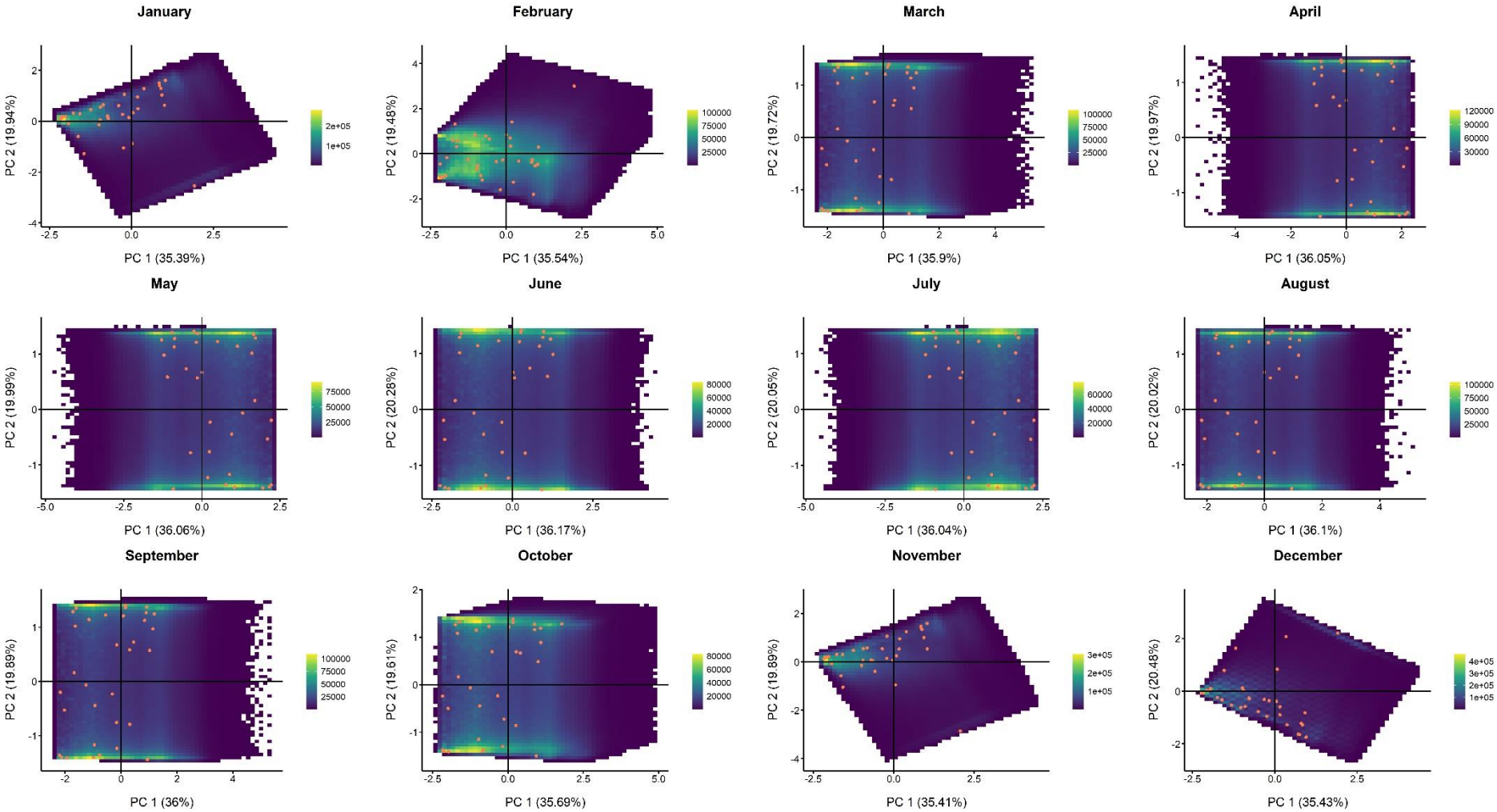

Figure A.14. Monthly bivariate plots of the PCAs that synthesize landscape complexity. Orange points indicate weather stations' locations.

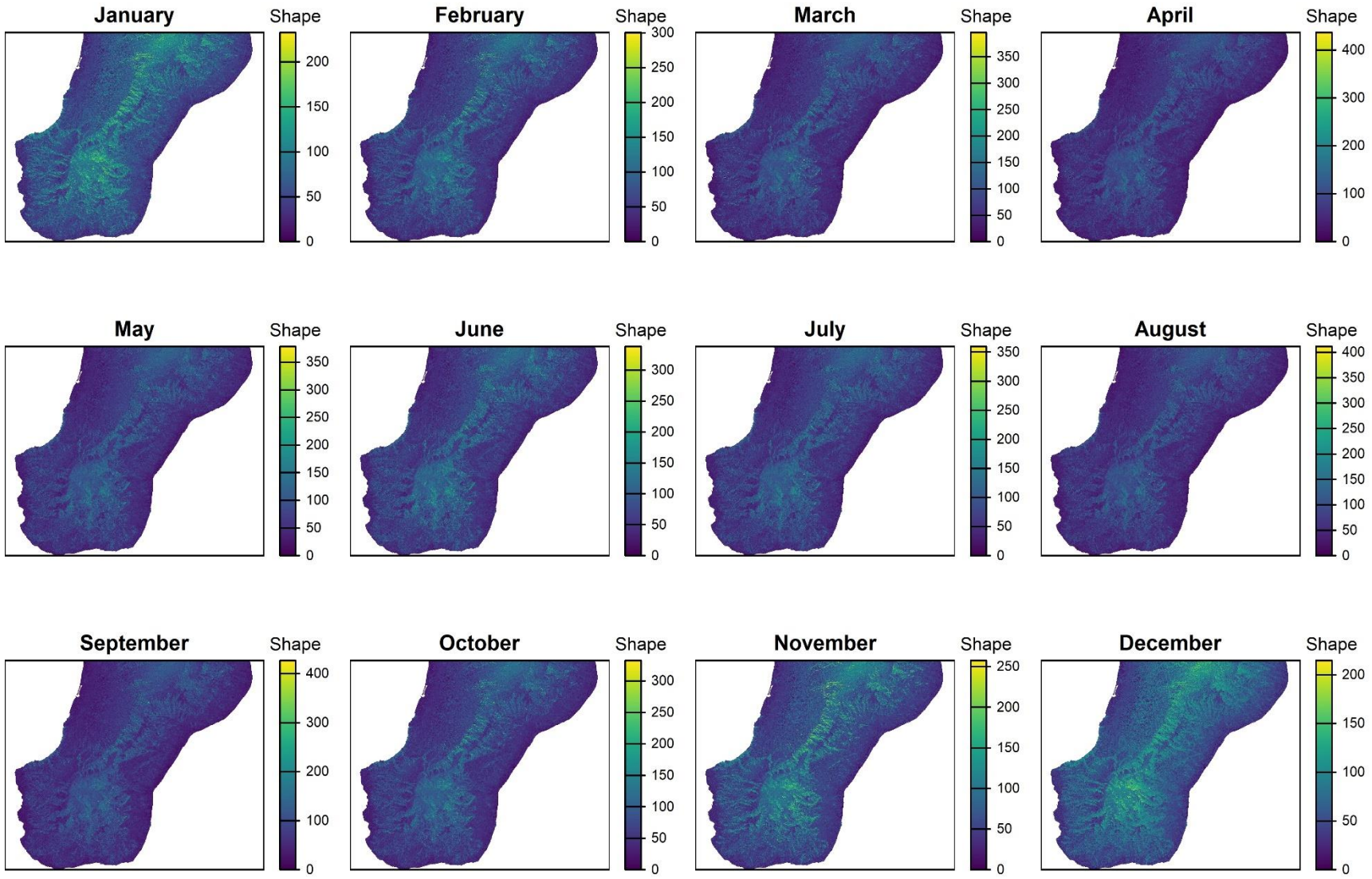

Figure A.15. Seasonal patterns of environmental extrapolation when interpolating weather station data. Extrapolation was quantified by the Shape method; higher Shape values indicate higher extrapolation degrees.

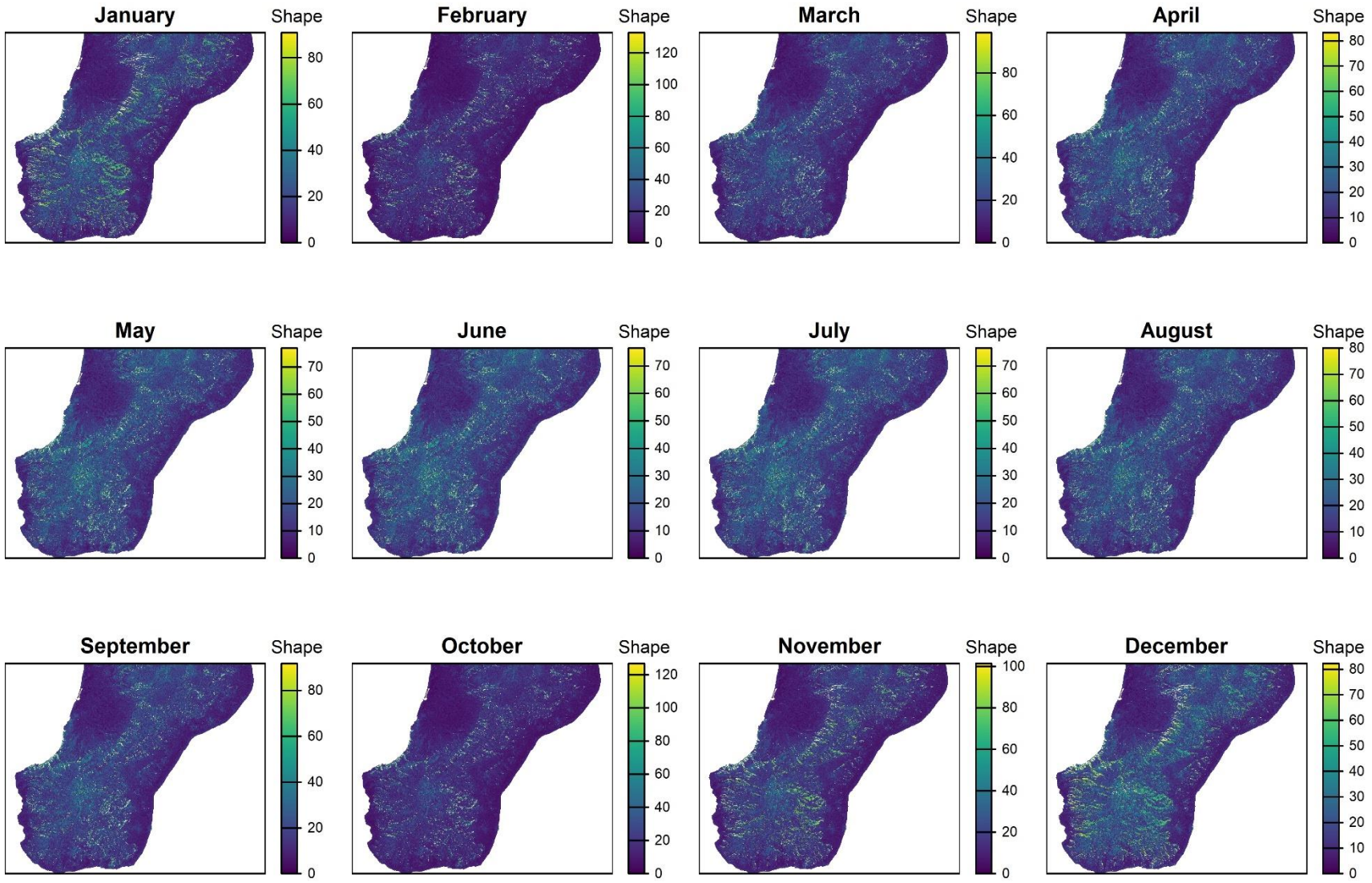

Figure A.16. Seasonal patterns of environmental extrapolation when downscaling WorldClim. Extrapolation was quantified by the Shape method; higher Shape values indicate higher extrapolation degrees. For graphical purposes, Shape values were capped at their 99th percentile.

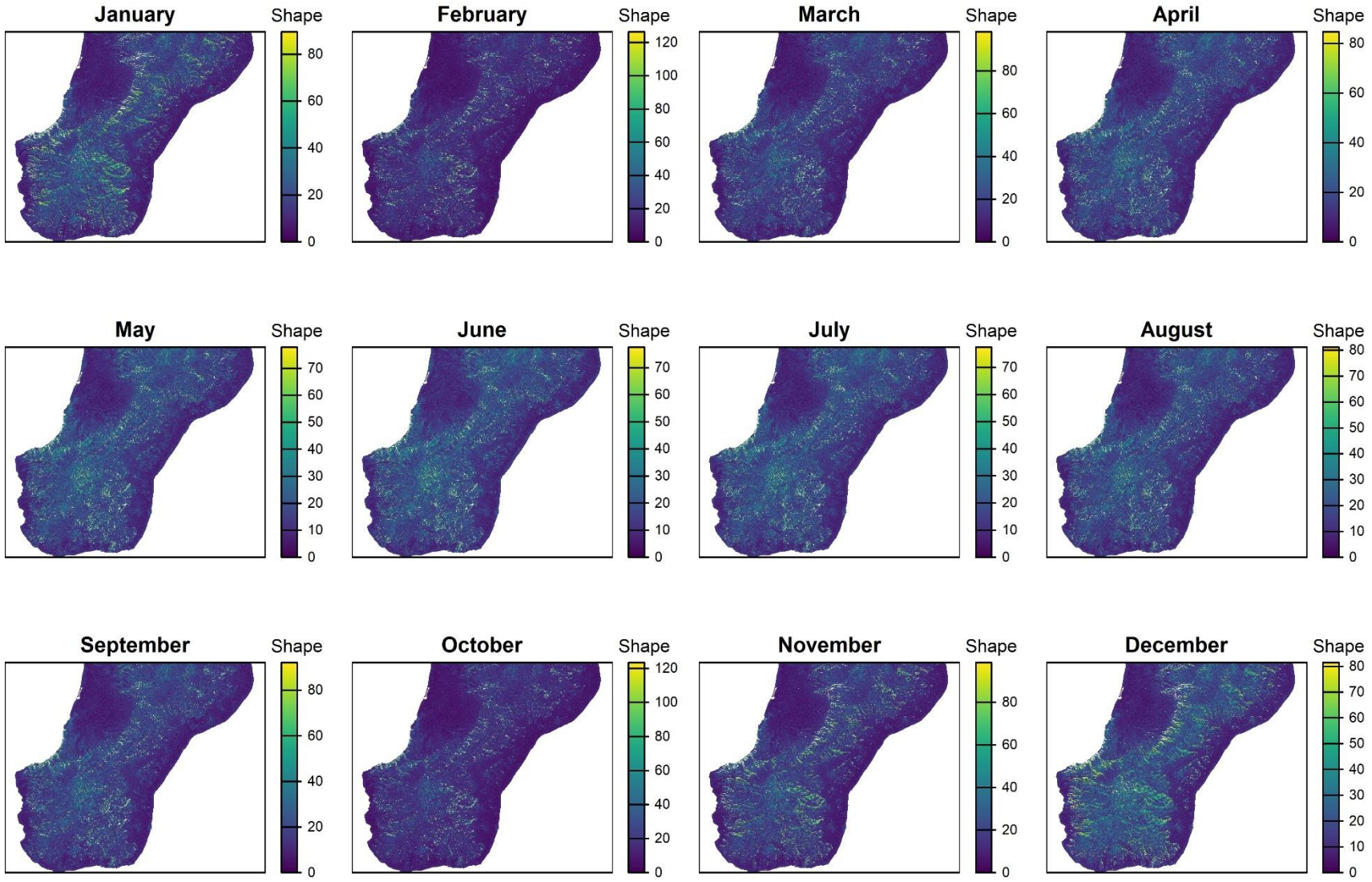

Figure A.17. Seasonal patterns of environmental extrapolation when downscaling CHELSA. Extrapolation was quantified by the Shape method; higher Shape values indicate higher extrapolation degrees. For graphical purposes, Shape values were capped at their 99th percentile.

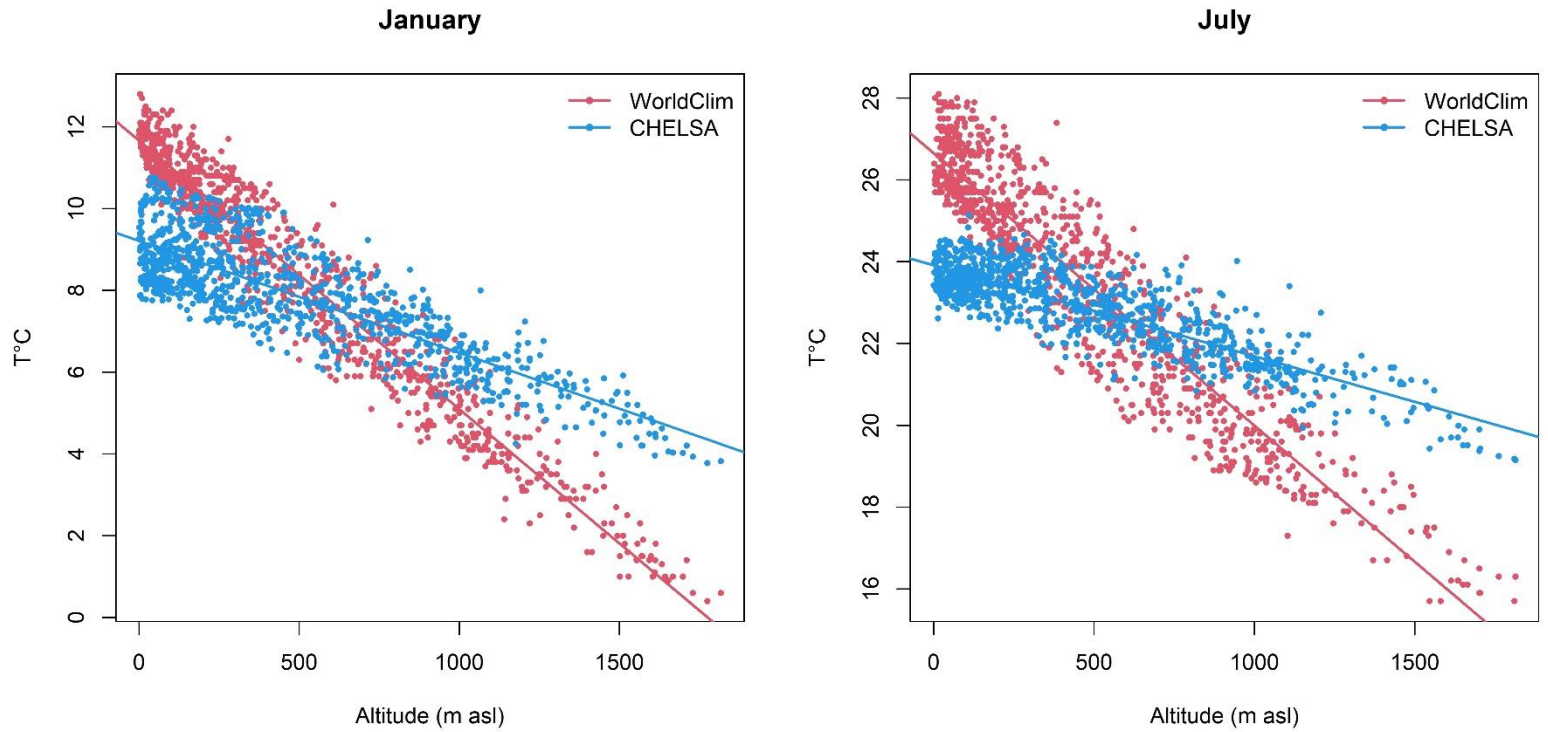

Figure A.18. Empirical temperature lapse rates of the native WorldClim and CHELSA macroclimate grids for January and July. Points indicate the altitude and coarse-grained temperature at 1000 random locations, while lines show the corresponding trend curves outputted by linear regression models.

Appendices of Chapter 3

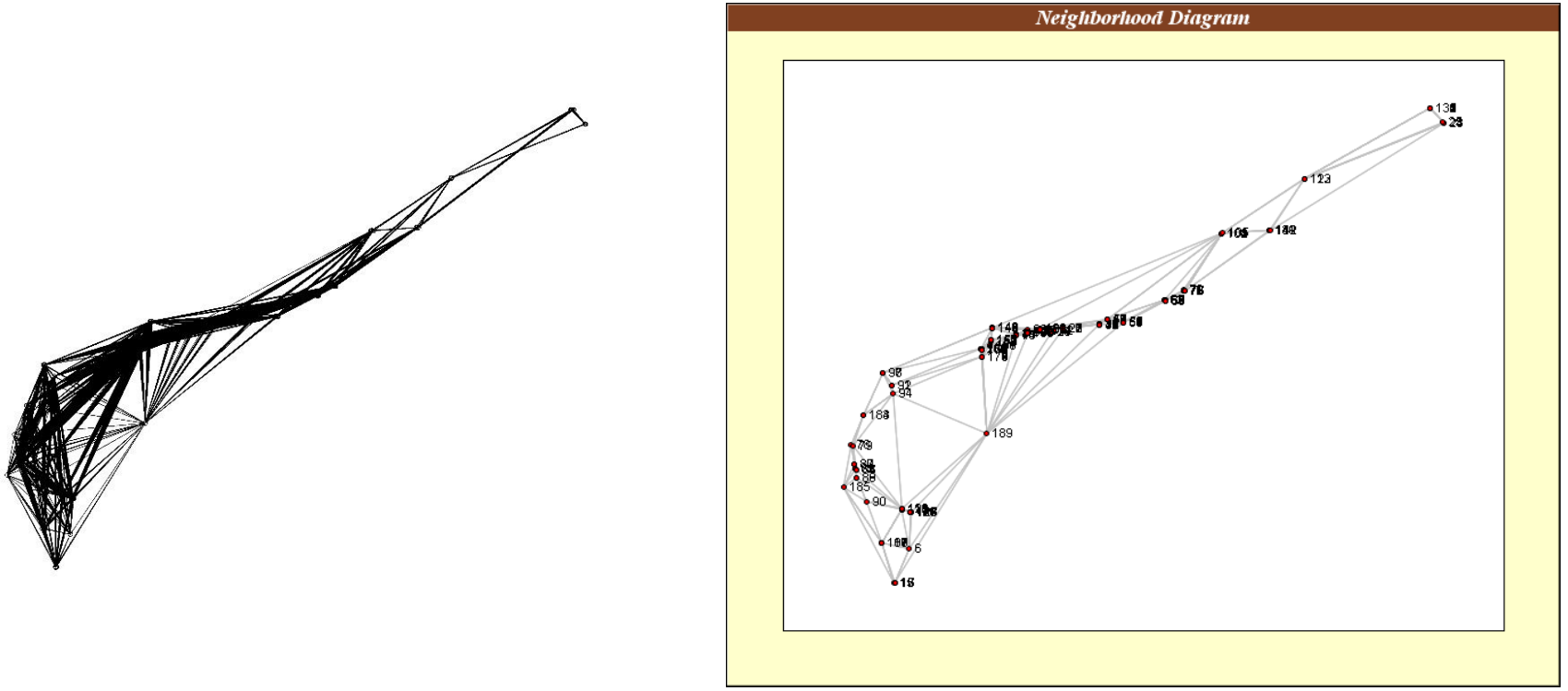

Figure A.1. The connection network we built for **a)** the sPCA and **b)** TESS.

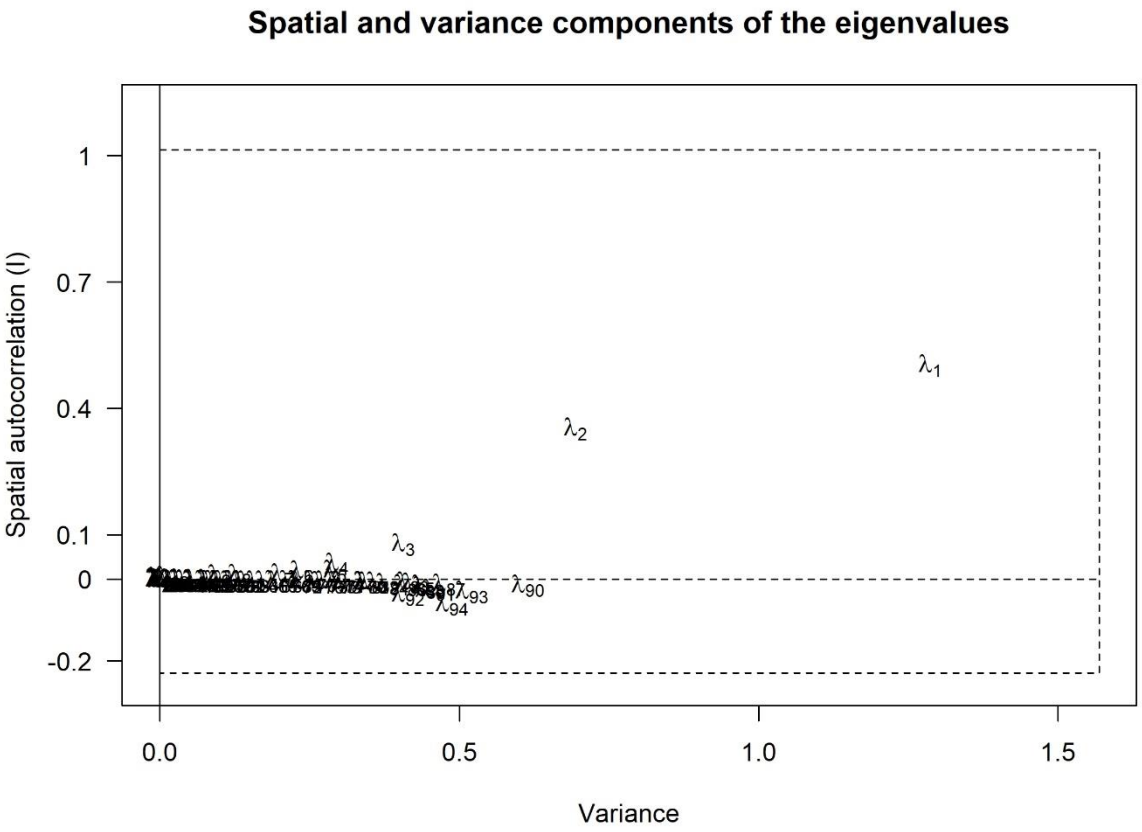

Figure A.2. Decomposition of the sPCA's eigenvectors into variance and autocorrelation.

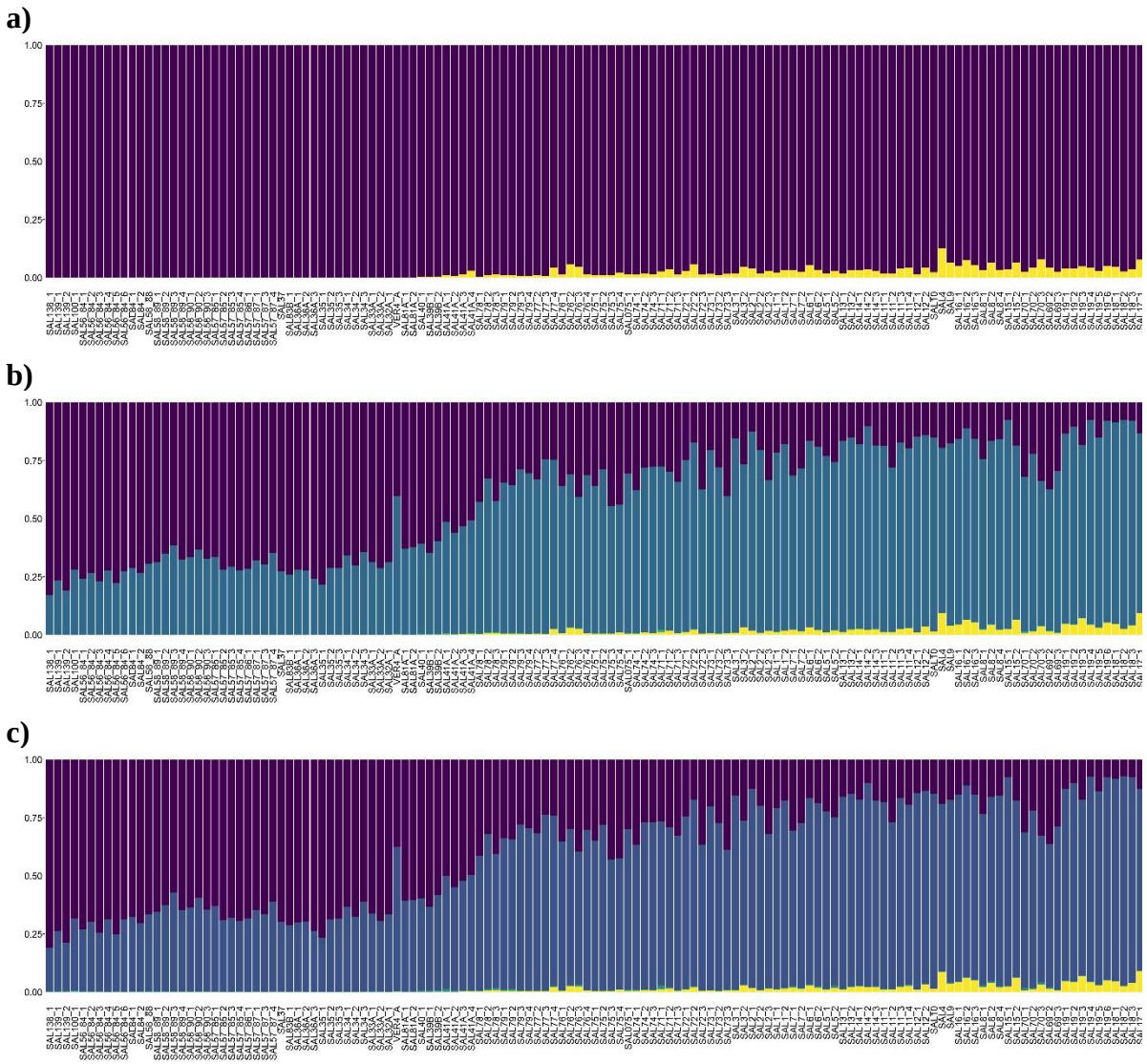

Figure A.3. The admixture proportions of each individual for **a)** K = 2, **b)** K = 4, and **c)** K = 5 that TESS inferred.

Appendices of Chapter 4

Table A.1. Coordinates, altitude, and hourly time series length for each data logger employed in the present study.

ID	Coordinates (EPSG: 32632)		Altitude	Hourly time series	
	longitude	latitude	(m a.s.l.)	start	end
001	1106657	4251742	1260.34	2021-06-21	2021-10-21
002	1110490	4252914	1163.76	2021-06-21	2021-10-21
003	1097303	4247003	1149.37	2021-06-21	2021-09-27
004	1109346	4250422	1523.42	2021-06-21	2021-10-21
005	1123513	4265159	941.45	2021-06-21	2021-10-22
006	1114640	4253143	1106.34	2021-06-21	2021-07-30
007	1105624	4245882	1874.98	2021-06-21	2021-10-19
008	1106734	4246934	1764.98	2021-06-21	2021-10-19
009	1114954	4256487	1073.05	2021-06-21	2021-10-21
010	1101898	4245058	1781.80	2021-06-21	2021-07-29
011	1109648	4242728	1387.13	2021-06-21	2021-10-20
012	1107736	4244158	1535.27	2021-06-21	2021-10-20
014	1118061	4247301	585.51	2021-06-21	2021-07-30
015	1120525	4261008	1021.49	2021-06-21	2021-07-30
016	1101632	4244220	1672.25	2021-06-21	2021-10-19
018	1109577	4244574	1504.07	2021-06-21	2021-07-29
019	1108463	4244589	1582.24	2021-06-21	2021-10-20
020	1110918	4246921	1113.19	2021-06-21	2021-07-29
021	1110857	4241673	1437.25	2021-06-21	2021-10-20
022	1104224	4247626	1715.24	2021-06-21	2021-10-19

Table A.2. The AICc table we built for multimodel inference. The box indicates the best models (ΔAICc ≤ 2), while the models highlighted in green are those we selected for the more conservative model averaging (ΔAICc ≤ 7). The blue line shows the rank of the null model (**CLC**: CORINE Land Cover; **FORESTS**: distance from the nearest old-growth forest; **DTR**: diurnal temperature range; **FLII**: Forest Landscape Integrity Index; **GCH**: Global Canopy Height; **log(β)**: logarithm of the buffering slope).

Intercept	CLC	FORESTS	DTR	FLII	GCH	log(β)	AICc	ΔAICc	weight
4.5755	*	-0.0727	-	-0.2390	-	-	204.694	-	0.37489
2.9450	*	-0.0881	-	-0.2192	0.0842	-	205.954	1.259	0.19972
1.3993	*	-0.0709	-	-	0.0872	-	206.526	1.831	0.15004
2.9487	*	-0.0527	-	-	-	-	207.438	2.743	0.09511
1.8018	*	-	0.0681	-	-	-	208.093	3.399	0.06852
2.2181	*	-0.0410	0.0517	-	-	-	209.003	4.308	0.04349
2.6991	*	-0.0567	-	-	-	-2.0050	211.315	6.620	0.01369
3.8556	*	-0.0622	0.0316	-0.1988	-	-	211.357	6.663	0.01340
4.3025	*	-0.0734	-	-0.2187	-	-1.1081	212.313	7.618	0.00831
2.6856	*	-	-	-	-	-	212.550	7.856	0.00738
1.2767	*	-0.0729	-	-	0.0818	-1.6511	213.011	8.317	0.00586
1.3089	*	-0.0602	0.0297	-	0.0687	-	213.643	8.949	0.00427
2.3376	*	-	0.0636	-0.0750	-	-	213.820	9.125	0.00391
1.5944	*	-	0.0658	-	0.0125	-	214.822	10.128	0.00237
1.8105	*	-	0.0707	-	-	0.3016	214.946	10.251	0.00223
3.4039	*	-	-	-0.1136	-	-	215.593	10.898	0.00161
2.8274	*	-0.0880	-	-0.2076	0.0818	-0.6306	216.261	11.567	0.00115
2.9105	*	-0.0867	0.0034	-0.2159	0.0822	-	216.494	11.800	0.00103
2.0008	*	-	-	-	0.0357	-	216.652	11.958	0.00095
2.4986	*	-	-	-	-	-1.3161	216.973	12.279	0.00081
2.2348	*	-0.0448	0.0428	-	-	-0.8755	217.023	12.328	0.00079
2.7504	*	-	-	-0.1008	0.0297	-	221.384	16.690	8.91e-05
3.8430	*	-0.0636	0.0278	-0.1960	-	-0.3812	221.841	17.146	7.09e-05
2.4753	*	-	0.0701	-0.0909	-	0.8764	221.851	17.156	7.05e-05
3.1938	*	-	-	-0.0977	-	-0.7703	222.102	17.408	6.22e-05
2.1585	*	-	0.0619	-0.0726	0.0097	-	222.156	17.461	6.06e-05
1.9354	*	-	-	-	0.0308	-1.0868	222.695	18.000	4.63e-05
1.5939	*	-	0.0686	-	0.0132	0.3492	223.191	18.497	3.61e-05
1.2620	*	-0.0671	0.0149	-	0.0735	-1.2934	223.323	18.628	3.38e-05
2.6365	*	-	-	-0.0896	0.0276	-0.5802	229.612	24.918	1.46e-06
2.8549	*	-0.0899	-0.0046	-0.2103	0.0841	-0.7372	229.811	25.117	1.32e-06
2.2784	*	-	0.0684	-0.0889	0.0111	0.9154	232.265	27.571	3.86e-07
0.7362	-	-	0.0433	-0.0853	0.0909	-	249.568	44.873	6.76e-11
0.4288	-	-	0.0427	-	0.0804	-	250.352	45.658	4.56e-11
0.8679	-	-	0.0395	-0.0832	0.0850	-0.6739	252.066	47.371	1.94e-11
0.5544	-	-	0.0383	-	0.0756	-0.7627	252.124	47.430	1.88e-11
0.4430	-	0.0114	0.0464	-	0.0740	-	252.714	48.019	1.40e-11
0.7532	-	-0.0032	0.0423	-0.0914	0.0935	-	253.140	48.446	1.13e-11
1.2635	-	-	-	-0.0828	0.1008	-	253.380	48.686	1.00e-11
1.3914	-	-	-	-0.0795	0.0907	-0.9377	254.191	49.496	6.70e-12
0.9388	-	-	-	-	0.0913	-	254.411	49.717	6.00e-12
1.0518	-	-	-	-	0.0827	-1.0293	254.430	49.735	5.94e-12
1.4983	-	-0.0270	-	-0.1327	0.1064	-1.4308	254.728	50.034	5.12e-12
1.0120	-	-0.0142	0.0331	-0.1102	0.0939	-0.9730	255.533	50.839	3.42e-12
0.5415	-	0.0060	0.0411	-	0.0730	-0.6294	255.561	50.866	3.38e-12

Table A.2. The AICc table we built for multimodel inference (*continued*).

Intercept	CLC	FORESTS	DTR	FLII	GCH	log(β)	AICc	ΔAICc	weight
1.2701	-	-0.0132	-	-0.1087	0.1114	-	255.640	50.946	3.24e-12
0.9581	-	0.0029	-	-	0.0897	-	257.148	52.453	1.53e-12
1.0243	-	-0.0056	-	-	0.0850	-1.1383	257.417	52.722	1.33e-12
1.5958	-	0.0237	0.0608	-	-	-	259.742	55.048	4.17e-13
1.8684	-	-	0.0472	-	-	-1.1061	259.959	55.264	3.74e-13
1.7726	-	-	0.0563	-	-	-	260.605	55.910	2.71e-13
1.7109	-	0.0168	0.0534	-	-	-0.7467	261.661	56.966	1.60e-13
2.1328	-	-	0.0478	-0.0453	-	-1.1539	261.986	57.292	1.36e-13
1.9669	-	-	0.0573	-0.0346	-	-	262.678	57.983	9.62e-14
1.6350	-	0.0230	0.0608	-0.0060	-	-	262.891	58.196	8.64e-14
1.9010	-	0.0125	0.0522	-0.0258	-	-0.8636	264.998	60.304	3.01e-14
2.6488	-	-	-	-	-	-1.4953	265.237	60.542	2.67e-14
2.9083	-	-	-	-0.04257	-	-1.5364	267.023	62.329	1.09e-14
2.6328	-	0.0049	-	-	-	-1.4012	267.890	63.196	7.10e-15
2.7279	-	-	-	-	-	-	269.990	65.295	2.48e-15
2.9383	-	-0.0023	-	-0.0463	-	-1.5837	270.168	65.473	2.27e-15
2.6543	-	0.0174	-	-	-	-	270.371	65.677	2.05e-15
2.8870	-	-	-	-0.0259	-	-	272.053	67.358	8.86e-16
2.6898	-	0.0168	-	-0.0054	-	-	273.150	68.456	5.12e-16

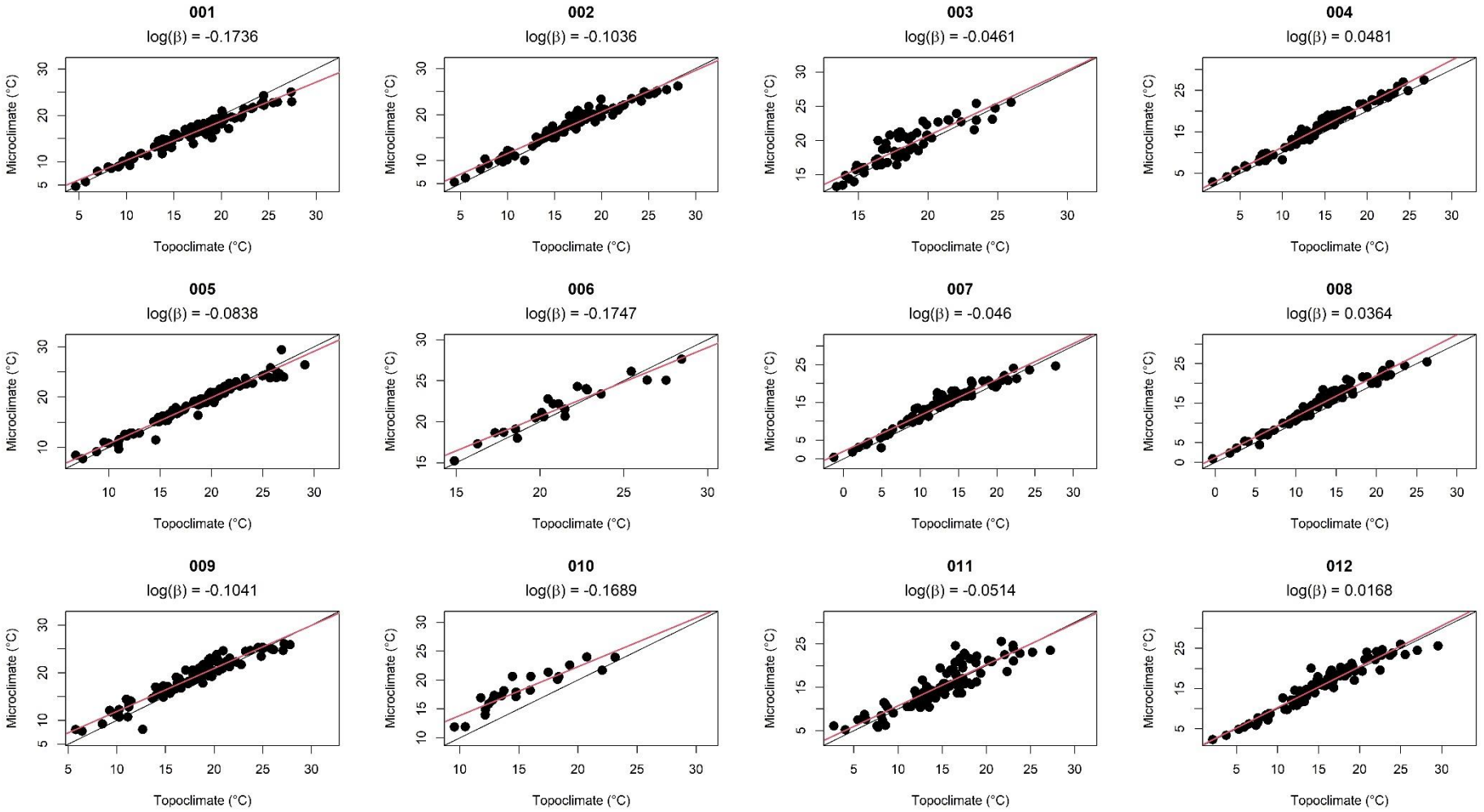

Figure A.1. The slope relating microclimate to topoclimate for data loggers 001 to 012. Negative log(β) values indicate buffering effects, where β are the slopes of the linear trend curves we draw in red.

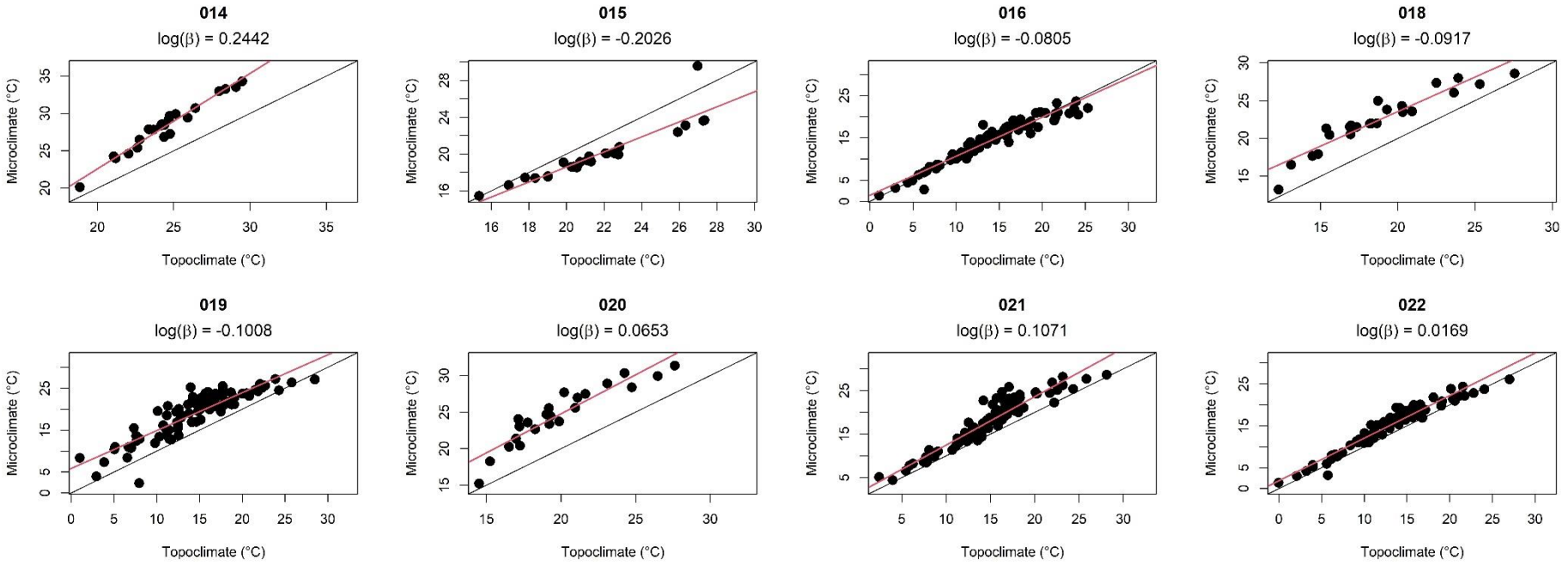

Figure A.2. The slope relating microclimate to topoclimate for data loggers 014 to 022. Negative log(β) values indicate buffering effects, where β are the slopes of the linear trend curves we draw in red.

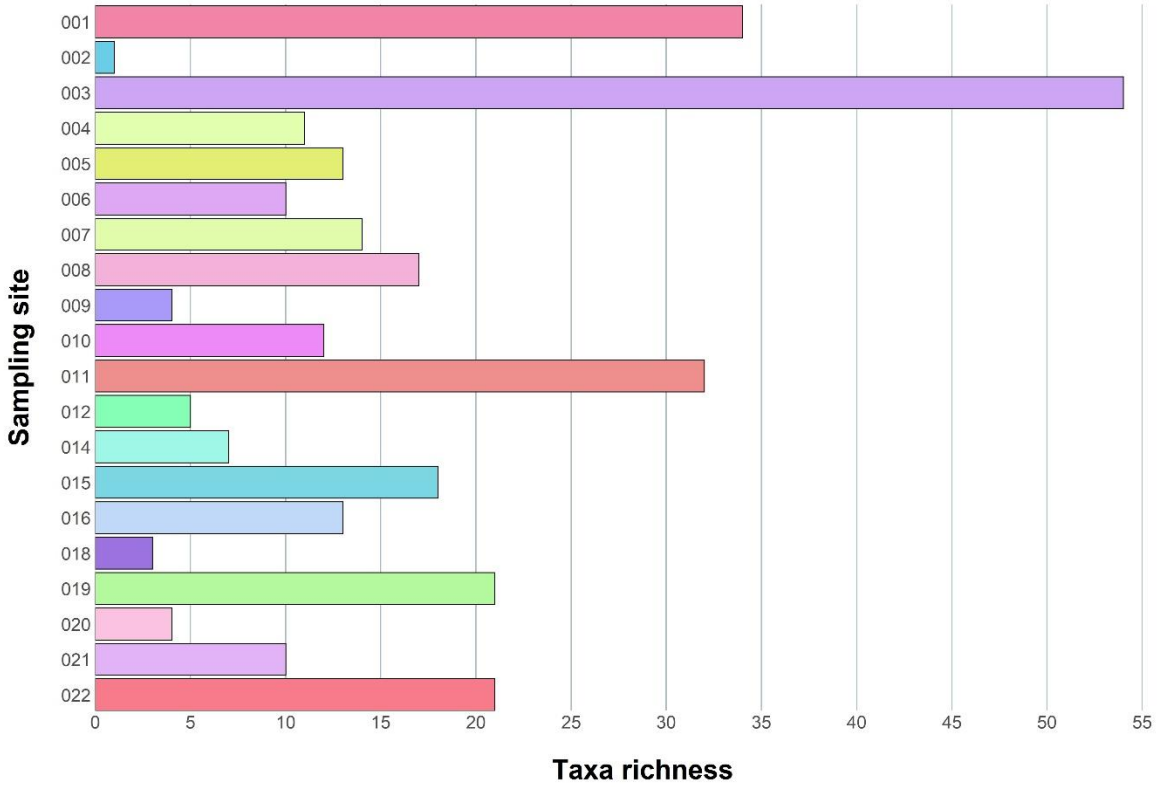

Figure A.3. Diversity of pollinating insects in the sampling sites we selected for this study, restituted by morphological and molecular identification.